Programa de Pós-graduação Multicêntrico em Química de Minas Gerais – Universidade Federal de Itajubá

Daniel Bragança Viana

Hybrid protein-polymer nanoparticles loaded with cisplatin: Synthesis and Characterization

Itabira

July/2021

Daniel Bragança Viana

Hybrid protein-polymer nanoparticles loaded with cisplatin: synthesis and Characterization

Dissertation presented at Universidade Federal de Itajubá – *Campus* Itabira – in partial fulfillment of the requirements for the degree of Master of Chemistry.

Concentration area: Química
Research field: Química Medicinal
Advisor: Prof(a). Dra. Marli Luiza Tebaldi
Co-advisor: Prof. Dr. Daniel Cristian Ferreira Soares

Itabira
July/2021

“Talk about a dream, try to make it real”

Bruce Springsteen, Badlands

Acknowledgment

To God who sustained me and gave me strength to reach the end.

My family for their unconditional support. My mother who never went out of her way to help me and of course always waited for me with a hot coffee, covering me with her care and love. To my brothers Daniela and Jhonniter for always being together bringing comfort and tranquility. Alice my girlfriend for all partnership and complicity, making my days lighter and happier.

My advisor Prof. Marli Luiza Tebaldi for all her dedication and donation. I am so grateful for the opportunity to learn and work with you. To my co-advisor Prof. Daniel Cristian, for his patience and availability to pass on his teachings, both academic and life. Without a doubt I could not have been guided by better people.

To colleagues at the Bioengineering Laboratory, for all the exchange of knowledge, support and companionship during these years of research, transforming the laboratory into one of the best places.

To the colleagues at the Fraunhofer IAP Institute who welcomed me and made every effort to contribute both to the research and to my stay in Germany, instructing me in every detail with all dedication.

CAPES, CNPq, FAPEMIG and Unifei for financial support.

To all my friends, especially Thais and Márcia who, even far away, were always present.

One more cycle ends and once again I realize that, alone, none of this would have been possible. To all those who contributed to the development of this work, I am very grateful!

Agradecimentos

Acknowledgment (Portuguese version)

A Deus que me sustentou e me deu forças para chegar até o fim.

A minha família pelo apoio incondicional. A minha mãe que nunca mediu esforços para me ajudar e claro sempre me esperava com um café quentinho, me cobrindo com seu cuidado e amor. Aos meus irmãos Daniela e Jhonniter por estarem sempre juntos trazendo conforto e tranquilidade. A Alice minha namorada por toda parceria e cumplicidade, tornando meus dias mais leves e felizes.

A minha orientadora Prof.ª Marli Luiza Tebaldi por toda dedicação e doação. Sou muito grato pela oportunidade de poder aprender e trabalhar com você. Ao meu co-orientador Prof. Daniel Crístian, pela paciência e disponibilidade em passar seus ensinamentos tanto os acadêmicos quanto de vida. Sem dúvidas eu não poderia ter sido orientado por pessoas melhores.

Aos colegas do laboratório de Bioengenharia, por toda troca de conhecimento, apoio e companheirismo durante estes anos de pesquisa, transformando o laboratório em um dos melhores lugares.

Aos colegas do Instituto Fraunhofer IAP que me acolheram e não mediram esforços para contribuir tanto com a pesquisa quanto com minha estadia na Alemanha, me instruindo em todos os detalhes com toda dedicação.

A CAPES, CNPq, FAPEMIG e a Unifei pelo apoio financeiro.

A todos os meus amigos, em especial Thais e Márcia que mesmo distantes estiveram sempre presentes.

Mais um ciclo se encerra e mais uma vez percebo que sozinho nada disso teria sido possível. A todos aqueles que contribuíram para o desenvolvimento deste trabalho o meu muito obrigado!

Abstract

Nowadays, many research related tovhybrid materials and the advances in Reversible-Deactivation Radical Polymerization (RDRP) techniques have enabled the development of responsive materials. These compounds respond to specific stimuli and have been integrating many research projects involving different drug delivery systems. In particular, hybrid conjugates based on protein−polymer have been integrating different formulations already approved by the Food and Drug Administration. In general, protein-polymer conjugates can increase the drug plasmatic half-life, altering the drug biodistribution profile and opening the possibility to reduce the dose administrated, which is a relevant advantage for patients. In this work, poly (N-vinylcaprolactam) (PNVCL) and poly (2-dimethylamino-ethyl methacrylate) (PDMAEMA) polymers were grafted to the surface of a protein model, the bovine serum albumin (BSA), by *grafting-from* approach, using the Atom Transfer Radical Polymerization (ATRP) technique. Firstly, a macroinitiator (BSA-MI) was successfully obtained and characterized by Sodium dodecyl sulfate polyacrylamide gel electrophoresis and Matrix-Assisted Laser Desorption Ionization Time of Flight Mass Spectrometry by modifying lysine groups present in the BSA. Then, the BSA-PNVCL-*co*-PDMAEMA hybrid was synthesized using BSA-MI as an initiator. The conjugate production was evaluated, revealing significant changes in the nanoparticles' molecular mass and zeta potential . Additionally, it is demonstrated that altering the monomers' ratio can further adjust the lower critical solution temperature (LCST) of the protein-polymer conjugates. The results indicate the obtaining of a BSA-PNVCL-co-PDMAEMA able to encapsulate approximately 1.9 mg of cisplatin for each 1 mg of the hybrid, making this conjugate a very promising hybrid material with desirable properties for a possible application in smart drug delivery systems.

Keywords: protein-polymer conjugate; Bovine Serum Albumin; thermally-responsive; Poly (N-vinyl caprolactam); Poly (2-dimethylamino-ethyl methacrylate); Cisplatin.

List of Figures

Figure 1.1: Representation of cisplatin structure……..14
Figure 3.1: Representation of a stimulus-responsive polymer behavior for PDMAEMA and the structures of NVCL and DMAEMA monomers and their respective polymers. Adapted from Precupas, Sandu, Popa (2016)……..19
Figure 3.2: Classification of hybrid materials adapted from Faustini *et al*. (2018)….21
Figure 3.3: Schematic representation of the *grafting-to* and *grafting-from* method adapted from Kaupbayeva and Russell (2019)……..22
Figure 3.4: Commonly lysine modification for *grafting-from.* Adapted from Messina *et al.* (2020)…….23
Figure 3.5: Mechanism of the traditional ATRP process. Adapted from MESSINA *et al*. (2019)…….24
Figure 4.1: Schematic representation of the steps to obtain N-2-Bromo-2-methylpropionyl-β-alanine N′-oxysuccinimide ester…….27
Figure 4.2: Schematic representation of the steps to obtain N-2-Chloropropionyl-β-alanine…….28
Figure 4.3: ATRP polymerization of homo PNVCL (I), PNVCL-co-PDMAEMA (II) and the Polymerization steps (III)……30
Figure 4.4: Synthesis of the conjugate via ATRP in A) synthesis of the macroinitiator and in B) synthesis of the hybrid by *grafting-from* approach……..34
Figure 5.1: ^{1}H-NMR spectrum of NHS-BIBA. Peaks are related to the respective structure……38
Figure 5.2: ^{1}H-NMR spectrum of N-ALA, recorded in $CDCl_3$, with peak assignments……..39
Figure 5.3: ^{1}H-NMR of NVCL reaction using ECP as an initiator, recorded in $CDCl_3$, with peak assignments……40
Figure 5.4: ^{1}H-NMR of NVCL and DMAEMA reaction using ECP as initiator, recorded in $CDCl_3$, with peak assignments……...……41
Figure 5.5: ^{1}H-NMR of NVCL reaction using BIBA as an initiator, recorded in $CDCl_3$, with peak assignments……42
Figure 5.6: ^{1}H-NMR of NVCL and DMAEMA reaction using BIBA as initiator, recorded in D_2O, with peak assignments……43

Figure 5.7: ^{1}H-NMR of NVCL reaction using N-ALA as an initiator and Me_6TREN as ligand, recorded in $CDCl_3$, with peak assignments……..……..…44
Figure 5.8: ^{1}H-NMR of NVCL and DMAEMA reaction using N-ALA as an initiator and Me_6TREN as ligand, recorded in $CDCl_3$, with peak assignments ……45
Figure 5.9: ^{1}H-NMR of NVCL reaction using N-ALA as an initiator and Me_6Cyclam as ligand, recorded in $CDCl_3$, with peak assignments. ……..…..…46
Figure 5.10: ^{1}H-NMR of NVCL and DMAEMA reaction using N-ALA as an initiator and Me_6Cyclam as a ligand, recorded in $CDCl_3$, with peak assignments……..46
Figure 5.11: ^{1}H-NMR analysis of polymerization of a) PNVCL-co-PDMAEMA and b) PDMAEMA. Samples were taken after specific time points (10, 60, 120, 240 minutes), recorded in D_2O, with peak assignments……..…….49
Figure 5.12: SDS-PAGE of BSA (line 1), BSA-MI (line 4) and BSA-MI, 10 times concentrated (line 10)……50
Figure 5.13: MALDI-ToF MS of BSA (blue spectrum) and BSA-MI (green spectrum).51
Figure 5.14: Hybrid material obtained from the first route after purification…….52
Figure 5.15: Particle size distributions: A) in PBS pH 7.4 BSA solution (1 mg/ml), B) in PBS pH 7.4 BSA-$PNVCL_{0.5}$-*co*-$PDMAEMA_{0.5}$ in PBS pH 7.4 (1 mg/ml)…….54
Figure 5.16: Aggregation point of BSA-PNVCL-*co*-PDMAEMA……55
Figure 5.17: SDS-PAGE of BSA (line 1) BSA-MI (line 4), BSA-MI 10 times concentrated (line 10), BSA-PNVCL-*co*-PDMAEMA (line 5) and BSA-PNVCL-*co*-PDMAEMA 10 times concentrated (line 11)……..56
Figure 5.18: MALDI-ToF MS of BSA-PNVCL-*co*-PDMAEMA……57
Figure 5.19: Aggregation point of BSA-PNVCL-*co*-PDMAEMA in PBS solution pH 7.4……58
Figure 5.20: Calibration curve for cisplatin in the range of 20 to 100 µg / mL obtained by the HPLC-DAD technique. The curve was obtained, given by the equation y = 0.00003643*X+ 0.6636 and r^2 = 0.9984 ……59

Abbreviations

ATRP – Atom Transfer radical Polymerization

BIBA - *N*-2-Bromo-2-methyl propanol-β-alanine

BSA – Bovine Serum Albumin

BSA-MI - Bovine Serum Albumin Macro Initiator

CRP – Controlled Radical Polymerization

CTA – Chain-transfer agent

DLS - Dynamic Light Scattering

DMAEMA - 2- (Dimethylamino) ethyl methacrylate

DP – Degree of Polymerization

DT – Dithranol

EC – Encapsulation capacity

ECP- Ethyl-2-chloropropionate

EP – Encapsulation percentage

FDA - United States Food and Drug Administration

^{1}H-NMR - Proton Nuclear Magnetic Resonance

HPLC – High-Performance Liquid Chromatography

HSA – Human Serum Albumin

LCST- Lower Critical Solubility Temperature

MALDI-ToF MS - Matrix-Assisted Laser Desorption Ionization Time of Flight Mass Spectrometry

Me_6TREM - Tris [2- (dimethylamino) ethyl] amine

MWCO – Molecular Weight Cut Off

N-ALA- N-2-chloropropionyl-β-alanine

NHS - N-hydroxysuccinimide ester

NHS-BIBA - *N*-2-Bromo-2-methyl propanol-β-alanine N′-oxysuccinimide ester

NMR - Nuclear magnetic resonance

NVCL - N-vinyl caprolactam

PBS - Phosphate-Buffered Saline

PDMAEMA - Poly (2-dimethylamino-ethyl methacrylate)

PEG - Polyethylene glycol

PNVCL - Poly (N-vinyl caprolactam)

RAFT – Reversible addition-fragmentation chain-transfer polymerization

RDRP – Controlled polymerization techniques, also known as Reversible Deactivation Radical Polymerization

SDS-PAGE – Sodium dodecyl sulfate polyacrylamide gel electrophoresis

Summary

1. Introduction……...13

2. Objectives……16

3. Theoretical Framework..……..17

3.1. Bovine Serum Albumin (BSA)……....17

3.2. Smart Polymers……18

3.3. Hybrids materials……..20

3.4. Protein-polymer conjugates……21

3.5. Controlled radical polymerization ……24

4. Metodology……..……25

4.1. Materials……..……25

4.2. Synthesis of ATRP initiators……25

4.2.1. N-2-Bromo-2-methylpropanoyl-β-alanine-N′-oxysuccinimide ester (NHS-BIBA).....26

4.2.2. N-2-Chloropropionyl-β-alanine.....27

4.3. Polymerization study……28

4.4. Kinetics studies for ATRP polymerization……30

4.5. Synthesis of BSA macroinitiator (BSA-MI)…..……31

4.6. Synthesis of the conjugate BSA-PNVCL-co-PDMAEMA……32

4.6.1. BSA-PNVCL-co-PDMAEMA (route 1)……..……32

4.6.2. BSA-PNVCL 0.5 -co-PDMAEMA 0.5 (route 2) ……..……33

4.6.3. BSA-PNVCL 0.7 -co-PDMAEMA 0.3 (route 3) ……..……33

4.7. Characterization methods… ……...34

4.7.1. Chemical characterization……..……34

4.7.2. Physical Characterization……35

4.7.3. Drug encapsulation efficiency ……36

5. Results and discussion……37

5.1. Synthesis of ATRP initiators……37

5.1.1. Synthesis of N-2-Bromo-2-methylpropanoyl-β-alanine-N′-oxysuccinimide ester (NHS-BIBA).....37

5.1.2. Synthesis of N-ALA……..38

5.2. Polymerization study……39

5.2.1. NVCL and DMAEMA reaction using the catalytic system ECP/Me 6 TREN……..……..40
5.2.2. NVCL and DMAEMA reaction using the catalytic system BIBA/Me 6 TREN...……41
5.2.3. NVCL and DMAEMA reaction using the catalytic system N-ALA and Me 6 Cyclan as a ligand……..43
5.2.4. NVCL and DMAEMA reaction using the catalytic system N-ALA and Me 6 TREN as a ligand……45
5.3. Kinetics studies for ATRP polymerization……..47
5.4. Synthesis of BSA BSA-MI……..……..…50
5.5. Synthesis of the BSA-PNVCL-co-PDMAEMA…….……51
5.5.1. Route 1……..……51
5.5.2. Route 2 ……..52
5.5.3. Route 3 ……55
5.6. Drug encapsulation efficiency ……...58
6. Conclusion ...……..……61
7. Work development and scientific production ……62
8. Perspectives ..……...63
References ……..64
Annex- Paper published……...68

1. Introduction

Throughout history, science has been concerned with developing systems that guarantee a better quality of life for human beings. With this same focus, several studies have been performed in the biomedical areas seeking to improve the diagnostic techniques and proposing innovative treatments, alleviating and prolonging the patients' lives (LANGER; PEPPAS, 2003).

Cancer has more than 277 variations and can be defined as a set of diseases characterized by mutations that imply significant disorders in cell growth, invading distant healthy tissues and organs. According to the World Health Organization (WHO), the disease is the second most cause of death globally, reaching in the year 2020 approximately 10 million people (HASSANPOUR, DEHGHANI; 2017). Once diagnosed, cancer can be treated through different chemotherapy approaches, radiation therapy, surgery, and through the combination of these treatments, depending mainly on the tumors' location and the stage of the disease. Nevertheless, chemotherapy and radiotherapy still promote numerous side effects to healthy tissues (INCA, 2019; WANG; ZHANG, 2017).

In particular, chemotherapy refers to using chemical substances to kill tumor cells, further preventing their spread (INCA, 2019). However, despite being efficient in killing cancer cells, conventional treatment has low selectivity, making these drugs toxic to normal tissues (VIEIRA; GAMARRA, 2015). In addition, many antitumor drugs are hydrophobic, a factor that hinders their solubilization and permanence in the bloodstream, reducing their stability, which facilitates their degradation in the body and hinders their transport through different biological barriers (KUDARHA; SAWANT, 2017).

As an example of a chemotherapy drug, we can mention *Cisplatin* (cis-Diaminedichloroplatinum) (Figure 1.1), an antineoplastic agent that had its anticancer properties accidentally discovered by Barnett Rosenberg in 1970, making it known for its high antitumor power for children and adults, mainly for the treatment of testicular and ovarian cancer (DASARI; TCHOUNWOU, 2014). It is a potent platinum-based compound that reacts with DNA causing cell death. Unfortunately, several side effects were associated with cisplatin usage, in which gastrointestinal toxicity, renal

dysfunction, hepatotoxicity, neurotoxicity, nephrotoxicity can be highlighted (KELLAND, 2007).

From the high toxicity of cisplatin, many studies were developed to find similar drugs with a lower level of toxicity, which would maintain antitumor activity. In this sense, the strategy of using delivery vehicles capable of directing the cytotoxic agent to the tumor stands out. Pharmaceutical preparations with this same approach are already clinically validated, in which liposomal formulations containing Doxorubicin (Doxil, Ortho Biotech Products) and paclitaxel linked to albumin (Abraxane, Abraxis BioScience) can be cited (GORDON *et al.*, 2004; GRADISHAR *et al*., 2005; KELLAND, 2007).

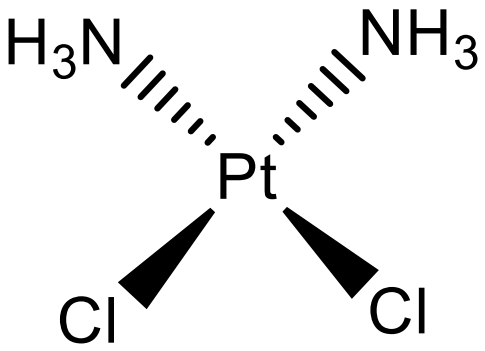

Figure 1.1: Representation of Cisplatin structure.

Drug delivery systems have shown the capacity of improving the safety and efficiency of drugs, allowing new therapeutic approaches. Currently, many studies have been performed, focused on developing increasingly selective and safe systems capable for complex drugs that are difficult to administer by conventional means. The main objective of these studies is to surpass the therapeutic inconveniences presented by drugs in their free form, which are: to minimize the toxicity of drugs, avoid degradation, maintain therapeutic concentration, and even selectivity in action (LANGER, 1990; LAVAN; GUIRE; LANGER, 2003)

It is desirable for this type of application that the system has a morphology capable of containing and protecting the drug. In addition, it allows high incorporation rates, relevant cytotoxic profile, low immunogenicity, accumulating preferably in the target tissues (QIN et al., 2016). Furthermore, the differences between ill and healthy sites, such as temperature and pH, allow designing systems that behave differently at

each location, decreasing the drug's affinity with healthy cells and facilitating interaction with the target cells (SRINIVASARAO; LOW, 2017).

Advances in materials science, chemistry, and bioengineering have paved the way for the development of responsive micro and nanoparticles, capable of undergoing modifications from stimuli such as pH, temperature, enzymes, light, and magnetic field, revolutionizing the way of transport and delivery of drugs (HU; CHEN; GU, 2018). These characteristics may enable the achievement of thermal and pH-sensitive nanostructured drug delivery systems activated in an endogenous and or exogenous manner (VIEIRA; GAMARRA, 2016). Another great advantage of this type of material is the possibility of associating therapy and simultaneous diagnosis (QIN et al., 2017).

In this application area, polymeric materials stand out as an important material class due to their great versatility of properties such as biocompatibility and biodegradability. The currently available diversity of monomers and polymerization techniques allows for obtaining monodisperse polymer chains with moldable properties, such as hydrophilicity and hydrophobicity, biodegradability, or even obtaining multifunctional and innovative structures (LANGER; PEPPAS, 2003).

This work propose is developing a new hybrid protein-polymer material based on BSA and the PNVCL-co-PDMAEMA copolymer loaded with cisplatin drug, obtained by the grafting-from methodology. Conjugating these materials make it possible to combine the biocompatibility and transport properties inherent of the albumin with the responsive behavior of the polymers used, enabling the achievement of an intelligent drug delivery system capable of minimizing the side effects caused by this potent drug.

2. Objective

This work aims to produce innovative thermal and pH-sensitive hybrid protein-polymer nanoparticles based on Bovine Serum Albumin and the copolymer PNVCL-PDMAEMA loaded with Cisplatin as a potential system against cancer. The set of specific objectives can be given by:

- Development of a viable BSA-Macroinitiator synthesis route;
- Study and develop an NVCL-DMAEMA polymerization process over the macro initiate species based on the ATRP technique;
- Characterize the physicochemical and morphological profile of all obtained materials;
- Develop an HPLC-DAD method for cisplatin quantification;
- Evaluate the cisplatin encapsulation rate.

3. Theoretical framework

During hybrid materials development it is essential to know their properties and limitations to determine the most appropriate techniques and guarantee the efficiency and reproducibility of their synthesis, seeking to achieve the desired properties. In order to elucidate the scenario and foundation of this study, a panorama of the Bovine Serum Albumin's central concepts, the polymers PDMAEMA and PNVCL, hybrids materials, protein-polymer conjugates, and controlled polymerization technique with emphasis on Atom Transfer Radical Polymerization technique (ATRP) will be presented.

3.1. Bovine Serum Albumin (BSA)

Albumin, the most abundant protein in the blood, is a natural biomacromolecule responsible for several essential functions for the human bodys' functioning, behaving as a deposit and transport for various compounds (JAHANBAN-ESFAHLAN et al., 2019; EVANS, 2002). In addition, this protein tends to bind a vast diversity of molecules, is responsible for transporting nutrients to cells (KHONDER et al., 2016).

Available with high purity and reduced cost, Bovine Serum Albumin (BSA) is a natural protein, highly water-soluble with an isoelectric point of 4.7 in water, at 25 °C (WANG; ZHANG, 2016). This protein has a chemical structure very similar to Human Serum Albumin (HSA). It is biocompatible, biodegradable, non-toxic, and non-immunogenic, making it widely used in the pharmaceutical industry (LI et al., 2017; ZHANG et al., 2018).

BSA is a protein with a molecular weight of approximately 66.8 KDa, with an acidic hydrophilic characteristic that maintains its native state in the pH range from 4 to 9 and can be heated at 60 °C for up to 10 hours without any deleterious effects. This protein comprises a single polypeptide chain consisting of 583 amino acid residues, organized in a secondary structure constituted by α-helical and β-sheets, forming three homologous domains in its tertiary structure, which is stabilized with 35 cysteine residues that form a total of 17 disulfide bonds (JAHANBAN-ESFAHLAN et al., 2019; WANG; ZHANG, 2016).

Biocompatibility, ease of preparation, and abundance of functional groups able to be covalently modified have stimulated the use of BSA in drug delivery, especially in the treatment of cancer. The diversity of functional sites in its structure, besides its compatibility with different types of drug, makes possible its modification and functionalization with different types of molecules (SALEHIABAR, 2018; WANG; ZHANG, 2016). On the other hand, low stability, enzymatic degradation, and the tendency to denaturation are factors that still limit its biomedical applications. In this sense, several strategies have been proposed to solve this issue. The conjugation of these proteins with synthetic polymers has presented very encouraging results (HE; LU; ZHAO, 2015).

3.2. Smart Polymers

Polymers, natural or synthetic, are defined as macromolecules formed by the repetition of equal units. These materials have various properties, which in the case of synthetic polymers, can be engineered. Furthermore, some polymers can reversibly respond to tiggers in the surrounding environment, they are called intelligent polymers. These external stimuli can be temperature, pH, ionic strength, electric and or magnetic fields, light, and radiation (KUMAR et al., 2007; TEBALDI et al., 2017). They affect the energy level, consecutively altering the intermolecular forces, changing shape, surface characteristics, solubility, and others (KUMAR et al., 2007). Due to its unusual behavior, these polymeric materials are desirable for application in biomedical areas, especially the thermal and pH-responsive ones (GALAEV; MATTIASSON, 1999). Two examples of polymers that exhibit this behavior are poly (N-vinyl caprolactam) (PNVCL) and poly (2-dimethylamino-ethyl methacrylate) (PDMAEMA), represented in Figure 3.2, with PNVCL being only thermally-responsive and PDMAEMA dual responsive (thermal and pH).

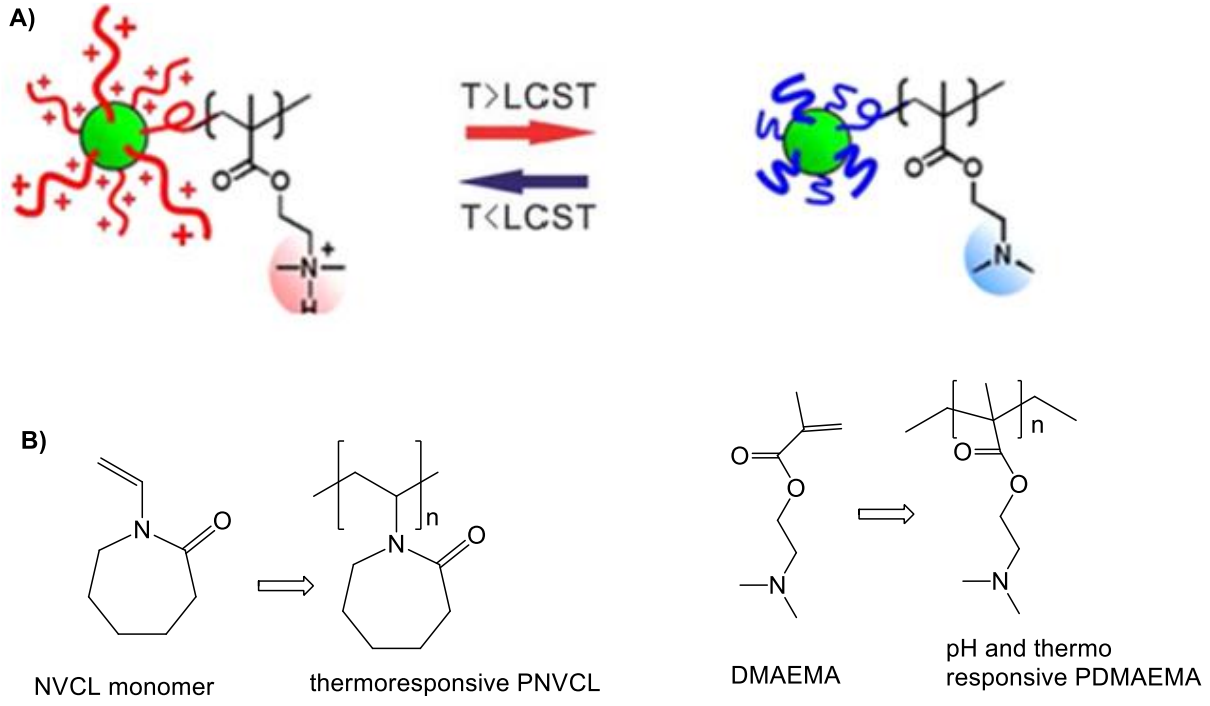

Figure 3.1: Representation of a stimulus-responsive polymer behavior for PDMAEMA (A) and the structures of NVCL and DMAEMA monomers and their respective polymers (B). Adapted from Precupas, Sandu, Popa (2016).

Thermoresponsive polymers have amphiphilic characteristics and an LCST behavior in which the phase change occurs by passing a specific temperature. These polymers are soluble in water at temperatures below LCST and become insoluble at higher temperatures due to variations in hydrophilic and hydrophobic interactions. These variations occur when the enthalpy of hydrogen bonds between the polymer and water becomes smaller than the entropic gain of the system in general, making the interactions between the polymer itself more favorable than the polymer-water interactions (KUMAR et al., 2007; ZHELAVSKYI; KYRYCHENKO, 2019).

On the other hand, in typical pH-responsive polymers, the protonation and deprotonation events can occur, generating new formal charges over the molecules. These events usually happen in amino and carboxylic groups that are strongly pH-dependent. This type of transition tends to be very noticeable and usually occurs in a range of 0.2-0.3 pH unit, causing the structure to collapse, and consequently, the polymer becomes insoluble (KUMAR et al., 2007; TEBALDI *et al*., 2019).

PDMAEMA is a cationic polymer that has attracted attention from several research groups due to its dual-responsive behavior. This polymer is capable of

undergoing structural transition below its pKa value (~ 7.4) in its phase transition temperature (LCST) around 45 ºC (MANOURAS, 2017), which values can vary according to the molar mass and also by inserting hydrophobic or hydrophilic comonomers, allowing the modeling of this phase transition (TEBALDI *et al*., 2014).

PNVCL is another polymer that has attracted the attention of researchers worldwide, mainly for biomedical applications. PNVCL is an unconjugated monomer and obtained by the polymerization of N-vinyl caprolactam (NVCL). The high reactivity of the radical species derived from the NVCL monomer makes radical polymerization a challenge. The control of its polymerization has proven difficult, however, several studies have been carried out for the development of efficient NVCL polymerization techniques (JIANG *et al.* 2013, MOHAMMED *et al., 2018;* YANG *et al.* 2015). PNVCL is a thermally-responsive, non-toxic, biocompatible feature and has stood out because it does not generate toxic groups when hydrolyzed (SHAO *et al*., 2012). In addition, this polymer typically presents an LCST behavior in the range of 32 ºC, a temperature that can be adjusted to higher values by adding hydrophilic comonomers (TEBALDI *et al*., 2014).

3.3. Hybrids materials

According to the International Union of Pure and Applied Chemistry (IUPAC), hybrid materials result from the intimate mixture of organic and or inorganic components in which interpenetration occurs on a scale smaller than 1 µm (ALEMÁN *et al*. 2007). In other words, the hybrids are formed by the union of two or more different components where at least one has a size between 1 and 1000 nm linked by specific interactions, which guarantees a synergistic improvement of properties overcoming limitations of the original materials (MA, 2019; SOARES et al., 2020; UNTERLASS, 2016).

These systems can be formed by the combination of inorganic-organic materials such as carbon nanotube, metal oxide nanoparticles, or other inorganic surfaces together with organic polymers, and also organic-organic, linking organic compounds such as proteins or lipids to natural or synthetic polymers (MA, 2019; SOARES *et al*., 2020; ANANIKOV, 2019). Unlike composite materials, hybrids are more than just a physical mixture of components and a simple sum of their properties. As a result, this

class of materials can possess properties different from those presented by its starting materials (GU *et al*. 2018).

The unique properties of hybrid materials are directly related to the interface between components and the types of interactions in that region. According to the interaction that predominates, hybrid materials can be classified into two groups, as shown in Figure 3.3. Class I - That corresponds to hybrids formed from by non-covalent interactions such as hydrogen, van der Waals, or electrostatic interactions; in other words, they are created by encapsulation. Class II - Hybrids formed from chemical bonds between components achieved with grafting methods (UNTERLASS, 2016; FAUSTINI *et al.*, 2018).

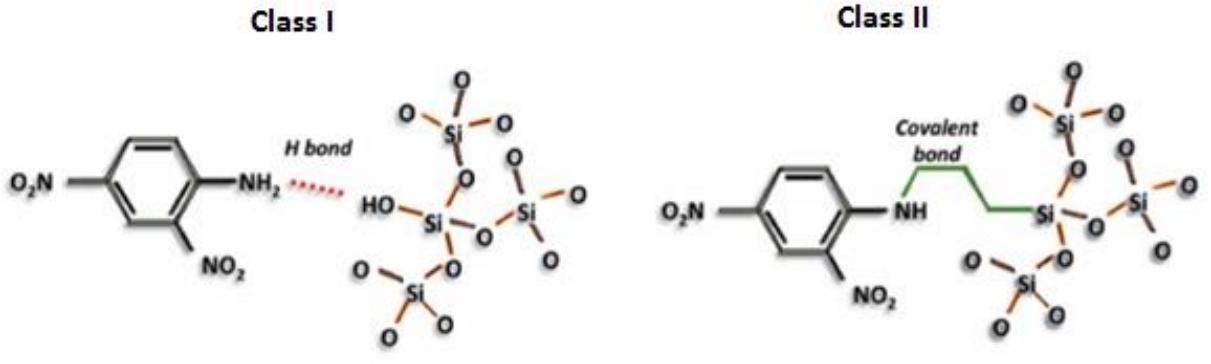

Figure 3.2: Classification of hybrid materials adapted from Faustini *et al*. (2018).

3.4. Protein-polymer conjugates

The first report of the synthetic binding polymer to a protein occurred in the 70s, when polyethylene glycol (PEG) was linked to protein, improving the circulation time considerably and reducing the immunogenic responses compared to the native protein. These improvements presented by the new material drove the development of numerous studies in this area, resulting in 17 different PEGylated protein formulations approved by the FDA (United States Food and Drug Administration) (KAUPBAYEVA; RUSSELL, 2019).

Since the appearance of the first PEGylated material until today, the insertion of synthetic polymers to proteins has made it possible to obtain new systems with significant improvement concerning the pharmacokinetics of these proteins, making this type of material a desirable option for biomedical applications, inspiring new studies for the development of innovative conjugation methodologies, using other polymers. (HUSSAIN et al., 2019; PFISTER; MORBIDELLI, 2014; RYAN et al., 2008; VERONESE; MERO, 2008).

Currently, protein-polymer bioconjugates are commonly synthesized by the *grafting-from* and *grafting-to* methods, as displayed in Figure 3.4. The *grafting-to* approach consists of linking pre-synthesized polymer chains directly to the protein, promoting a low graft density since it involves the connection of two macromolecules. On the other hand, in the *grafting-from* method, first small-molecules (initiators or chain transfer agent (CTA) are linked to the protein, and after that the polymer chains grow from the modified protein (GARCIA; LAVIGNAC, 2016; CARMALI, 2018 and Ji; LU; ZHAO, 2017).

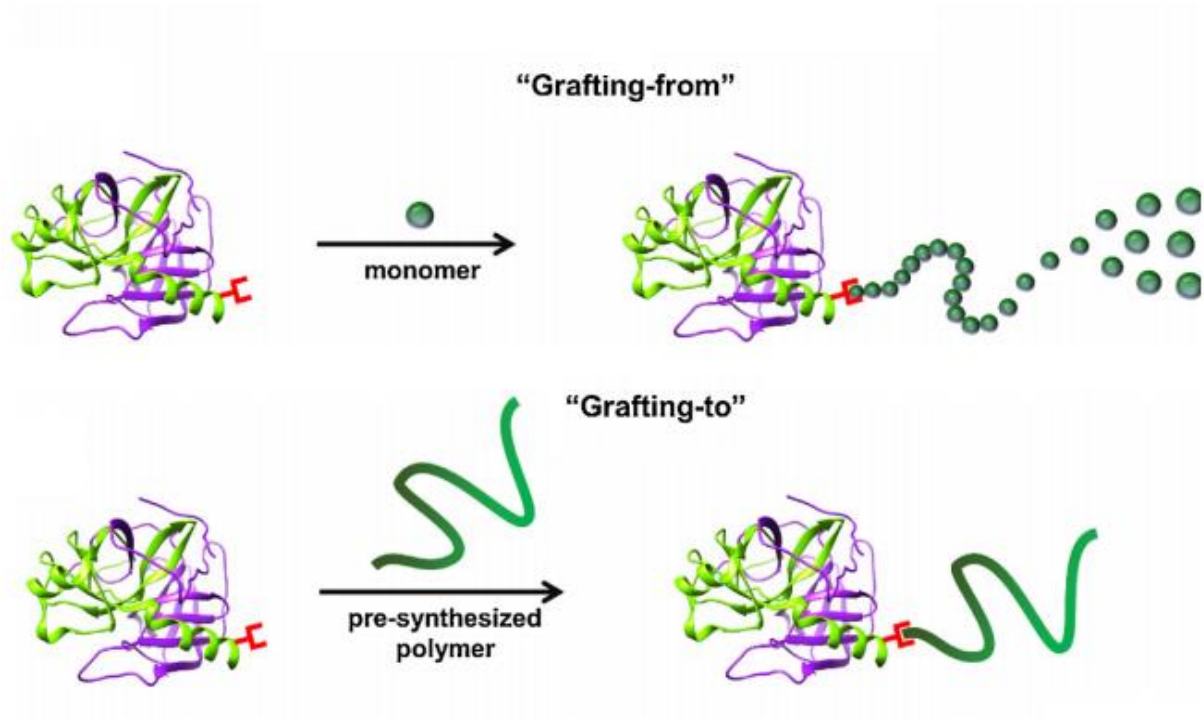

Figure 3.3: Schematic representation of the *grafting-to* and *grafting-from* method adapted from Kaupbayeva and Russell (2019).

The amino acid residues present in proteins are essential conjugation sites as they can react in different ways with side-chain−initiator/polymer. The reactions of such

groups can be influenced by different factors such as the side-chain pKa, exposed surface area, polarity, and hydrophobicity, which causes some groups to react quickly and others not. Therefore, it is essential to understand the protein structure to make it possible to choose the reactive target site (CARMALI, 2018; JI; LU; ZHAO, 2017).

The success of protein graft reactions is mainly due to cysteine and lysine, frequently used as targeted modification sites. Lysine residues are usually present in large amounts in the proteins and are functional groups capable of being modified. In addition, studies are under development aiming at new conjugation strategies with molecules such as acid halides, N-hydroxysuccinimide (NHS- ester), as available in Figure 3.5. In this reaction, the amino group acts as a nucleophile, attacks the carbonyl group (electron-deficient), leading to the displacement of the NHS group and, consequently, the covalent bonding of the initiator to the protein (MESSINA *et al*. 2020; CARMALI, 2017; CARMALI, 2018).

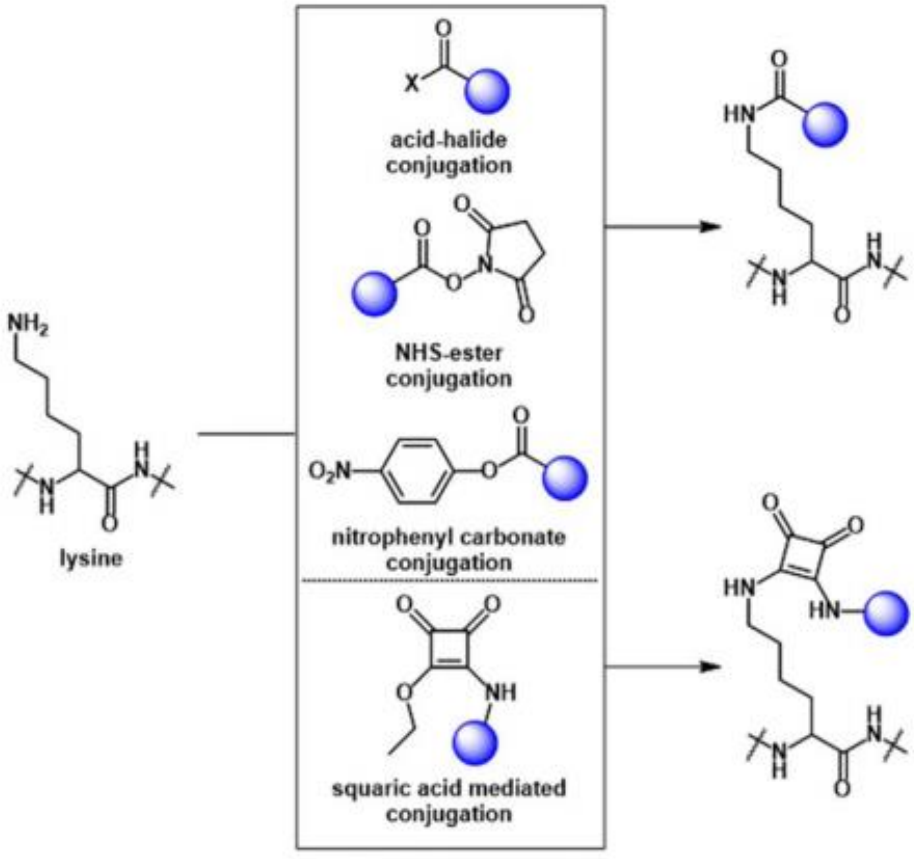

Figure 3.4: Commonly lysine modification for *grafting-from.* Adapted from Messina *et al.* (2020).

3.5. Controlled radical polymerization

Despite the advantages achieved by PEGylation, many studies have determined limitations such as hypersensitivity, immune response, and accumulation in tissue, stimulating the search for other polymers capable of replacing PEG. The need to synthesize macromolecules with controlled sequences and configurations has led to improved polymerization techniques (KAUPBAYEVA; RUSSELL, 2019).

Controlled polymerization techniques, also known as Reversible Deactivation Radical Polymerization (RDRP), such as the Atom Transfer Radical Polymerization (ATRP) and Reversible Addition-Fragmentation Chain-Transfer polymerization (RAFT), allow obtaining polymers with well-defined composition, low molar mass distribution, complex architectures, and with the insertion of functional interest groups, allowing the development of water-soluble, non-toxic, biodegradable and easily eliminated polymers from the body (VANPARIJS et al., 2010; SOARES *et al.* 2020).

In the ATRP mechanism, represented schematically in Figure 3.6, the propagation stage of polymerization occurs through reversible redox reactions between a halogen specie present in the ATRP initiators' structure, usually chlorine (Cl) or bromine (Br), and a transition metal complex. In this process, the halogen atom is transferred to the transition metal complex, forming the propagation radical. Reversibly, the metal can deactivate radical species, moving the halogen back to the end of the propagation chain. These reversible reactions are responsible for maintaining a small number of radicals in the solution, avoiding unwanted terminations (MESSINA *et al.*, 2019; KAUPBAYEVA; RUSSELL, 2019).

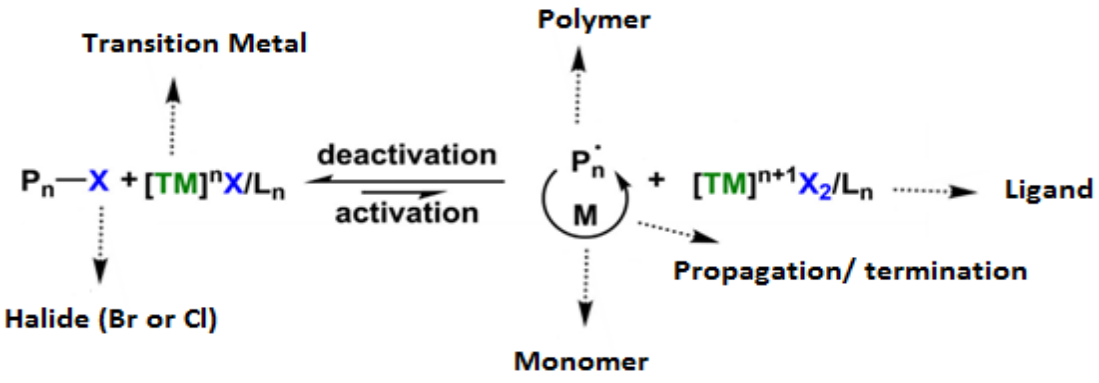

Figure 3.5: Mechanism of the traditional ATRP process. Adapted from MESSINA *et al*. (2019).

4. Methodology

4.1. Materials

Copper(I) chloride (CuCl, Aldrich, ≥99%) and Copper(I) bromide (CuBr, Aldrich 98%) were purified by stirring in glacial acetic acid (2 × 8 h), washed first with ethanol, then with diethyl ether, and finally dried under reduced pressure; 2-Dimethylaminoethyl methacrylate (DMAEMA, Sigma-Aldrich, 98%) was passed through a column with aluminum oxide to remove inhibitors; N-Vinylcaprolactam (NVCL, Sigma-Aldrich, 98%) was recrystallized from *n*-hexane; 1,4-dioxane (Chemsolute, ≥99%) was distilled before use; BSA (Sigma-Aldrich, ≥99%) was diluted in PBS pH 7.4 and used without further purification. The following materials were used as received: 2-bromo-2-methylpropionyl bromide (98%, ACROS Organics™), dichloromethane (Sigma-Aldrich, ≥99%), β-alanine (Sigma-Aldrich, ≥99%), sodium hydrogen carbonate (carlroth, ≥99%), hydrochloric acid (HCl, Sigma-Aldrich, 37%), ethyl acetate (Chemsolute, ≥99%), Magnesium sulfate ($MgSO_4$, carlroth, ≥99%), n-hexane (Sigma-Aldrich, ≥99%), N, N′-diisopropylcarbodiimide (Sigma-Aldrich, ≥99%), N-hydroxysuccinimide (Sigma-Aldrich, 98%), 2-propanol (Chemsolute, ≥99%), Deuterated chloroform ($CDCl_3$, Sigma-Aldrich, ≥99%), 2-chloropropionyl chloride (Alfa Aesar™, 96 %), diethyl ether (Chemsolute, ≥99%), Ethyl-2-chloropropionate (Alfa Aesar, 97%), Tris [2- (dimethylamino) ethyl] amine (Me_6TREN, Alfa Aesar, 98%), 5,5,7,12,12,14-hexamethyl-1,4,8,11- tetraazacyclotetradecane (Me_6Cyclam, Sigma-Aldrich, ≥99%) were used as received without further purification. Cisplatin was acquired from Bergamo Pharmaceutical Chemical Laboratory (Taboão da Serra, Brazil).

4.2. Synthesis of ATRP initiators

In order to obtain macro initiators from proteins, it is necessary to improve the reactions in water since the reaction with proteins needs to be done in an aqueous medium. In this sense, two ATRP initiators were synthesized, focused on good solubility in aqueous media and capable of polymerizing NVCL and DMAEMA monomers. Based on the literature, we chose to synthesize N-2-Bromo-2-

methylpropanoyl-β-alanine N′-oxysuccinimide ester (NHS-BIBA) and N-2-Chloropropionyl-β-alanine as described below.

4.2.1. N-2-Bromo-2-methylpropanoyl-β-alanine-N′-oxysuccinimide ester (NHS-BIBA)

N-2-Bromo-2-methylpropanoyl-β-alanine N′-oxysuccinimide ester was synthesized following the previously described procedure by Murata *et al*. (2013), and the steps are summarized in Figure 4.1. Briefly, 2-bromo-2-methylpropionyl bromide (6.2 mL, 50 mmol) and dichloromethane (25 mL) were mixed and slowly added into the solution of β-alanine (4.45 g, 50 mmol) and sodium hydrogen carbonate (10, 5 g, 125 mmol) in deionized water (100 mL) at 0 °C. The obtained mixture was stirred at room temperature for 2 h. The aqueous phase was treated with dichloromethane (100 mL × 3), aiming to remove eventual impurities. Then, the pH was adjusted to 2 with HCl (solution 1.0 mol/L) at 0 °C. The product was extracted with ethyl acetate (6 x 100 mL). The organic phase was dried with $MgSO_4$, filtered, and the solvent removed by a rotary evaporator. N-2-Bromo-methylpropionyl-β-alanine was isolated by recrystallization from a mixture of diethyl ether and *n*-hexane (1/9 volume ratio).

N,N′-diisopropyl carbodiimide (1.6 g, 9.13 mmol) was slowly added to the solution of N-2-bromo-2-methylpropionyl-β-alanine (2.0 g, 8.3 mmol), and N-hydroxysuccinimide (1.03 g, 9.13 mmol) in dichloromethane (100 mL) at 0 °C. The mixture was stirred at room temperature for 4 h. After filtering out the precipitated urea, the solvents were removed by a rotary evaporator. N-2-Bromo-2-methylpropionyl-β-alanine. N′-oxysuccinimide ester was purified by recrystallization using 2-propanol alcohol. The chemical structure was confirmed by ^1H NMR using $CDCl_3$ as a solvent.

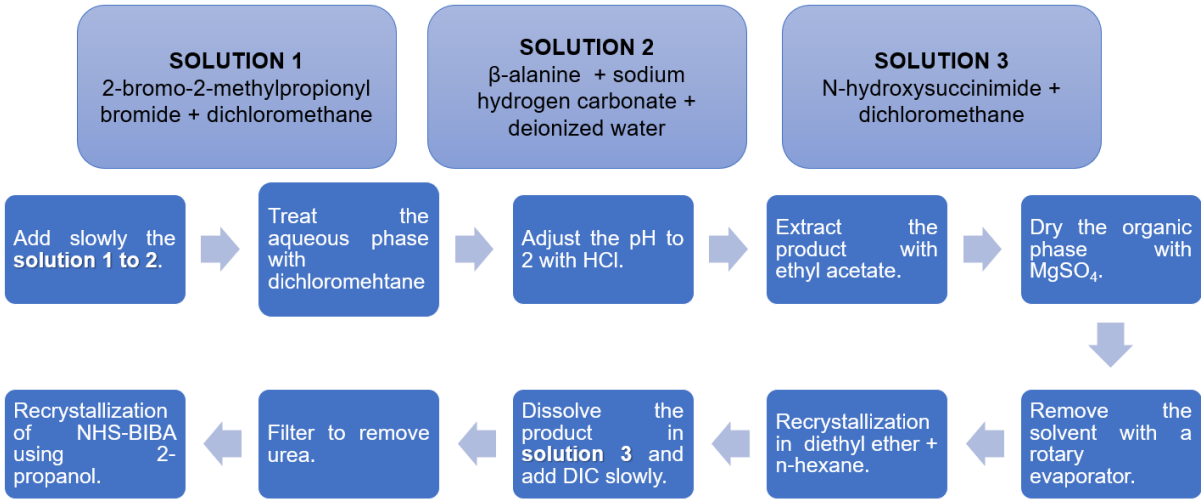

Figure 4.1: Schematic representation of the steps to obtain N-2-Bromo-2-methylpropionyl-β-alanine N′-oxysuccinimide ester

4.2.2. N-2-Chloropropionyl-β-alanine

N-2-Chloropropionyl-β-alanine was synthesized by the following procedure, previously described by Cummings *et al.* (2014). A solution of 2-chloropropionyl chloride (9.7 mL, 100 mmol) in 1,4-dioxane (50 mL) was slowly added into a solution of ß-alanine (8.9 g, 100 mmol) and sodium hydrogen carbonate (21 g, 250 mmol) in 200 mL of a mixture of deionized water and 1,4-dioxane (1:1 volume ratio) at 0 °C. The mixture was stirred at room temperature for 2 hours. The water phase was treated with diethyl ether (3 x 100 mL), and then the pH of the aqueous phase was adjusted to 2 using HCl solution (5%) at 0 °C. The product was extracted with ethyl acetate (6 x 150 mL). The organic phase was dried with sodium sulfate, and a rotary evaporator was used to remove the solvent. N-2-chloropropionyl-ß-alanine (N-ALA) was isolated by recrystallization from a mixture of diethyl ether and n-hexane (1:1 volume ratio). The chemical structure was confirmed by ^{1}H NMR using $CDCl_3$ as a solvent. The steps are summarized in Figure 4.2.

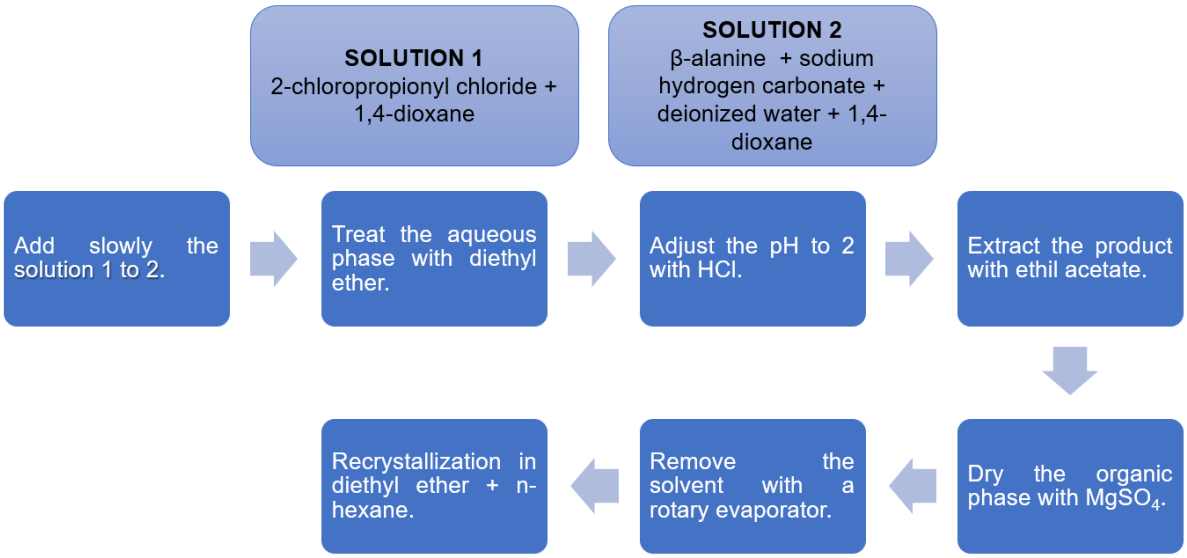

Figure 4.2: Schematic representation of the steps to obtain the N-2-Chloropropionyl-β-alanine specie.

4.3. Polymerization study

The ATRP initiators were tested in homo- and copolymerization using NVCL and DMAEMA monomers to obtain the best polymerization conditions and acquire the desired copolymer. In this stage, the initiators tested were: Ethyl-2-chloropropionate (ECP) and the produced BIBA and N-ALA. For N-ALA, two different ligands were evaluated, Me_6TREN and Me_6Cyclam. For the other initiators (BIBA and ECP), only the Me_6TREN was used. All tested formulations are summarized in Table 1 and the experiments are described below.

Table 4.1: Tested conditions for the study of polymerizations.

EXPERIMENT	MONOMER	INITIATOR	CATALYST	LIGAND	SOLVENT	T °/ TIME
1.3.1 Homopolymerization	NVCL (411.7 mg, 2.9 mmol, 200 eq.),	ECP (2.02 mg, 14.8 µmol, 1 eq.),	CuCl (1.5 mg, 14.8 µmol, 1 eq.)	Me_6TREN (3.95 µL, 14.8 µmol, 1 eq.)	1,4-dioxane (1 mL)	25 °C/ 6 h
1.3.1 Copolymerization	DMAEMA (232.5 mg,14.8 mmol, 100 eq.) NVCL (205.9 mg, 14.8 mmol, 100 eq.)	ECP (2.02 mg, 14.8 µmol, 1 eq.),	CuCl (1.5 mg, 14.8 µmol, 1 eq.)	Me_6TREN (3.95 µL, 14.8 µmol, 1 eq.)	1,4-dioxane (1 mL)	25 °C/ 6 h
1.3.2 Homopolymerization	NVCL (633 mg, 4.5 mmol, 380 eq.)	BIBA (2 mg, 11,98 µmol)	CuBr (12 mg, 83.9 µmol, 7 eq.)	Me_6TREN (32 µL, 119.8 µmol, 10 eq.)	1,4-dioxane (25 mL)	80 °C/ 24 h
1.3.2 Copolymerization	DMAEMA (357.7 mg, 2.25 mmol, 190 eq.) NVCL (316.7 mg, 2.25 mmol, 190 eq.)	BIBA (2 mg, 11,98 µmol),	CuBr CuBr (12 mg, 83.9 µmol, 7 eq.)	Me_6TREN (32 µL, 119.8 µmol, 10 eq.),	PBS (25 mL)	25 °C/ 24 h
1.3.3 Homopolymerization	NVCL (465 mg, 3.3 mmol, 200 eq.)	N-ALA (3 mg, 16.7 µmol, 1 eq.)	CuCl (1.7 mg, 16.7 µmol, 1 eq.)	Me_6Cyclan (3.3 mg, 16.7 µmol, 1 eq.)	1,4-dioxane (0.93 mL)	25 °C/ 6 h
1.3.3 Copolymerization	DMAEMA (262.6 mg, 1.7 mmol, 100 eq.) NVCL (232.5 mg, 1.7 mmol, 100 eq.)	N-ALA (3 mg, 16.7 µmol, 1 eq.)	CuCl (1.7 mg, 16.7 µmol, 1 eq.)	Me_6Cyclan (3.3 mg, 16.7 µmol, 1 eq.)	1,4-dioxane (0.93 mL)	25 °C/ 6 h
1.3.4 Homopolymerization	NVCL (465 mg, 3.3 mmol, 200 eq.)	N-ALA (3 mg, 16.7 µmol, 1 eq.)	CuCl (1.7 mg, 16.7 µmol, 1 eq.)	Me_6TREN (4.46 µL, 16.7 µmol, 1 eq.),	1,4-dioxane (0.92 mL).	25 °C/ 6 h
1.3.4 Copolymerization	DMAEMA (262.6 mg, 1.7 mmol, 100 eq.) NVCL (232.5 mg, 1.7 mmol, 100 eq.)	N-ALA (3 mg, 16.7 µmol, 1 eq.)	CuCl (1.7 mg, 16.7 µmol, 1 eq.)	Me_6TREN (4.46 µL, 16.7 µmol, 1 eq.),	1,4-dioxane (0.92 mL).	25 °C/ 6 h

The reactions were performed as described below, following the conditions described in the table 4.1. A round-bottom flask A was loaded with the catalyst and deoxygenated by N_2 bubbling for 30 minutes. Another round-bottom flask B was loaded with the ATRP initiator, the ligand, solvent, and the monomers, and the flasks were *deoxygenated* using three freeze-pump-thaw cycles (except for the experiments 1.3.2, which were deoxygenated by bubbling N_2 for 30 minutes). After deoxygenation, the

solution into the flasks B was transferred to the flasks using a transfer needle. According to the time and temperature described previously, polymerizations were carried out and stopped by bubbling oxygen into the samples. Figure 4.3 illustrates the expected reaction for homopolymerization and copolymerization and the polymerization steps.

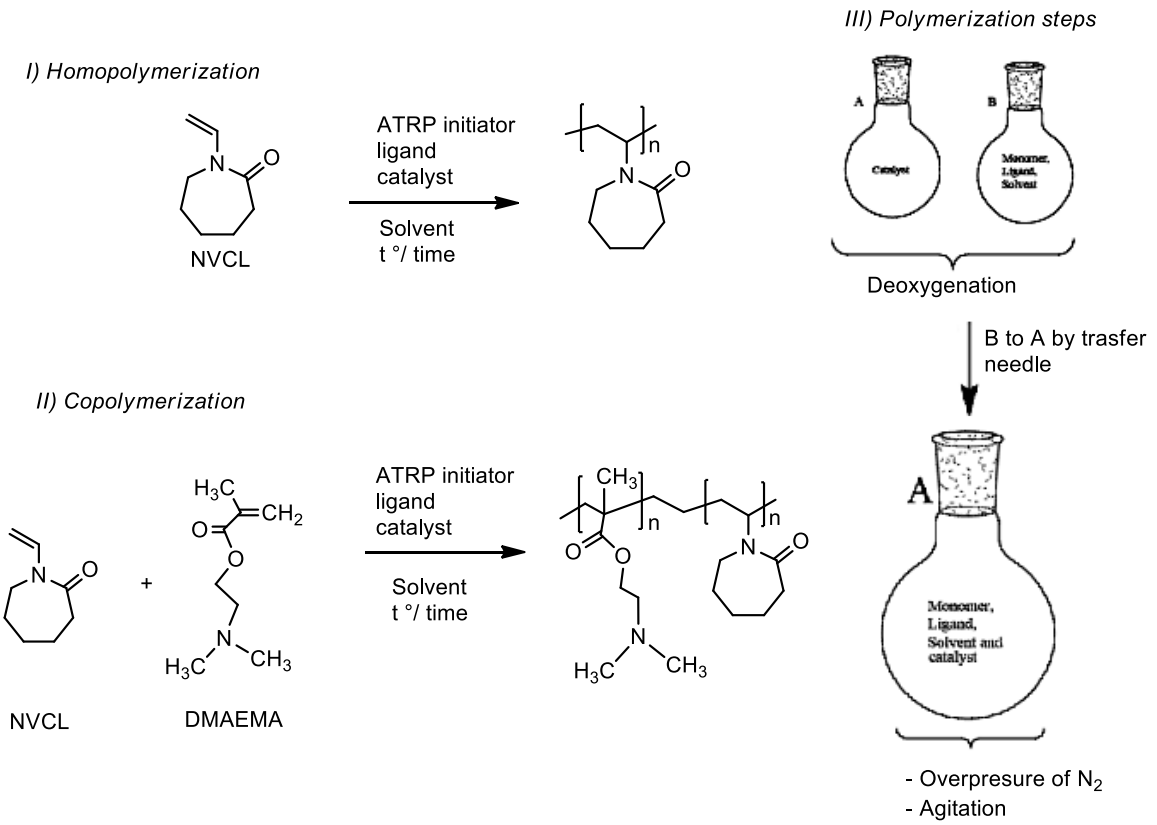

Figure 4.3: ATRP PNVCL homopolymerization (I), PNVCL-*co*-PDMAEMA copolymerization (II) and the Polymerization steps (III).

4.4. Kinetics studies for ATRP polymerization using BIBA as initiator

The kinetics studies were conducted to evaluate how fast the conversion of the monomers occurred. In this study, BIBA was used as an initiator to clarify the monomer's peaks on ^{1}H-NMR without BSA signal interference. At this stage, the study was carried out for both the desired copolymer and the homopolymer PDMAEMA. The homopolymer PDMAEMA was chosen to guarantee a sufficient polymerization condition since DMAEMA polymerizes more easily than NVCL. PDMAEMA and PNVCL-*co*-PDMAEMA) were prepared using PBS buffer pH 7.4 (25 mL), BIBA (2 mg, 11,98 µmol) Me_6TREN (32 µL, 119.8 µmol, 10 eq.) and CuBr (12 mg, 83.9 µmol, 7

eq.). For the PDMAEMA synthesis, was used a solution of DMAEMA (715 mg, 4.5 mmol, 380 eq.), while for copolymer was used the solutions of DMAEMA (358 mg, 2.3 mmol, 190 eq.) and NVCL monomers (317 mg, 2.3 mmol, 190 eq.). For these experiments, two different flasks were loaded with BIBA, Me_6TREN, PBS buffer, and the solutions of the cited monomers. In a round-bottom flask, was added only DMAEMA (Flask M1). In another round-bottom flask was added DMAEMA and NVCL (flask M2). Two other similar flasks (Flasks C1 and C2) were loaded with CuBr, and all flasks (M1, M2, C1, and C2) were bubbled with N_2 for 30 min. The polymerizations were initiated by transferring the flask M1 to C1 and M2 to C2 in one shot. The reactions were kept under stirring in an ice bath. Samples were taken in 10, 60, 120, and 240 minutes stopped by bubbling air into the sample, lyophilized, and analyzed by ^{1}H-NMR. The conditions used in the ^{1}H-NMR analyzes are mentioned in section 5.2.

The degree of conversion was calculated considering only the monomer DMAEMA, using the Equation 4.1, where *j* corresponds to the integral of polymer signal and *i* to the monomer. *J* was divided by two in this equation because this signal corresponds to two protons from a CH_2 group. From this monomer/polymer, it is possible to identify well-defined peaks, avoiding possible overlapped with other reagents present in the reactional system. This fact allows an integral with better precision and simplification of the calculations, which is impossible for the NVCL / PNVCL set.

$$\%\ of\ conversion = \frac{\frac{j}{2}}{\frac{j}{2}+i} \qquad (4.1)$$

4.5. Synthesis of BSA macroinitiator (BSA-MI)

Initially, different synthesis conditions were tested for the BSA-MI preparation in which different reagents concentrations, reaction time, and temperature were considered. The best route was chosen and is described as follows (schematically represented in the Figure 4.4 A).

First, 100 mg of BSA (1.5 µmol) was dissolved in 50 mL of PBS buffer (pH 7.4) in a round-bottom flask. Next, was added 50 mL of a solution of sodium bicarbonate (0.2 mol/L) and the pH of the medium was adjusted to around 9.0 using NaOH (1 mol/L) to ensure the non-protonation of the BSA amino groups. Sequentially, 75 mg

(223 µmol) of NHS-BIBA was added, yielding a turbid solution. The solution was kept in a refrigerator, under overnight stirring.

Finally, the crude product was purified by dialysis with a 12.4 kDa Molecular Weight Cut Off (MWCO) dialysis membrane against PBS buffer at pH 7.4 into the refrigerator for additional 72 hours. MALDI-Tof and SDS-PAGE were used to characterize the macroinitiator.

4.6. Synthesis of BSA-PNVCL-co-PDMAEMA hybrid nanoparticles

A total of three different synthesis routes have been carried out, aiming to optimize the protein-polymer conjugate production, mainly to obtain a material with a transition temperature around 40 °C. In this stage, different reaction times, the proportion between monomers, and even preparing the reaction were tested.

4.6.1. BSA-PNVCL-co-PDMAEMA (Route 1)

The first experiment was carried out mainly to test the viability of the studied system. In this assay, the system was kept for 48 hours to guarantee the end of the polymerization reaction. The used methodology is described as follows. In a round bottom flask was added BSA-MI (2 mL of BSA-MI in PBS buffer solution pH 7.4 concentration 10 mg/mL content, 9.6 µmol expected reactive moieties), water ultrapure (1.5 mL), NVCL (470 mg, 3.38 mmol, 350 eq.), DMAEMA (530 mg, 3.38 mmol, 350 eq.) and bipyridine (4.9 mg, 30.8 µmol, 3 eq.). Then the flask was deoxygenated by Argon (Ar) bubbling for 30 minutes. After, were added CuBr (6.7 mg, 46.6 µmol, 5 eq.) and sodium ascorbate (2 mg, 10.1 µmol, 1 eq.) previously dissolved in water ultrapure (0.4 mL). The reaction mixture was performed at room temperature for 48 hours and stopped by bubbling air into the sample. The obtained product was purified by dialysis with a 12.4 kDa MWCO membrane using PBS buffer at pH 7.4 for 72 hours. The final material was analyzed by the FTIR and DLS techniques.

4.6.2. BSA-PNVCL$_{0.5}$-co-PDMAEMA$_{0.5}$ (Route 2)

In the second route, CuBr (5.4 mg, 37.4 µmol, 7 eq.) and Me_6TREN (14.3 µL, 53.5 mmol, 10 eq.) were dissolved in 1 mL of PBS buffer pH 7,4 in a round bottom flask (A). In another flask (B) were added BSA-MI (8.5 mL of BSA-MI in PBS buffer solution pH 7.4 concentration 1 mg/mL content, 5.3 µmol expected reactive moieties), NVCL (140 mg, 1.16 mmol, 190 eq.) and DMAEMA (160 mg, 1.16 mmol, 190 eq.). All flasks were deoxygenated by N_2 bubbling for 30 minutes. The polymerization was initiated by t transferring the content of flask B into flask A in one shot. The reaction was allowed to proceed initially at 0 °C and gradually rising to room temperature as the ice melted. The polymerization was stopped after 5 hours by bubbling air into the sample. The crude product was purified by dialysis with a 12.4 kDa MWCO dialysis membrane against PBS buffer at pH 7.4 for 72 hours. The BSA-PDMAEMA-*co*-PNVCL was analyzed by DLS in order to verify the cloud point temperature.

4.6.3. BSA-PNVCL$_{0.7}$-*co*-PDMAEMA$_{0.3}$ (Route 3)

The following reagents were added to a sealed Schlenk flask: (*i*) solution of BSA-MI (6 mL in PBS, pH 7.4, concentration 1 mg/mL content, 2.9 µmol expected reactive moieties); (*ii*) DMAEMA (52.3 mg, 332 µmol, 114 eq.); (*iii*) NVCL (108 mg, 776.1 µmol, 266 eq.) and (iv) Me_6TREN (7.8 µL, 29.2 µmol, 10 eq.). Next, the content was bubbled with N_2 for 30 min. Using another similar bottle, was added CuBr (2.9 mg, 20.4 µmol, 7 eq.) sealed and bubbled with N_2 for 30 min. The polymerization was initiated by transferring the BSA MI/monomer mixture to the CuBr flask via a gas-tight syringe. The reaction was allowed to proceed initially from 0 °C and gradually rising to room temperature using a bath of ice melted and a heat plate. The polymerization was stopped after 16 hours by bubbling air into the sample, and the product was purified by dialysis with a 12.4 kDa MWCO membrane using PBS buffer (pH 7.4) for 72 hours. The BSA-PDMAEMA-*co*-PNVCL was analyzed by the MALDI-ToF MS, SDS-Page, and Dynamic Light Scattering (DLS) techniques (Figure 4.4 B).

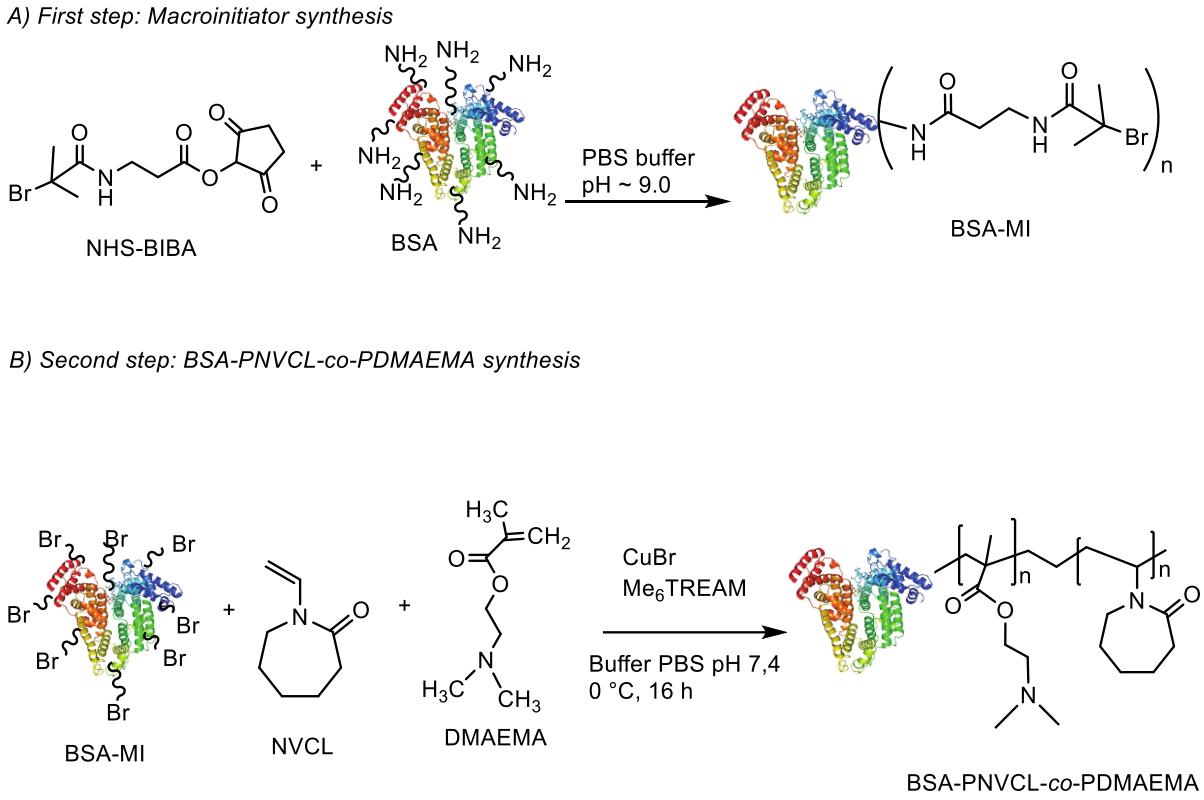

Figure 4.4: Synthesis of the conjugate via ATRP in A) synthesis of the macroinitiator and in B) synthesis of the hybrid by *grafting-from* approach.

4.7. Characterization methods

4.7.1. Chemical Characterization

In order to elucidate the structure of the synthesized ATRP initiators, verify the occurrence of polymerization and the related polymerization kinetics, the technique of Nuclear Magnetic Resonance of hydrogen (^{1}H NMR) was used.^{1}H NMR spectra were recorded on an INOVA 500 spectrometer from Varian Inc. at 500 MHz. According to the material analyzed, $CDCl_3$ or D_2O were used as solvents. The signal of the non-deuterated solvent was used as an internal standard.

SDS-Page analysis was performed on samples of in Natura BSA, BSA-MI, and BSA-conjugates in order to evaluate possible changes in the molecular mass of the protein. The samples were prepared by diluting 0.4 µl of the sample to be analyzed (initial concentration 1 mg/mL) in 14.6 µl of PBS (pH 7.4, 0.1 mol/L) and adding 5 µl of the denaturing agent 2-mercaptoethanol, thus obtaining a solution with a final protein concentration of 0.1 mg/mL. This solution was then heated to 90 °C for 10 minutes and

then cooled again in the refrigerator for 10 minutes. 5 µl of each sample was loaded onto 4-15% gradient polyacrylamide gels and 2 µl of Roti®-Mark TRICOLOR XTRA was used as a standard. The gels were maintained at 100 V and 18 mA for 1.5 hours in a Mini-PROTEAN®Electrophoresis System-Bio-Rad (München, Germany). Coomassie blue protocol was used to resolve the gel.

MALDI-ToF Mass Spectroscopy (MALDI-ToF MS) spectra were acquired using a 337 nm laser Bruker Microflex MALDI-ToF mass spectrometer (Bruker, Bremen, Germany) with pulsed ion extraction. The molar masses were determined in positive ion linear mode. The sample solutions were applied on a ground steel target using the dried droplet technique with $ZipTip_{C18}$ pipette tips (Millipore, Darmstadt, Germany). Dithranol (DT) was used as matrix substance in a 50 mg mL^{-1} solution in Millipore water:acetonitrile (v/v, 1:1) with 0.1% trifluoroacetic acid. Mass calibration was performed with external calibration.

4.7.2. Physical Characterization

The DLS technique was performed on a Malvern (Worcestershire, England) Zetasizer Nano ZS device. DLS technique was used to determine the mean particle size and the polydispersity index (PDI), a dimensionless measure of the amplitude of the particle size distribution in a sample. Results are expressed as the mean and standard deviation of at least three different lots of each analyzed sample. This technique was also used to determine the Lower Critical Solubility Temperature (LCST). For the LCST analysis, a heating ramp of 0.5 °C min^{-1} and an equilibration time of 120 s was used. Zeta Potential was also evaluated on a Malvern (Worcestershire, England) Zetasizer Nano ZS device and the measurements were carried out at 25 °C in a U-type zeta cell filled with the respective samples. The multiparameter analysis was performed on an average of three runs for every data point. All the DLS analyzes were performed in samples with a concentration of 1 mg/mL at PBS buffer (pH 7.4 0.1 mol/L).

4.7.3. Drug encapsulation efficiency

The encapsulation percentage (EP) of cisplatin into the BSA-PNVCL$_{0.7}$-*co*-PDMAEMA$_{0.3}$ was determined through the High-Performance Liquid Chromatography technique (HPLC-DAD). The encapsulation solution (ES) was prepared using 1.6 mL of cisplatin solution (1000 µg/mL) and 0.4 mL of a buffered solution (PBS at pH 7.4; 0.1 M) of BSA-PNVCL$_{0.7}$-*co*-PDMAEMA$_{0.3}$ at 1mg/mL. The suspension was incubated in an orbital shaker (Nova Ética São Paulo, Brasil) for 24 hours at room temperature. The dialysis technique was used to remove the non-encapsulated cisplatin. Dialysis membrane (12.4 kDa - MWCO) was used to prepare the dialysis bags, immersed in ultrapure water, for 24 hours at room temperature, ratio 1:10 (ES: water). After, samples of the dialyzed were analyzed through HPLC-DA.

The HPLC analyzes were conducted following the previous work conducted by Kaushik et al. (2010) with some modifications. Briefly, in a VWR Hitachi 5260 system (Tokyo), constituted by a quaternary pump (600 bar), autosampler, column oven, and a DAD detector, the separations were carried out at 25°C using a 150 x 3 mm and 3µm ACE 5 Generix™ C18 chromatography column. The mobile phase consisted of deionized water (Phase A- 25%) and methanol (Phase B- 75%). The calibration curve was obtained through five different drug concentrations (100, 80, 50, 30, 20 µg/mL). As a result, a linear regression curve was obtained. The detection wavelength was 210 nm, and the injection volume was 50 µl. The mobile phase flow was eluted isocratically at 1.5 mL/min. The percentage rate of encapsulation was calculated by the difference between the initial concentration of added cisplatin (C_i) and the residual concentration of cisplatin (C_r) present in the solution (multiplied by a dilution factor equal to 11) during the dialysis process (Equation 4.2). The encapsulation capacity (EC), the mass of cisplatin encapsulated per unit mass of hybrid, was calculated using equation 4.3.

$$EP\ (\%) = \frac{Ci - Cr}{\mathrm{Ci}} * 11\ X\ 100 \quad (4.2)$$

$$EC\ (\%) = \frac{Weight\ of\ initial\ Cisplatin - Weight\ of\ residual\ Cisplatin}{\mathrm{Weight\ of\ Hybrid}} X\ 100 \quad (4.3)$$

5. Results and discussion

5.1. Synthesis of ATRP initiators

Two different ATRP initiators were synthesized, N-2-Bromo-2-methylpropanoyl-β-alanine N′-oxysuccinimide ester and N-2-Chloropropionyl-β-alanine (N-ALA), in order to verify which one would be more efficient for the NVCL polymerization and also for the synthesis of the BSA macroinitiator. At this stage, the aim was to obtain ATRP initiators with good solubility in aqueous media, avoiding organic solvents since the polymerizations would also involve protein.

5.1.1. NHS-BIBA synthesis

After the synthesis of N-ALA, this compound was activated with the oxysuccinimide ester. Oxysuccinimide is an activated ester characterized by an excellent leaving group. Thus, this modification was performed to make this species more reactive and facilitating the protein binding process. The results of ^{1}H-NMR for N-2-Bromo-2-methylpropanoyl-β-alanine N′-oxysuccinimide ester synthesis is available in Figure 5.1, where similar results were previously described by Murata *et al.,* 2013. It is possible to observe a singlet at 1.91 ppm, which was associated with two methyl groups (6H, -NHC=OC(CH_3)$_2$Br, C_a and C_b); a double triplet around 2.84 ppm with an integral of 6, which can be associated with three methylene groups, (2H, HOOCCH_2-, C9 and 4H, -N-CO-CH_2-CH_2-CO-, C_f and C_g). The hydrogens linked to the "f" and "g" carbons are equivalent, presenting a single absorption without multiplicity. However, the hydrogens' of the C_e present themselves as a triplet, showing that this group has two adjacent protons. The quadruplet around 3,66 ppm (2H,-CH_2NHC=O, C_d) refers to the methylene adjacent to the amide group. There is also an absorption at 7.18 ppm, which refers to the amide groups' hydrogen (broad s, 1 H, -NHC=O, N_c). Yield: 6.7 g (56.5 %).

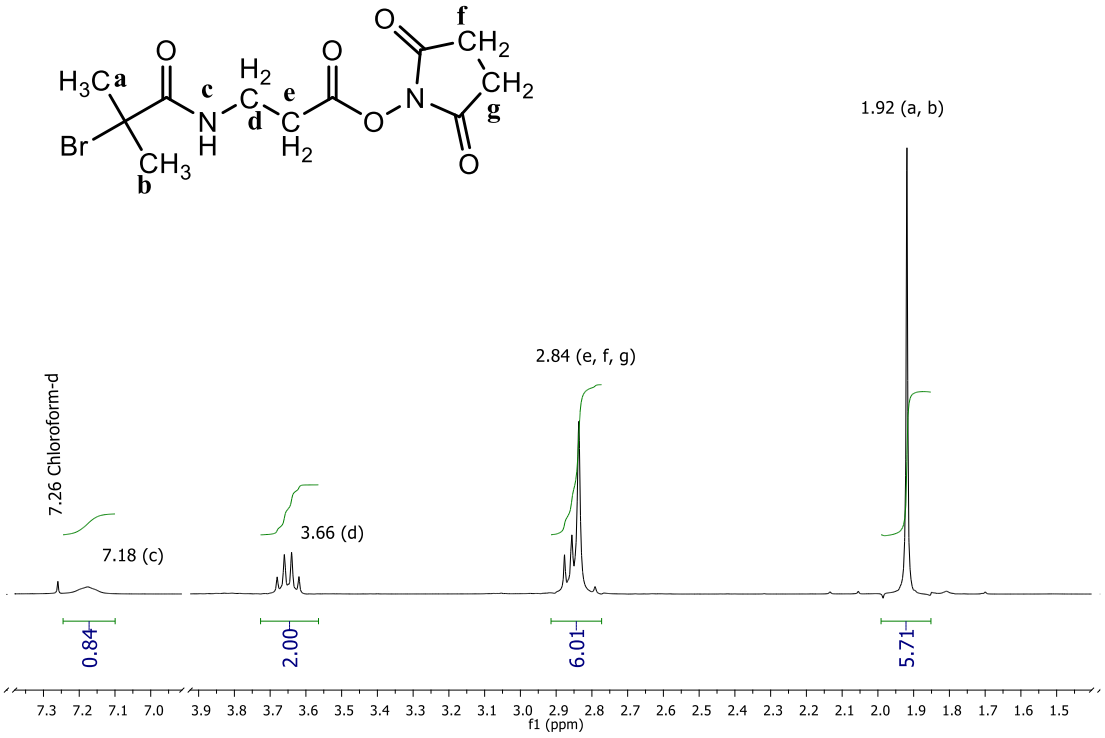

Figure 5.1: ^{1}H-NMR spectrum of N-2-Bromo-2-methylpropanoyl-β-alanine N′-oxysuccinimide ester, recorded in $CDCl_3$, with peak assignments.

5.1.2. N-ALA synthesis

N-ALA was synthesized, and its formation was confirmed by the ^{1}H-NMR spectrum available in Figure 5.2. Similar results was previously described by Cummings *et al.,* 2014. In the spectrum, it is possible to observe a signal represented by a doublet at 1.7 ppm, which refers to a methyl (3H, C*H*$_3$- CHClCONH-, C_b); a triplet at 2.64 ppm, corresponding to the methylene group (2H, -C*H*$_2$-COOH, C_e); a quadruplet around 3.56 ppm, which refers to methylene adjacent to the amide group (2H, -C*H*$_2$-NH-CO-CHCl-CH$_3$, C_d); a quadruplet at 4.41 ppm corresponding to the hydrogen linked to the C_a (1H, CH$_3$-C*H*-Cl-CO-NH-). Finally, we can observe a broad singlet at 7.17 ppm, referring to secondary amide hydrogen (1H, -N*H*CO-CH-Cl-CH$_3$, N_c). Yield: 2.20 g (79 %).

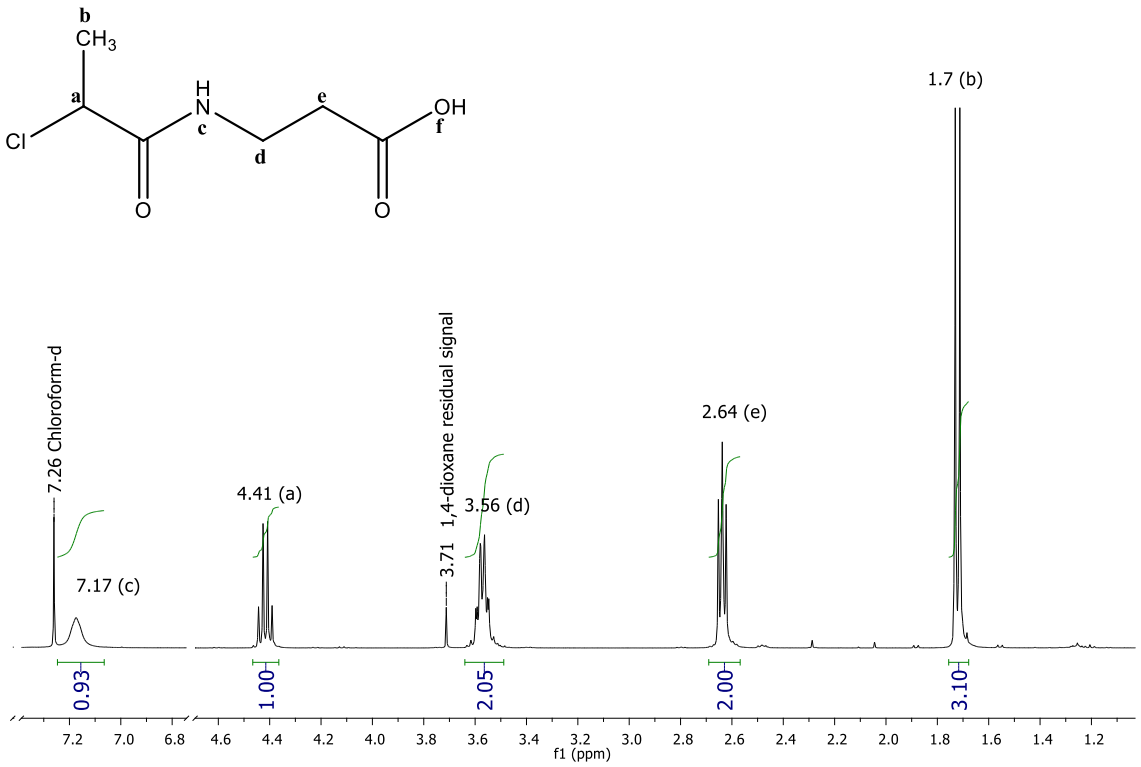

Figure 5.2: ^{1}H-NMR spectrum of N-ALA, recorded in $CDCl_3$, with peak assignments.

5.2. Polymerization study

Three studies with different reaction media were conducted in this step to seek the best route for PDMAEMA and PNVCL monomers homo- and copolymerization. The ^{1}H-NMR technique was used to study the proposed polymerizations focused on searching for the existence or not of broad peaks, which are evidence of monomers' conversion into macromolecules.

In the ^{1}H-NMR spectrum of the PDMAEMA, a clear and non-overlapping broad signal around 4.27 ppm can be observed. This signal was associated with the methylene repetition adjacent to the ester group macromolecules (DE JESÚS-TÉLLEZ *et al*., 2020), indicating the polymer formation. On the other hand, for the PNVCL, enlarged regions, such as 1.7, 3.15, and 4.38 ppm, cover practically the entire spectrum (KOZANOĞLU; ÖZDEMI; USANMAZ, 2011).

5.2.1. NVCL and DMAEMA reaction using the catalytic system ECP/Me_6TREN

In route 1, ECP was used as an initiator and Me_6TREN as a ligand. The procedure was previously described in item 4.3.1. The ^{1}H-NMR spectra obtained from the analysis of the tested routes reaction medium are available in Figure 5.3, and the results revealed the presence of narrow peaks, indicating the failure of polymerization. Furthermore, peaks referring to the structure of the monomer NVCL, such as multiplet at 7.30 ppm; duple duplet at 4.86 and 4.72 (hydrogens of the vinyl group C_a and C_b, respectively), can be observed. The slight broad signal at 1.77 and 1.87 ppm was associated with the overlapping signals from the hydrogens linked to carbons C_d, C_e, and C_f (Figure 5.3).

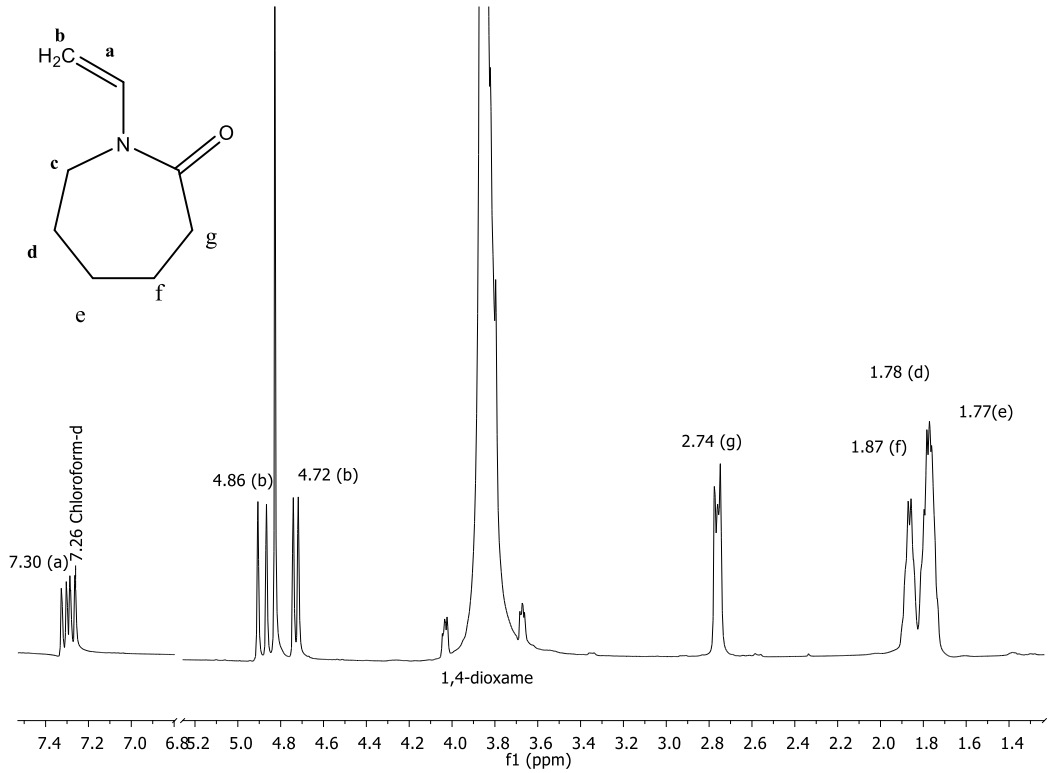

Figure 5.3: ^{1}H-NMR of NVCL reaction using ECP as an initiator, recorded in $CDCl_3$, with peak assignments.

The results of the ^{1}H-NMR spectrum, obtained from samples constituted by NVCL and DMAEMA, are available in Figure 5.4. The obtained data revealed absorptions related to the protons linked to unsaturated carbons from the DMAEMA

structure, at 5.87 and 6.29 ppm. Furthermore, these absorptions were associated with the cis and trans protons of the ethylene group (C_b) and a clear triplet at 4.48 ppm, referring to the protons of the methylene (C_c), which becomes quite broad in the case of polymerization. On the other hand, the signals of the protons linked to unsaturated carbons of NVCL at 7.31 ppm can also be seen. Such observation indicates that the polymerization of DMAEMA and NVCL did not occur under these conditions.

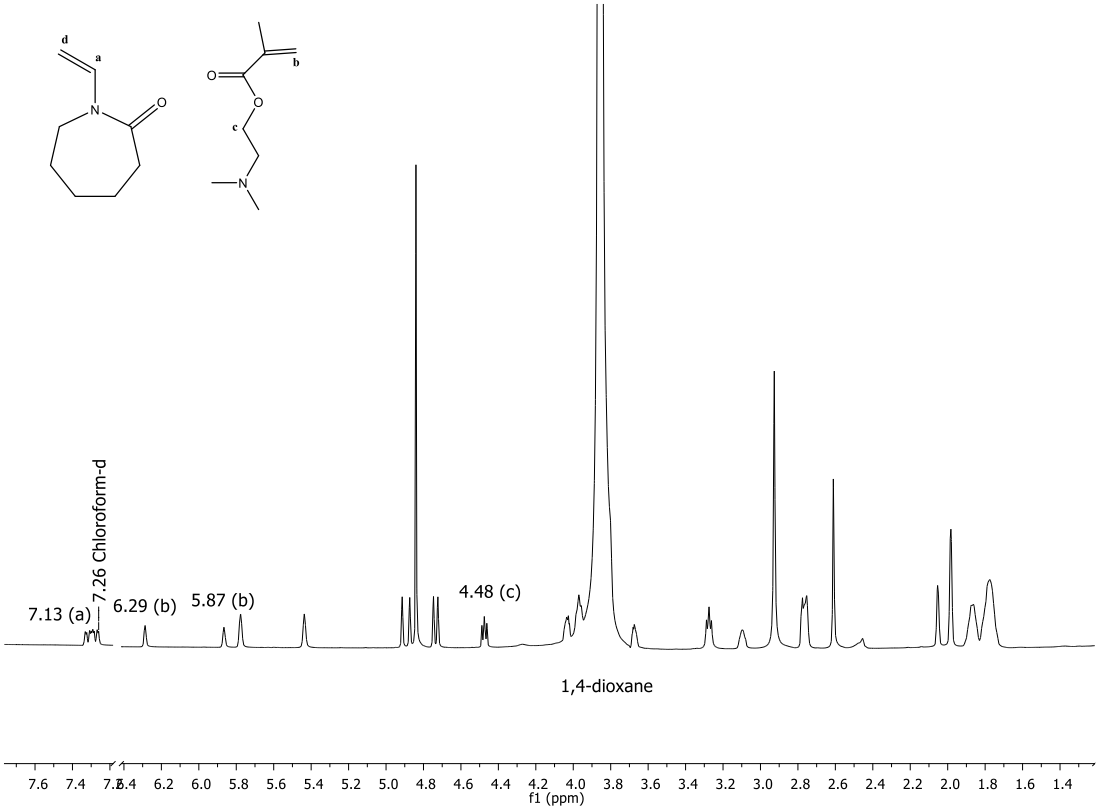

Figure 5.4: ^{1}H-NMR of NVCL and DMAEMA reaction using ECP as initiator, recorded in $CDCl_3$, with peak assignments.

The analyses presented show that the system using ECP, under the conditions tested, was not efficient in polymerizing NVCL or DMAEMA.

5.2.2. NVCL and DMAEMA reaction using the catalytic system BIBA/Me_6TREN

The spectrum obtained from reaction related to NVCL using BIBA/Me_6TREN is available in Figure 5.5. Unfortunately, it was not possible to observe broad peaks

related to the macromolecule structure. In this sense, only peaks related to the NVCL monomers, as described in the previous section, were identified.

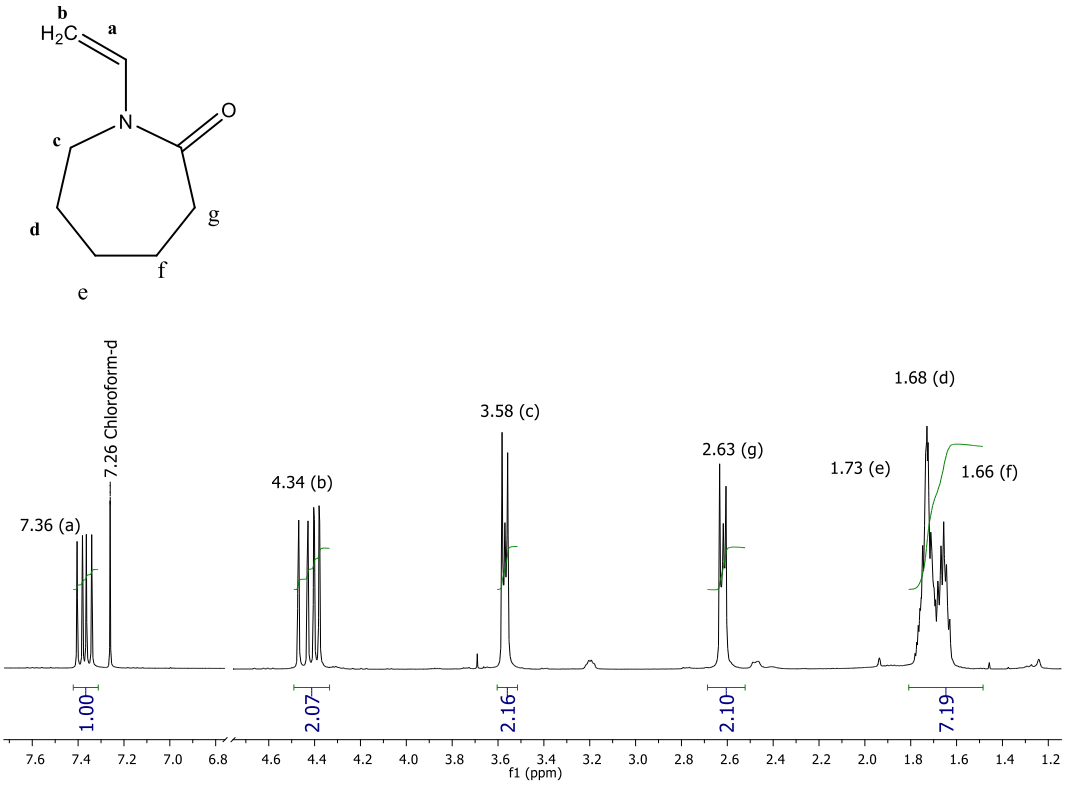

Figure 5.5: ^{1}HNMR of NVCL reaction using BIBA as an initiator, recorded in $CDCl_3$, with peak assignments.

On the other hand, according to the spectrum available in Figure 5.6, the presence of broad peaks such as the found at 4.26 ppm can be associated with DMAEMA polymerization. Furthermore, it is even possible to notice peaks at 5.65 and 5.35 ppm (protons signals from unsaturated carbon of the DMAEMA), which shows the remaining DMAEMA monomer. Besides, it is also possible to notice broad peaks that join throughout the region from 1 ppm to 3.5 ppm, indicating the NVCL polymerization.

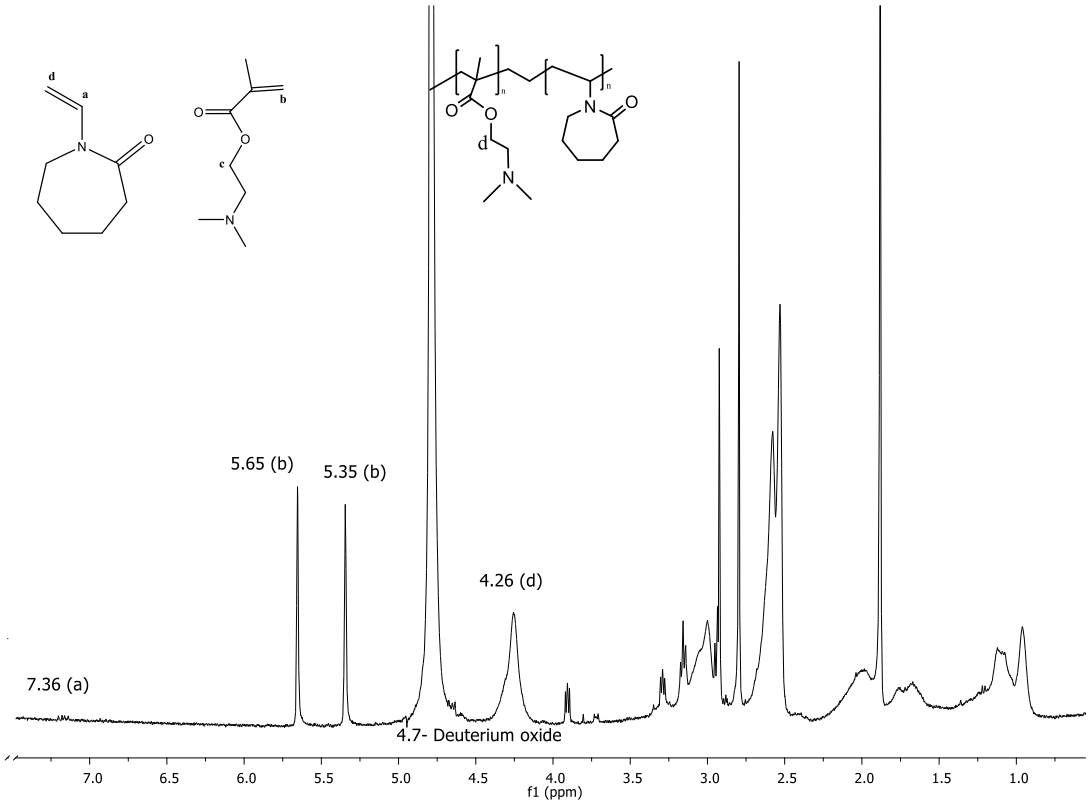

Figure 5.6: ^{1}HNMR of polymerization of NVCL and DMAEMA using BIBA as initiator, recorded in D_2O, with peak assignments.

Using BIBA/Me6TREN as a catalytic system, the occurrence of polymerization was not verified for NVCL homopolymerization. On the other hand, the polymerization occurred for the copolymerization of NVCL and DMAEMA. This behavior may indicate that the use of another monomer (DMAEMA in this case) helps stabilize the NVCL radical, making possible the polymerization. However, other detailed studies must be conducted to amplify the comprehension of these reactions.

5.2.3. NVCL and DMAEMA reaction using the catalytic system N-ALA/Me$_6$TREN

The homo- and copolymerization were tested using the catalytic system N-ALA/Me$_6$TREN under the conditions mentioned in section 4.2.3. Figures 5.7 and 5.8 are available ^{1}H-NMR spectra, which allow verifying that nonsignificant homopolymerization or copolymerization occurred, respectively. Furthermore, the results observed in the spectra revealed only signs related to the respective

monomers, without broad peaks, demonstrating the low efficiency of the system to allow in obtaining the significant quantities of the desired polymer.

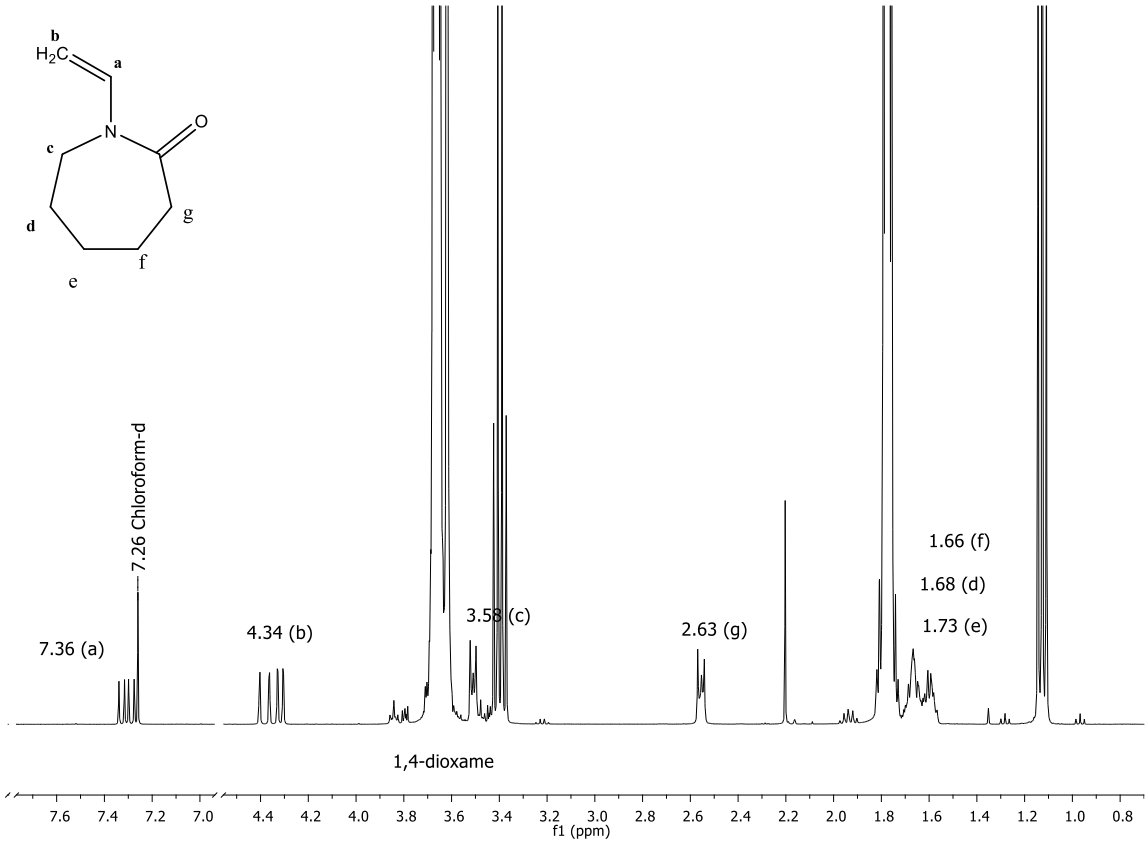

Figure 5.7: ^{1}HNMR of NVCL reaction using N-ALA as an initiator and Me_6TREN as ligand, recorded in $CDCl_3$, with peak assignments.

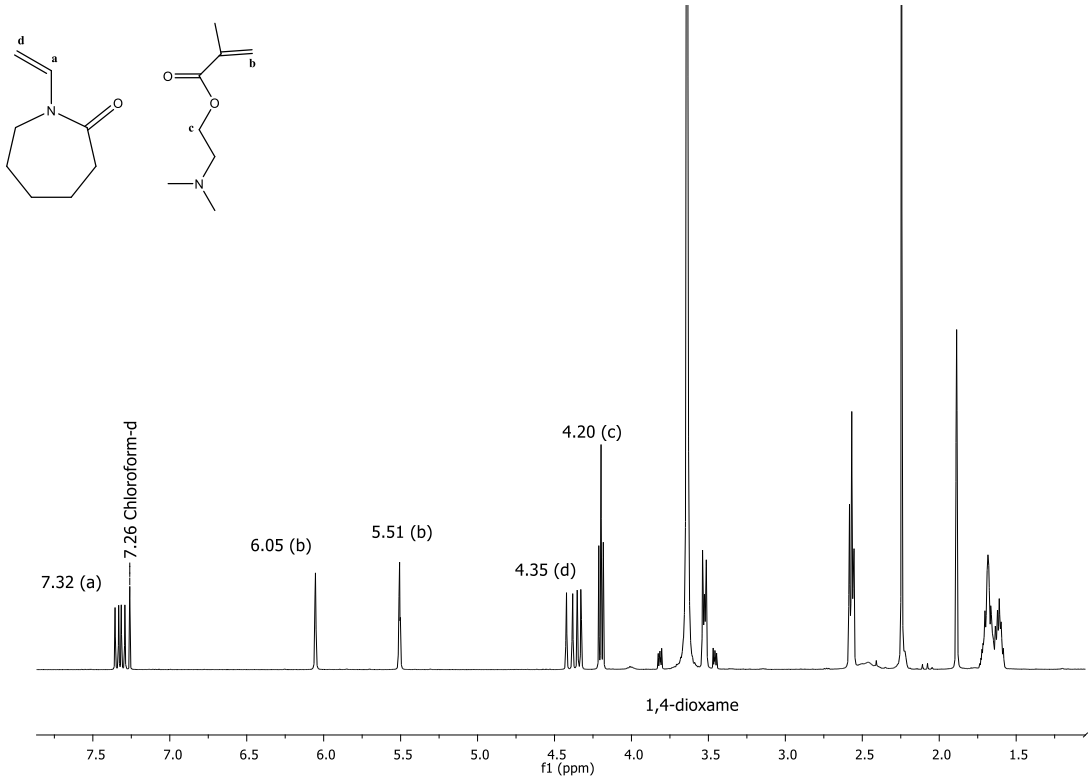

Figure 5.8: ^{1}H-NMR of NVCL and DMAEMA reaction using N-ALA as an initiator and Me_6TREN as ligand, recorded in $CDCl_3$, with peak assignments.

5.2.4. NVCL and DMAEMA reaction using as catalytic system N-ALA/Me_6Cyclam

In this step, the initiator used was the same related in item 5.2.3. The tests were performed by changing the ligand Me_6TREN to Me_6cyclam. Figures 5.9 and 5.10, are available the spectra of the homo- and copolymerization processes, respectively. The results revealed only narrow signs related to the monomers' structure, as previously mentioned. In this sense, the catalytic system did not prove to be a good option for obtaining the desired polymers.

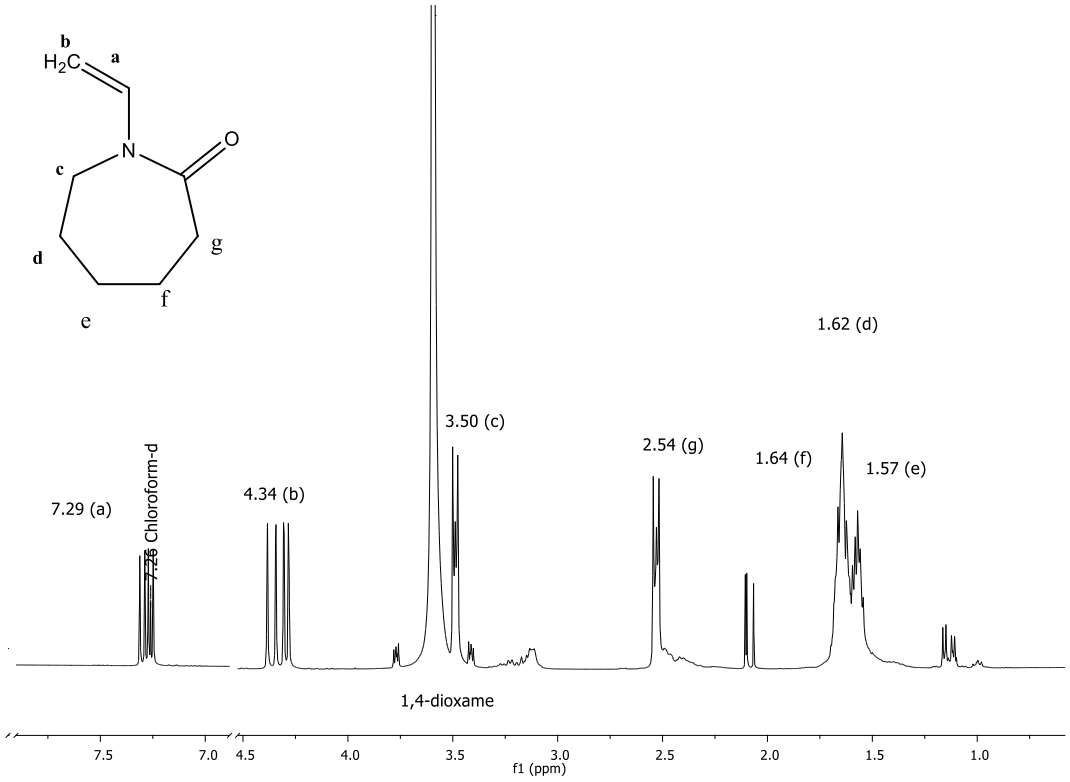

Figure 5.9: ^{1}H-NMR of NVCL reaction using N-ALA as an initiator and Me_6Cyclam as ligand, recorded in $CDCl_3$, with peak assignments.

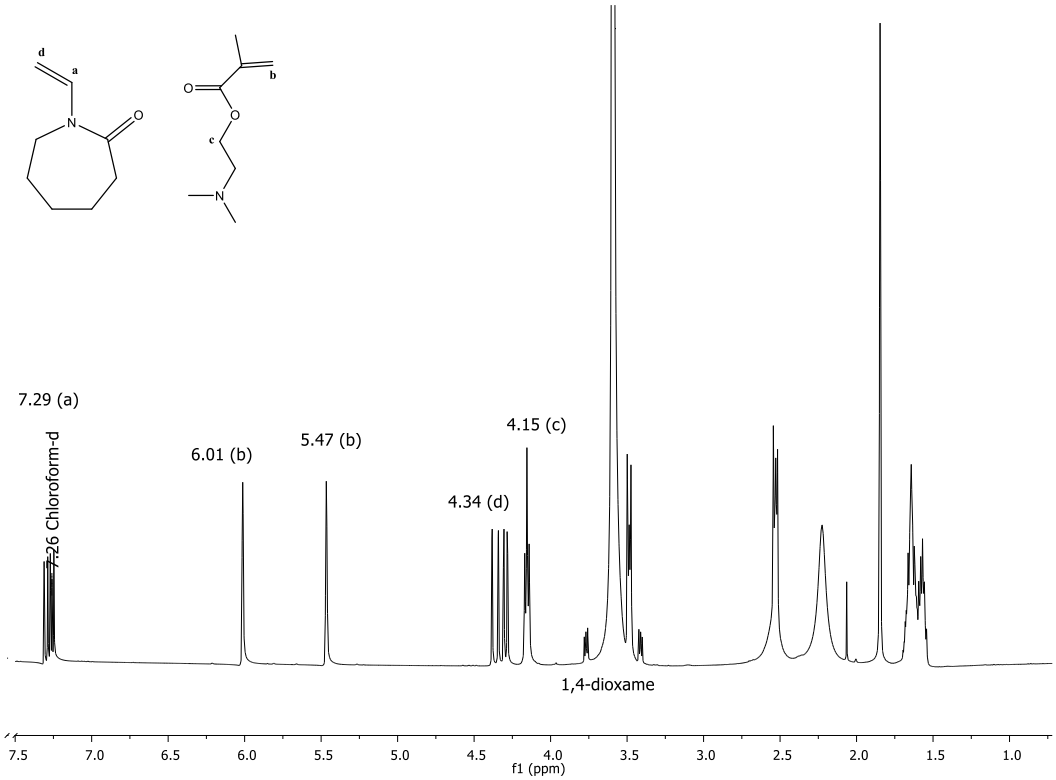

Figure 5.10: ^{1}H-NMR of NVCL and DMAEMA reaction using N-ALA as an initiator and Me_6Cyclam as a ligand, recorded in $CDCl_3$, with peak assignments.

Some previously published works have indicated that the chlorinated catalytic systems are more efficient than brominated in the polymerization of NVCL since they have less reactive groups and can stabilize the monomeric radicals, allowing a well-controlled polymerization process (QUIAN *et al*. 2014). However, this behavior was not verified in the conducted experiments. This fact may be related to the reaction conditions used, requiring additional tests, amplifying the parameters used such as type of solvent, temperature, and proportion between the reagents.

The BIBA initiator revealed better performance for obtaining the desired hybrid from the obtained results using the different polymerization routes. Thus, this initiator was used to obtain the macroinitiator by modifying the BSA and sequentially used for getting BSA-PNVCL-*co*-PDMAEMA conjugate by *grafting from using* Me_6TREN /CuBr as a catalytic system.

5.3. Kinetics studies for ATRP polymerization

The kinetic studies for the PDMAEMA and PNVCL-*co*-PDMAEMA polymerization were performed to determine the minimum reaction time, seeking to prevent protein denaturation. For NVCL, it was not possible to carry out homopolymerization kinetics under the conditions studied due to the instability of the formed radicals. So, it can only be polymerized under specific conditions.

^{1}H-NMR was used to carry out the kinetic studies of the PDMAEMA and PNVCL-co-PDMAEMA polymerization, and the obtained results are available in Figure 5.11. The presence of broad signals without multiplicity and associated with a significant reduction in the intensity of the signals corresponding to the vinyl protons can be used as tools confirming the polymerization success.

The conversion degree was calculated by comparing the integral of the peaks refers to the vinyl protons of the monomer (C_a and $C_{a'}$) in the region 5.66 ppm and the broad signal in the area 4.32 ppm (referring to ethylene groups of PDMAEMA C *h*). The results are available in Table 5.1, where it is possible to verify that copolymerization becomes slower than homopolymerization. Compared with the homopolymer, while it was observed more than 80% of conversion in 60 minutes, this degree of conversion is not reached before 120 minutes of reaction for the copolymer. This behavior can be explained due to the high reactivity of radical species derived

from the NVCL monomer, which becomes difficult for this polymerization process (JIANG et al., 2013).

Table 5.1: Conversion degree for copolymer PNVCL-co-PDMAEMA and homopolymer PDMAEMA in different reaction times.

Reaction time	**PNVCL-*co*-PDMAEMA**	**PDMAEMA**
10 min	40%	68%
60 min	76%	87%
120 min	78%	88%
240 min	92%	84%

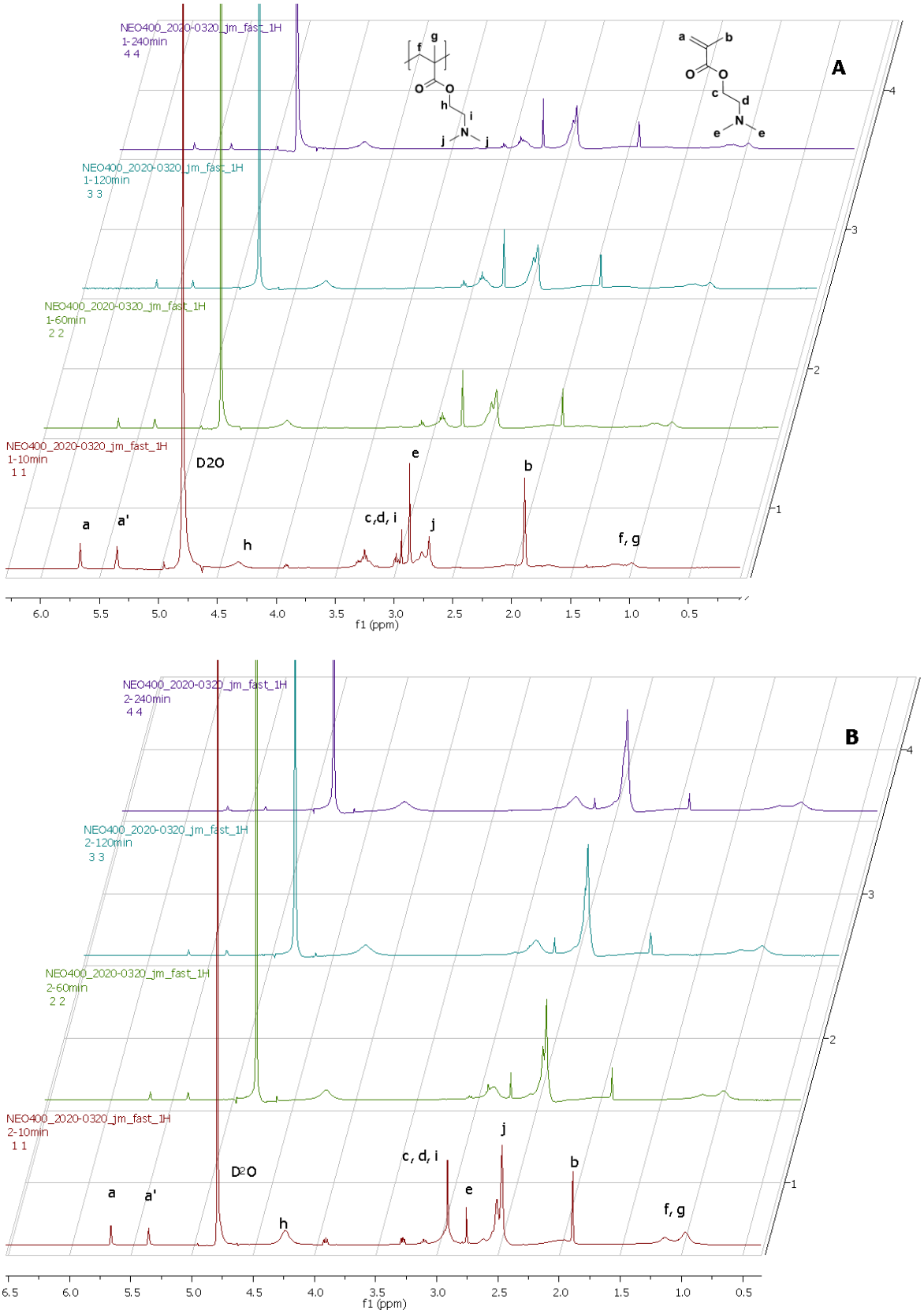

Figure 5.11: ^{1}H-NMR analysis of polymerization of a) PNVCL-*co*-PDMAEMA and b) PDMAEMA. Samples were taken after specific time points (10, 60, 120, 240 minutes), recorded in D_2O, with peak assignments.

5.4. Synthesis of BSA-MI

The preparation of the BSA-MI was done by lysine residue modification into the BSA structure using NHS-BIBA, an ATRP initiator activated with an ester (N-Hydroxysuccinimide). Considering the low solubility of the NHS-BIBA in an aqueous medium, the employment of a low concentration of BSA was the best way to synthesize the macroinitiator (1 mg/mL), also leading to a low concentration of NHS-BIBA (0.75 mg/mL) and consequently, better homogeneity of the reaction medium. The temperature and reaction time were also adjusted for 4 °C and 16 hours, respectively. The macroinitiator formation, BSA-MI, was characterized by SDS-PAGE and MALDI-ToF MS.

The SDS-PAGE analysis (Figure 5.12) was used to qualitatively verify the modification of the BSA and revealed an increase in the BSA molecular mass when compared with unmodified BSA (line 1) and BSA-MI (lines 4 and 10) sugesting the binding NHS-BIBA onto the protein.

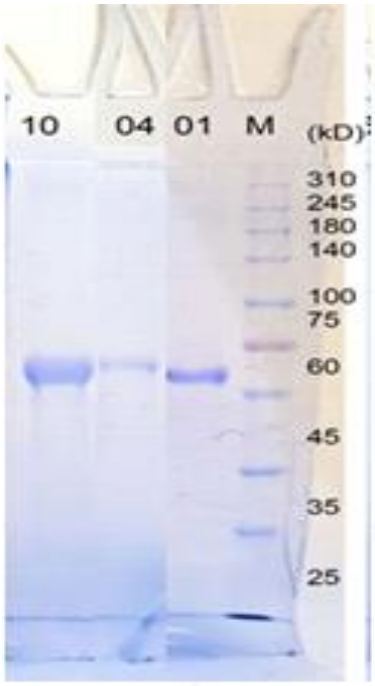

Figure 5.12: SDS-PAGE of BSA (line 1), BSA-MI (line 4) and BSA-MI, 10 times concentrated (line 10).

To quantify the protein modification MALDI-ToF was performed and the mass spectra of the BSA and BSA-MI (Figure 5.13) were obtained using Zip Tip sample preparation and the matrix dithranol (DT). The unmodified BSA was detected with a

molecular mass of 66,8 kDa, while for BSA-MI, the molecular mass detected was around 75,7 KDa. This difference between the BSA and BSA-MI molecular mass proposes that the modification of lysines groups on BSA has occurred to a considerable range.

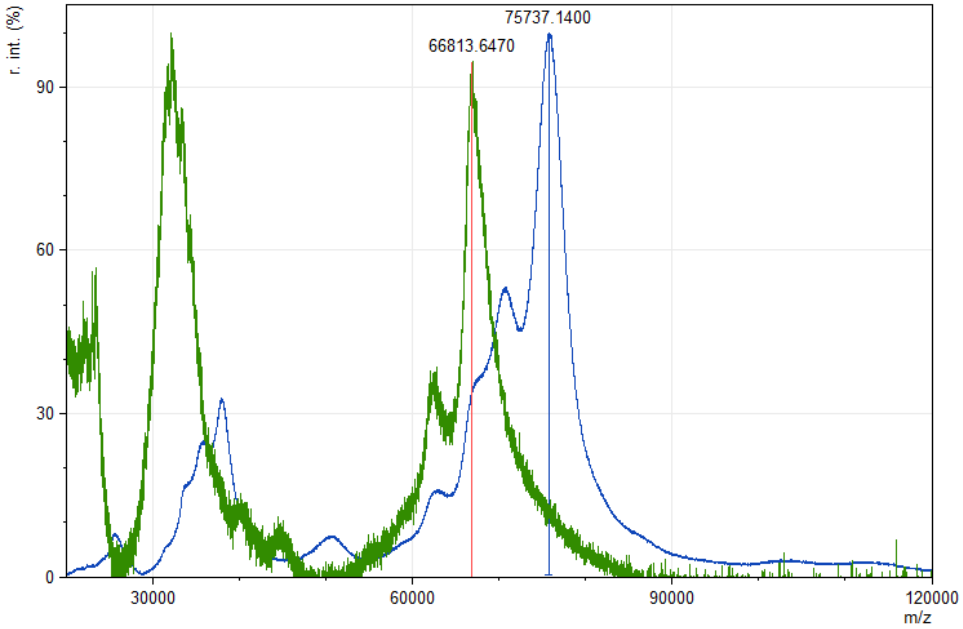

Figure 5.13: MALDI-ToF MS of BSA (blue spectrum) and BSA-MI (green spectrum).

5.5. Synthesis of BSA-PNVCL-*co*-PDMAEMA

The synthesis of BSA-MI proved to be successful, enabling the modification of the lysine groups present in the BSA structure, as shown in the previous section. This obtained macroinitiator was used to obtain the conjugate, varying other parameters to optimize the synthesis of the material with the desired properties such as a system soluble in an aqueous medium, particle size around 100 nm maximum, and LCST at around 40 °C.

5.5.1. Route 1

In the first route, the aim was to prove the macroinitiator polymerization efficiency. The theoretical degree of polymerization was 700 in the ratio 1:1 (NVCL / DMAEMA), and the reaction was kept for 48 hours. The obtained final product presented as a viscous gel, as shown in Figure 5.14, suggesting the success of the

polymerization and forming a hybrid material. However, it was impossible to solubilize this material after its lyophilization, suggesting a possible crosslinking of this material, making its Characterization unfeasible. In this sense, the proposed methodology was optimized (route 2) to obtain the desired hybrid material.

Figure 5.14: Hybrid material obtained from the first route after purification.

5.5.1. Route 2

In this step, the main objective was to obtain a non-crosslinked material. Thus, some modifications were made in the synthetic route combining the best synthesis conditions seeking to adjust the particle size and consequently collapse temperature of the conjugate around 40 ºC. Thus, in this step, the Characterization was limited to particle size and the transition temperature.

The decrease in the average particle size was tested by reducing the degree of theoretical polymerization from 700 (route 1) to 380, maintaining the ratio of 1:1 (NVCL/DMAEMA). Figure 5.15 are available the results of BSA and BSA-PNVCL-*co*-PDMAEMA average size. The obtained data revealed a significant increase in the average size of the conjugate nanoparticles compared with the in-nature protein. The average diameter of BSA particles is around 7 nm (11.23 ± 4.86 nm by intensity, 6.98 ± 2.83 nm by volume and 5.26 ± 1.56 nm by number) , and agrees with the results found by Li *et al.* (LI; YANG; MEI, 2011). On the other hand, BSA-PNVCL-*co*-PDMAEMA presented an average size between 20 and 30 nm (35.46 ± 14.40 nm by intensity, 24.70 ± 8.86 nm by volume and 19.82 ± 5.29 nm by number). When analyzing the size distribution by intensity, it is possible to observe three peaks, for the protein and also for the hybrid. These data may be related to the presence of dimers and

aggregates. However, this behavior is not observed in the distribution by volume or by numbers, suggesting that they are not representative populations for these sizes. The size of nanoparticles ranging around 100nm is essential for intravenous applications since it may avoid clot formation and thrombosis phenomena (ZHAO *et al*., 2019).

Another indication of the conjugate formation is the Zeta Potential changing. BSA and BSA-PNVCL-co-PDMAEMA presented values of -11,1 ± 1,3 mV and 10,6 ± 0,4 mV, respectively, changing from the negative modulus to positive after polymerization over the surface of the protein showing that in module the systems have equivalent stabilities.

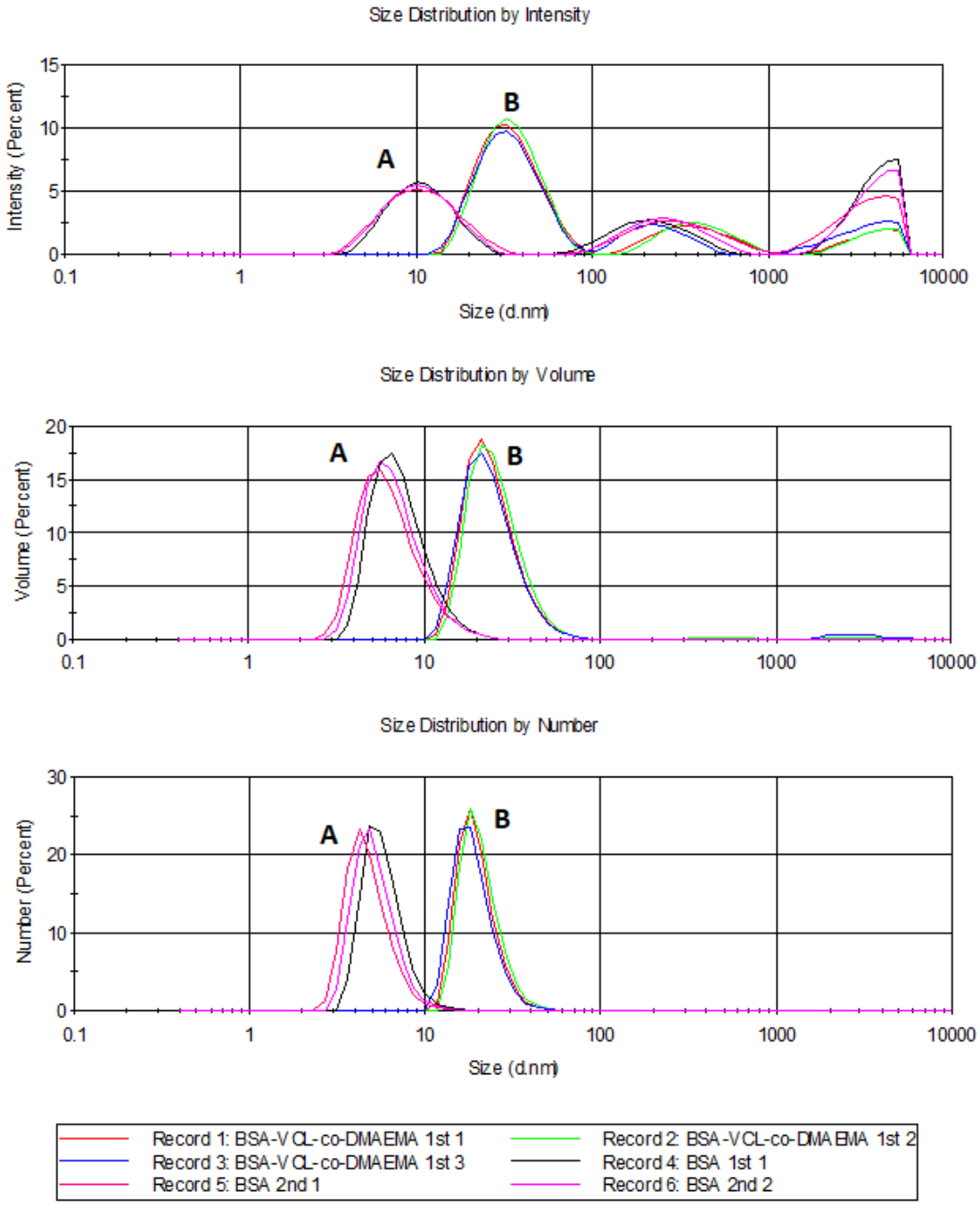

Figure 5.15: Particle size distributions: A) in PBS pH 7.4 BSA solution (1 mg/mL), B) in PBS pH 7.4 BSA-PNVCL$_{0.5}$-*co*-PDMAEMA$_{0.5}$ in PBS pH 7.4 (1 mg/mL)

The temperature dependence on the phase transition of the BSA-PNVCL$_{0.5}$-*co*-PDMAEMA$_{0.5}$ conjugates by DLS was investigated in PBS solution pH 7.4. As displayed in Figure 5.16, was observed an aggregation point around 45 °C.

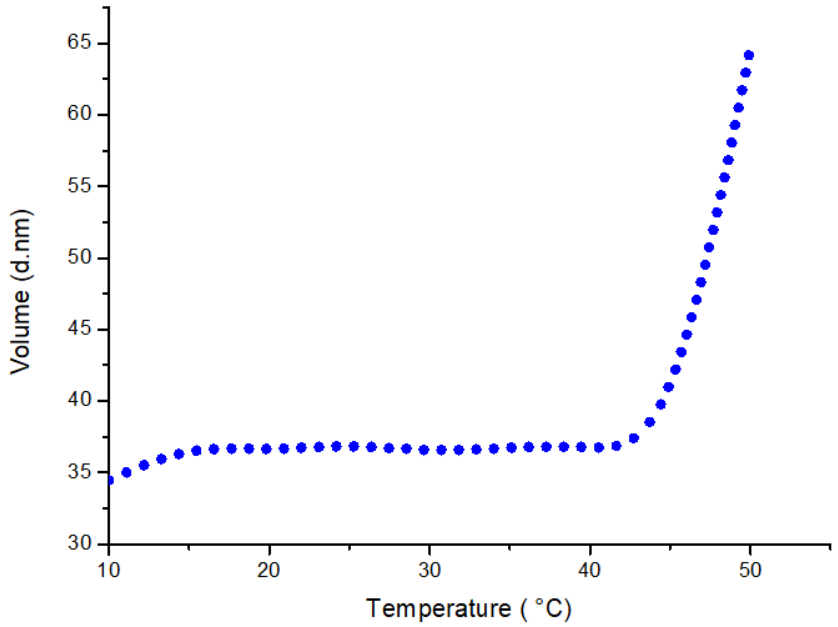

Figure 5.16: Aggregation point of BSA-PNVCL-*co*-PDMAEMA.

From synthesis route 2, there are indications of obtaining the hybrid material with thermo-responsive behavior. However, the aggregation point observed around 45 ºC is above the desired application as a carriers' systems drug. Thus, additional characterizations were not conducted in this material. Therefore, seeking to optimize the synthesis and reduce the transition temperature to approximately 40 ° C, route 3 was developed as follows.

5.5.3 Route 3

This essay aimed to reduce the transition temperature of the material obtained to values of approximately 40 ºC. The LCST values for homopolymers, PNVCL is around 32 °C and PDMAEMA, is around 45 °C. In this sense, the polymerization with different proportions between these two monomers was performed, seeking to obtain an intermediate value among them. The experiment was conducted keeping the DP at 380 and changing the ratio between monomers, which 70% NVCL and 30% DMAEMA, a higher proportion of the monomer with lower LCST. SDS-PAGE, MALDI-ToF, and DLS were used to characterize the final product.

The formation of hybrid BSA-PNVCL-*co*-PDMAEMA was successfully confirmed by SDS-PAGE, according to Figure 5.17. The conjugate indicated in lines 5

and 11(10 times concentrated) shows a significant increase in the molecular mass, passing from 60 to 75 KDa (BSA and BSA-MI, respectively), while for the conjugate, BSA-PNVCL-*co*-PDMAEMA, the observed band appears around 310 KDa.

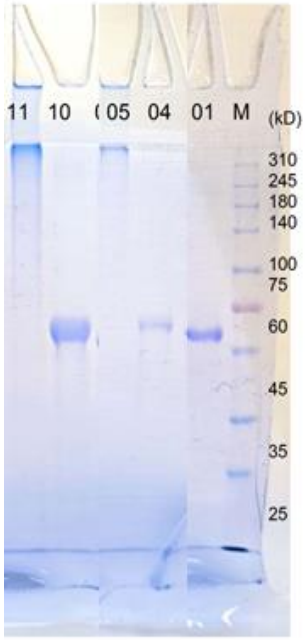

Figure 5.17: SDS-PAGE of BSA (line 1) BSA-MI (line 4), BSA-MI 10 times concentrated (line 10), BSA-PNVCL-*co*-PDMAEMA (line 5), and BSA-PNVCL-*co*-PDMAEMA 10 times concentrated (line 11).

The MALDI-ToF mass spectra (Figure 5.18) is no more possible to see a straight peak referring to BSA or BSA-MI, but a pronounced and broad peak. However, in this analysis, it is challenging to calculate the number of polymer chains attached to BSA, not even the polymer's molecular mass.

Tebaldi et al. (2017) reported that the mass of 310 kDa observed in the SDS-PAGE and the high mass observed in the MALDI-Tof do not represent a single mass conjugate but may be related to the agglomerates, that is, several subunits together. This agglomeration can be facilitated by introducing polymeric chains to the protein, a behavior that is not observed for the unmodified protein. Typically, it is challenging to obtain mass spectra of conjugates because of the two linked compounds' different properties and the broad molecular weight distribution.

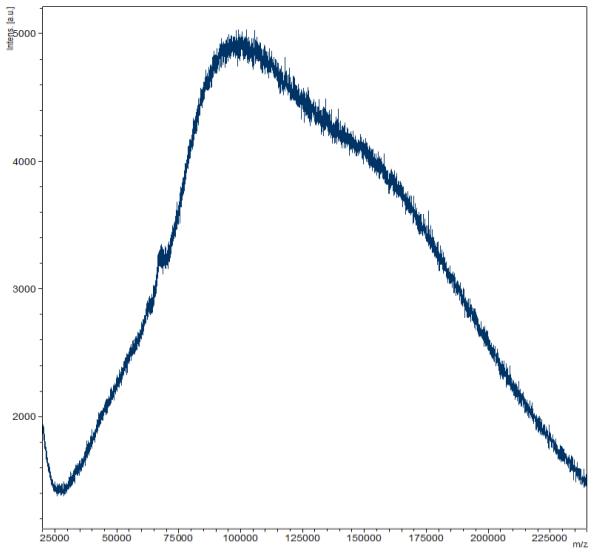

Figure 5.18: MALDI-ToF MS of BSA-PNVCL-*co*-PDMAEMA.

PDMAEMA and PNVCL are temperature-sensitive polymers, conferring these sensitivities to the conjugate. However, the LCST, for example, of the hybrid material can differ from that of the pure polymer. On the other hand, PDMAEMA is pH- and temperature-sensitive, and its LCST can change in different pH solutions.

Here, we investigated the temperature dependence on the phase transition of the BSA-PNVCL-*co*-PDMAEMA conjugates by DLS studies in PBS solution pH 7.4. As displayed in Figure 5.19, around 39 °C, a high particle size variation is observed. The chains are partially protonated in these conditions and undergo a phase transition, resulting in aggregated particles related to the LCST behavior.

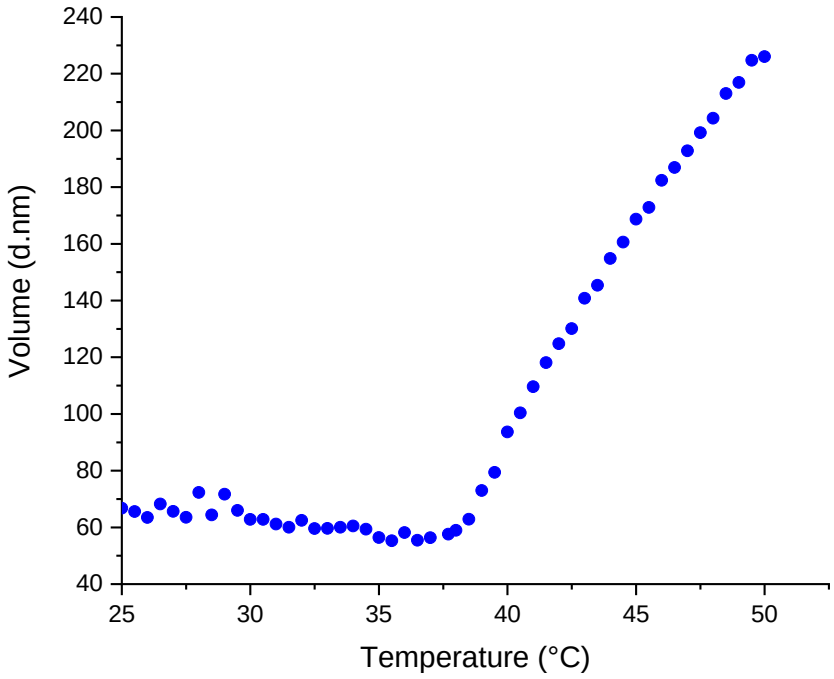

Figure 5.19: Aggregation point of BSA-PNVCL-*co*-PDMAEMA in PBS solution pH 7.4.

This conjugate obtained is very promising for application as a drug delivery system, considering mainly its transition temperature range and particle size, which remained below 100 nm when below the LCST. These characteristics may enable its intravenous use associated with the selective release of the drug in tumor tissues in cancer therapy. However, further studies are still needed to verify the influence of pH on the LCST of the product obtained, considering the presence of PDMAEMA in the structure, thermal and pH-responsive polymer.

5.6. Drug Encapsulation Efficiency

The HPLC-DAD technique was used to quantitatively determine the amount of cisplatin encapsulated in BSA-PNVCL$_{0.7}$-*co*-PDMAEMA$_{0.3}$ samples. For this purpose, a calibration curve was prepared, where the used concentration ranged from 20 to 100 µg/mL. The curve obtained is shown in Figure 5.20, and the obtained data revealed a coefficient of determination (r^2) equal to 0.9984.

According to RDC 166 (Brazilian government resolution) of the National Health Surveillance Agency (ANVISA), for analytical methods of drugs, including the HPLC technique, calibration curves must have minimum r^2 values of 0.99 or closer to 1. It is

also recommended that the curve have at least five standards of different concentrations. The data obtained meet both recommendations and are therefore considered adequate for cisplatin quantification studies.

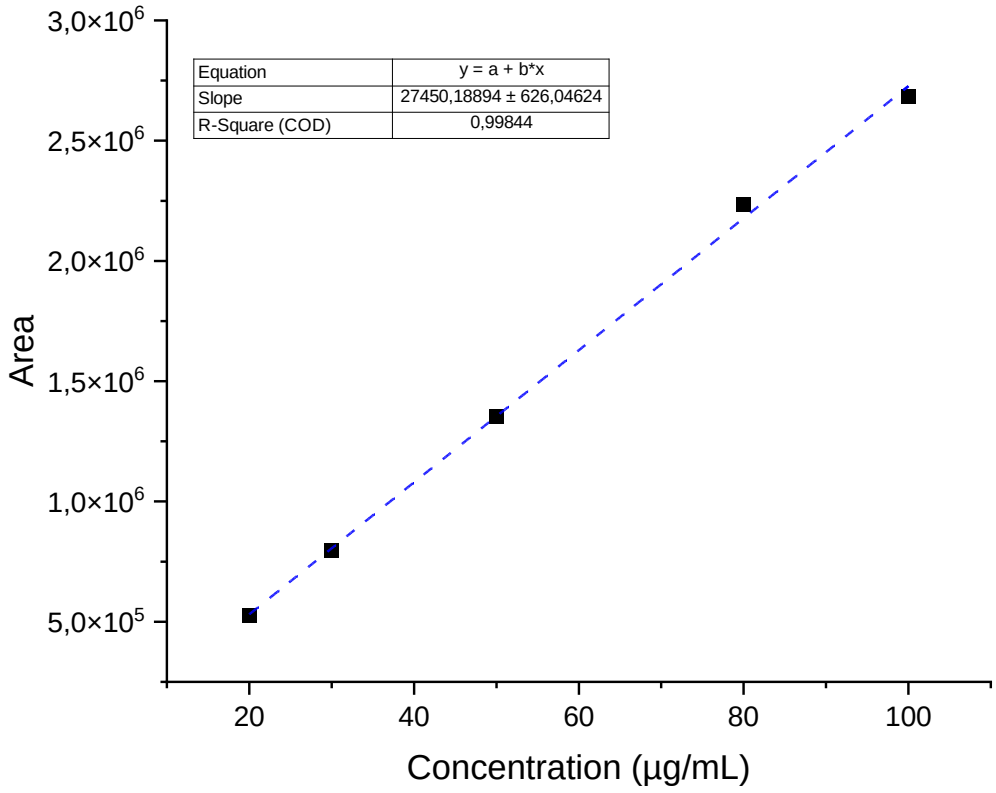

Figure 5.20: Calibration curve for cisplatin in the range of 20 to 100 µg / mL obtained by the HPLC-DAD technique. The curve was obtained, given by the equation y = 0 .00003643*X+ 0.6636 and r^2 = 0.9984.

Samples constituted by hybrid materials were incubated with cisplatin solution (1000 µg/mL). After 24 hours, the nanoparticles were dialyzed and analyzed (n=3) through the HPLC-DAD technique. From equation 4.2 (section 4.7.3), the obtained results revealed an average EP of 40 ± 2.7 %, which means incorporating 390 ± 20 µg of cisplatin within the hybrid. Furthermore, from equation 4.3 (section 4.7.3), an EC of approximately 195% was determined. This percentage indicates that the obtained system could encapsulate approximately 1.9 mg of cisplatin for each 1 mg of the hybrid BSA-PNVCL$_{0.7}$-*co*-PDMAEMA$_{0.3}$.

Previous studies were conducted by Banihashem and coworker (2020) which prepared hybrid nanosystems based on polymer PNVCL and protein chitosan loaded with cisplatin. The authors reported an incorporation efficiency of 96 % and an incorporation capacity of 33.6%, using cisplatin solutions in different concentrations. Studies conducted by Wang and collaborators (2019) also evaluated the encapsulation efficiency for the system for the chitosan/hyaluronic acid nanoparticles co-encapsulated with doxorubicin and cisplatin. The results showed EP and EC 20.55% and 21.4% for doxorubicin and 9.53% and 81.71% for cisplatin. Catanzaro *et al.* (2018) obtained BSA nanoparticles with approximately 100% EP and 20% EC. Tiwari *et al*. (2020) also obtained BSA nanoparticles with an EP of 75% and an EC of 9.4%.

From the obtained results, it is possible to notice that the produced nanosystem displayed EP inferior to homologous systems loaded with cisplatin, compared to data previously described in the literature. However, such studies have employed cisplatin concentrations, which were significantly lower than those used in this work. In this sense, the EC was significantly higher.

These differences may be related mainly to the methodologies used for the encapsulation process. In all the described works, significant proportions of nanostructures (hybrid systems or nanoparticles) were used for encapsulation than cisplatin during the encapsulation process, unlike the current work, in which an excess of cisplatin was used concerning the hybrid BSA-PNVCL$_{0.7}$-*co*-PDMAEMA$_{0.3}$. The results obtained in this work suggest that the fabricated nanosystem can be considered as a potential alternative nanocarrier for cisplatin delivery since they can encapsulate large amounts of cisplatin in a relatively small amount of hybrid system.

6. Conclusion

The hybrid system based on BSA-PNVCL-*co*-PDMAEMA was successfully synthesized and characterized as a thermal responsive conjugate. BSA was modified with NHS-BIBA, an ATRP initiator. The efficiency of this reaction was verified by SDS-PAGE and calculated by MALDI-ToF, showing that a relevant number of lysine residues present in the protein has been modified. After obtaining the BSA-MI, DMAEMA and NVCL were polymerized from the protein by ATRP using the *grafting-from* strategy. The success of hybrid formation was confirmed by SDS-PAGE, showing a significant increase in the molecular weight, evaluated by MALDI- ToF. DLS was employed to investigate the phase transition behavior of the conjugates in response to temperature. The thermoresponsive behavior of the conjugates in PBS pH 7.4 was demonstrated and adjusted to approximately 39 °C, close to tumor cells temperature. Furthermore, the developed system showed a high encapsulation capacity of the drug cisplatin.

The new hybrid system obtained by combining the benefits of albumin with the responsiveness of polymers shows interesting properties for biomedical applications, especially as a drug delivery system. Furthermore, this system can minimize the side effects caused by antitumor agents used in conventional therapies, optimizing the drug administrations.

7. Work development and scientific production

Part of this work was fulfilled in partnership with the Fraunhofer IAP Institute in Potsdam – Germany, with the collaboration and supervision of Professor Dr. Alexander Böker, Dr. Ulrich Glebe, Maria Mathieu, and Johanes Martin.

During the execution of this work, a review paper was prepared and published in the journal Biomedicine & Pharmacotherapy in collaboration with Professor Dr. Daniel Crístian Ferreira Soares, Professor Dr. Marli Luiza Tebaldi, and Stephanie Calazans Domingues. The full paper is found at the end of this work.

A first article with the results presented in this work, entitled "Polymer-protein conjugation based on PVCL and PDMAEMA by ATRP: New smart hydrides materials," is being prepared in collaboration with Professor Dr. Marli Luiza Tebaldi, Professor Dr. Daniel Cristiam Ferreira Soares, Maria Mathieu, Dr. Ulrich Glebe and Professor Dr. Alexander Böker.

8. Perspectives

As perspectives for the continuity of studies, we may mention:

1- Evaluation of the LCST of the hybrid at different pH;

2- Study of the release profile of cisplatin;

3- Conducting in vitro assays involving tumor and healthy cell cultures aiming to evaluate the cytotoxicity of the system;

4- Conduct in vivo studies to assess the toxicity of the system and to verify its biodistribution.

References

ALEMÁN, J. V. et al. Definitions of terms relating to the structure and processing of sols, gels, networks, and inorganic-organic hybrid materials (IUPAC Recommendations 2007). **Pure and Applied Chemistry**, v. 79, n. 10, p. 1801-1829, 2007.

AN, Fei-Fei; ZHANG, Xiao-Hong. Strategies for preparing albumin-based nanoparticles for multifunctional bioimaging and drug delivery. **Theranostics**, v. 7, n. 15, p. 3667, 2017

ANANIKOV, V.P. Organic—inorganic hybrid nanomaterials. **Nanomaterials** 9, 1197, 2019.

ANVISA, BRAZIL. National Health Surveillance Agency. Resolution of the Collegiate Board of Directors-RDC No. 166. 2017.

BANIHASHEM, Solmaz; NEZHATI, Mahshid Nikpour; PANAHIA, Homayon Ahmad. Synthesis of chitosan-grafted-poly (N-vinylcaprolactam) coated on the thiolated gold nanoparticles surface for controlled release of cisplatin. **Carbohydrate polymers**, v. 227, p. 115333, 2020.

CARMALI, Sheiliza et al. Tertiary structure-based prediction of how ATRP initiators react with proteins. **ACS Biomaterials Science & Engineering**, v. 3, n. 9, p. 2086-2097, 2017.

CARMALI, Sheiliza et al. Tailoring site specificity of bioconjugation using step-wise atom-transfer radical polymerization on proteins. **Biomacromolecules**, v. 19, n. 10, p. 4044-4051, 2018.

CATANZARO, Giuseppina et al. Albumin nanoparticles for glutathione-responsive release of cisplatin: New opportunities for medulloblastoma. **International Journal of Pharmaceutics**, v. 517, n. 1-2, p. 168-174, 2017.

CUMMINGS, Chad et al. Dramatically increased pH and temperature stability of chymotrypsin using dual block polymer-based protein engineering. **Biomacromolecules**, v. 15, n. 3, p. 763-771, 2014.

DASARI, Shaloam; TCHOUNWOU, Paul Bernard. Cisplatin in cancer therapy: molecular mechanisms of action. **European Journal of Pharmacology**, v. 740, p. 364-378, 2014

DE JESÚS-TÉLLEZ, Marco A. et al. Kinetic Investigations of Quaternization Reactions of Poly [2-(dimethylamino) ethyl methacrylate] with Diverse Alkyl Halides. **Macromolecular Chemistry and Physics**, v. 221, n. 9, p. 1900543, 2020.

EVANS, T. W. albumin as a drug—biological effects of albumin unrelated to oncotic pressure. **Alimentary Pharmacology & Therapeutics**, v. 16, p. 6-11, 2002.

FAUSTINI, Marco et al. History of organic–inorganic hybrid materials: prehistory, art, science, and advanced applications. **Advanced Functional Materials**, v. 28, n. 27, p. 1704158, 2018.

FAUSTINI, Marco et al. History of organic–inorganic hybrid materials: prehistory, art, science, and advanced applications. **Advanced Functional Materials**, v. 28, n. 27, p. 1704158, 2018.

GARCIA, Diana R.; LAVIGNAC, Nathalie. Poly (amidoamine)–BSA conjugates synthesised by Michael addition reaction retained enzymatic activity. **Polymer Chemistry**, v. 7, n. 47, p. 7223-7229, 2016.

GORDON, Alan N. et al. Long-term survival advantage for women treated with pegylated liposomal doxorubicin compared with topotecan in a phase 3 randomized study of recurrent and refractory epithelial ovarian cancer. **Gynecologic oncology**, v. 95, n. 1, p. 1-8, 2004.

GRADISHAR, William J. et al. Phase III trial of nanoparticle albumin-bound paclitaxel compared with polyethylated castor oil–based paclitaxel in women with breast cancer. **Journal of clinical oncology**, v. 23, n. 31, p. 7794-7803, 2005.

GU, Hongbo et al. Introducing advanced composites and hybrid materials. **Advanced Composites and Hybrid Materials**, 2018.

HASSANPOUR, Seyed Hossein; DEHGHANI, Mohammadamin. Review of cancer from perspective of molecular. **Journal of Cancer Research and Practice**, v. 4, n. 4, p. 127-129, 2017.

HE, Naipu; LU, Zhenwu; ZHAO, Weigang. pH-responsive double hydrophilic protein-polymer hybrids and their self-assembly in aqueous solution. **Colloid and Polymer Science**, v. 293, n. 12, p. 3517-3526, 2015.

HU, Quanyin; CHEN, Qian; GU, Zhen. Advances in transformable drug delivery systems. **Biomaterials**, v. 178, p. 546-558, 2018

HUSSAIN, Zahid et al. PEGylation: a promising strategy to overcome challenges to cancer-targeted nanomedicines: a review of challenges to clinical transition and promising resolution. **Drug Delivery and Translational Research**, v. 9, n. 3, p. 721-734, 2019.

INCA-**Quimioterapia.** Disponível em:< http://www.inca.gov.br>. Acesso em 10 setembro 2020

J. V. Alemán, A. V. Chadwick, J. He, M. Hess, K. Horie, R. G. Jones, P. Kratochvíl, I. Meisel, I. Mita, G. Moad, S. Penczek, R. F. T. Stepto, Pure Appl. Chem. 2007, 79, 1801.

JAHANBAN-ESFAHLAN, Ali et al. Recent developments in the detection of bovine serum albumin. **International Journal of Biological Macromolecules**, v. 138, p. 602-617, 2019.

JI, Xiaotian; LIU, Li; ZHAO, Hanying. The Synthesis and self-assembly of bioconjugates composed of thermally-responsive polymer chains and pendant lysozyme molecules. **Polymer Chemistry**, v. 8, n. 18, p. 2815-2823, 2017.

JIANG, Xiuyu et al. A novel poly (N-vinylcaprolactam)-based well-defined amphiphilic graft copolymer synthesized by successive RAFT and ATRP. **Polymer Chemistry**, v. 4, n. 5, p. 1402-1411, 2013.

JIANG, Xiuyu et al. A novel poly (N-vinylcaprolactam)-based well-defined amphiphilic graft copolymer synthesized by successive RAFT and ATRP. **Polymer Chemistry**, v. 4, n. 5, p. 1402-1411, 2013.

KELLAND, Lloyd. The resurgence of platinum-based cancer chemotherapy. **Nature Reviews Cancer**, v. 7, n. 8, p. 573-584, 2007.

KAUPBAYEVA, Bibifatima; RUSSELL, Alan J. Polymer-enhanced biomacromolecules. **Progress in Polymer Science**, v. 101, p. 101194, 2020.

KHODER, Mouhamad et al. Efficient approach to enhance drug solubility by particle engineering of bovine serum albumin. **International Journal of Pharmaceutics**, v. 515, n. 1-2, p. 740-748, 2016.

KOZANOĞLU, Selin; ÖZDEMIR, Tonguç; USANMAZ, Ali. Polymerization of N-vinylcaprolactam and characterization of poly (N-vinylcaprolactam). **Journal of Macromolecular Science, Part A**, v. 48, n. 6, p. 467-477, 2011.

KUDARHA, Ritu R.; SAWANT, Krutika K. Albumin based versatile multifunctional nanocarriers for cancer therapy: fabrication, surface modification, multimodal therapeutics and imaging approaches. **Materials Science and Engineering: C**, v. 81, p. 607-626, 2017.

KUDARHA, SAWANT 2017

LANGER, Robert. New methods of drug delivery. **Science**, v. 249, n. 4976, p. 1527-1533, 1990.

LANGER, Robert; PEPPAS, Nicholas A. Advances in biomaterials, drug delivery, and bionanotechnology. **AIChE Journal**, v. 49, n. 12, p. 2990-3006, 2003.

LAVAN, David A.; MCGUIRE, Terry; LANGER, Robert. Small-scale systems for in vivo drug delivery. **Nature biotechnology**, v. 21, n. 10, p. 1184-1191, 2003.

LI, Jinhua et al. Binding of carbendazim to bovine serum albumin: Insights from experimental and molecular modeling studies. **Journal of Molecular Structure**, v. 1139, p. 303-307, 2017.

LI, Yunfang; YANG, Guangzhong; MEI, Zhinan. Spectroscopic and dynamic light scattering studies of the interaction between pterodontic acid and bovine serum albumin. **Acta Pharmaceutica Sinica B**, v. 2, n. 1, p. 53-59, 2012.

Ma, D., 2019. Hybrid Nanoparticles: An Introduction. pp. 12–15. https://doi.org/10.1016/ B978-0-12-814134-2.00001-2.

MANOURAS, Theodore et al. A facile route towards PDMAEMA homopolymer amphiphiles. **Soft Matter**, v. 13, n. 20, p. 3777-3782, 2017.

MESSINA, Marco S. et al. preparation of biomolecule-polymer conjugates by grafting-from using ATRP, RAFT, or ROMP. **Progress in Polymer Science**, v. 100, p. 101186, 2020.

MOHAMMED, Marwah N.; YUSOH, Kamal Bin; SHARIFFUDDIN, Jun Haslinda Binti Haji. Poly (N-vinyl caprolactam) thermoresponsive polymer in novel drug delivery systems: a review. **Materials Express**, v. 8, n. 1, p. 21-34, 2018.

MURATA, Hironobu et al. Polymer-based protein engineering can rationally tune enzyme activity, pH-dependence, and stability. **Biomacromolecules**, v. 14, n. 6, p. 1919-1926, 2013.

PAKEN, Jessica et al. Cisplatin-associated ototoxicity: a review for the health professional. **Journal of Toxicology**, v. 2016, 2016.

PRECUPAS, Aurica; SANDU, Romica; POPA, Vlad T. Quercetin influence on thermal denaturation of bovine serum albumin. **The Journal of Physical Chemistry B**, v. 120, n. 35, p. 9362-9375, 2016.

PFISTER, David; MORBIDELLI, Massimo. Process for protein PEGylation. **Journal of Controlled Release**, v. 180, p. 134-149, 2014.

QIAN, Wenhao et al. Synthesis of PAA-g-PNVCL Graft Copolymer and Studies on Its Loading of Ornidazole. **Chinese Journal of Chemistry**, v. 32, n. 10, p. 1049-1056, 2014.

QIN, Si-Yong et al. Drug self-delivery systems for cancer therapy. **Biomaterials**, v. 112, p. 234-247, 2017

SALEHIABAR, Marziyeh et al. Production of biological nanoparticles from bovine serum albumin as controlled release carrier for curcumin delivery. **International Journal of Biological Macromolecules**, v. 115, p. 83-89, 2018.

RYAN, Sinéad M. et al. Advances in PEGylation of important biotech molecules: delivery aspects. **Expert Opinion on Drug Delivery**, v. 5, n. 4, p. 371-383, 2008.

SHAO, Lidong et al. RAFT polymerization of N-vinylcaprolactam and effects of the end group on the thermal response of poly (N-vinylcaprolactam). **Reactive and Functional Polymers**, v. 72, n. 6, p. 407-413, 2012.

SOARES, Daniel Crístian Ferreira et al. Polymer-hybrid nanoparticles: Current advances in biomedical applications. **Biomedicine & Pharmacotherapy**, v. 131, p. 110695, 2020.

SRINIVASARAO, Madduri; LOW, Philip S. Ligand-targeted drug delivery. **Chemical reviews**, v. 117, n. 19, p. 12133-12164, 2017.

TEBALDI, Marli Luiza et al. Dual-Stimuli Sensitive Hybrid Materials: Ferritin–PDMAEMA by Grafting-From Polymerization. **Macromolecular Chemistry and Physics**, v. 218, n. 11, p. 1600529, 2017

TEBALDI, Marli Luiza et al. Poly (-3-hydroxybutyrate-co-3-hydroxyvalerate)(PHBV): Current advances in synthesis methodologies, antitumor applications and biocompatibility. **Journal of Drug Delivery Science and Technology**, v. 51, p. 115-126, 2019.

TEBALDI, Marli Luiza. et al. Synthesis of stimuli-sensitive copolymers by RAFT polymerization: potential candidates as drug delivery systems. **Materials Research**, v. 17, p. 191-196, 2014.

TIWARI, Rahul et al. Cisplatin-loaded albumin nanoparticle and study their internalization effect by using β-cyclodextrin. **Journal of Receptors and Signal Transduction**, v. 41, n. 4, p. 393-400, 2021.

UNTERLASS, Miriam M. Green synthesis of inorganic–organic hybrid materials: State of the art and future perspectives. **European Journal of Inorganic Chemistry**, v. 2016, n. 8, p. 1135-1156, 2016.

VANPARIJS, Nane et al. Polymer-protein conjugation via a 'grafting to'approach–a comparative study of the performance of protein-reactive RAFT chain transfer agents. **Polymer Chemistry**, v. 6, n. 31, p. 5602-5614, 2015.

VERONESE, Francesco M.; MERO, Anna. The impact of PEGylation on biological therapies. **BioDrugs**, v. 22, n. 5, p. 315-329, 2008.

VIEIRA, Débora Braga; GAMARRA, Lionel Fernel. Avanços na utilização de nanocarreadores no tratamento e no diagnóstico de câncer. **Einstein (São Paulo)**, v. 14, n. 1, p. 99-103, 2016.

WANG, Jun; ZHANG, Bingbo. Bovine serum albumin as a versatile platform for cancer imaging and therapy. **Current Medicinal Chemistry**, v. 25, n. 25, p. 2938-2953, 2018.

WANG, Yaping et al. Doxorubicin/cisplatin co-loaded hyaluronic acid/chitosan-based nanoparticles for in vitro synergistic combination chemotherapy of breast cancer. **Carbohydrate Polymers**, v. 225, p. 115206, 2019.

YANG, Yaozong et al. High-efficiency synthesis of well-defined cyclic poly (N-vinylcaprolactam) and its solution properties. **Polymer**, v. 68, p. 213-220, 2015.

ZHANG, Hongmei et al. Changing the activities and structures of bovine serum albumin bound to graphene oxide. **Applied Surface Science**, v. 427, p. 1019-1029, 2018.

ZHAO, Shurui et al. Nano-scaled MTCA-KKV: for targeting thrombus, releasing pharmacophores, inhibiting thrombosis and dissolving blood clots in vivo. **International Journal of Nanomedicine**, v. 14, p. 4817, 2019.

ZHELAVSKYI, Oleksii S.; KYRYCHENKO, Alexander. Atomistic molecular dynamics simulations of the LCST conformational transition in poly (N-vinylcaprolactam) in water. **Journal of Molecular Graphics and Modelling**, v. 90, p. 51-58, 2019.

Annex 1- Paper published

Paper: "Polymer-hybrid nanoparticles: Current advances in biomedical applications" Authors: Daniel Crístian Ferreira Soares, Stephanie Calazans Domingues, Daniel Bragança Viana and Marli Luiza Tebald.

Biomedicine & Pharmacotherapy 131 (2020) 110695

Contents lists available at ScienceDirect

Biomedicine & Pharmacotherapy

journal homepage: www.elsevier.com/locate/biopha

Review

Polymer-hybrid nanoparticles: Current advances in biomedical applications

Daniel Crístian Ferreira Soares *, Stephanie Calazans Domingues, Daniel Bragança Viana, Marli Luiza Tebaldi

Universidade Federal de Itajubá, campus Itabira, Laboratório de Bioengenharia, Rua Irmã Ivone Drumond, 200, Itabira, Minas Gerais, Brazil

ARTICLE INFO

Keywords:
Polymer-hibrid nanoparticles
Lipid-polymer hybrid nanoparticle
Hybrid silica nanoparticles

ABSTRACT

The unique properties of polymer-hybrid nanosystems enable them to play an important role in different fields such as biomedical applications. Hybrid materials, which are formed by polymer and inorganic- or organic-base systems, have been the focus of many recently published studies whose results have shown outstanding improvements in drug targeting. The development of hybrid polymer materials can avoid the synthesis of new molecules, which is an overall expensive process that can take several years to get to the proper elaboration and approval. Thus, the combination of properties in a single hybrid system can have several advantages over non-hybrid platforms, such as improvements in circulation time, structural disintegration, high stability, premature release, low encapsulation rate and unspecific release kinetics. Thus, the aim of the present review is to outline a rapid and well-oriented scenario concerning the knowledge about polymer-hybrid nanoparticles use in biomedical platforms. Furthermore, the ultimate methodologies adopted in synthesis processes, as well as in applications *in vitro/in vivo,* are the focus of this review.

1. Introduction

Nanostructured systems have been considered by many researchers the most powerful tool to find materials with unique chemical and physical properties [1,2]. Likewise, nanosystems have been the focus of different biotech research projects in the biomedical context, whose aims were only reached through the use of nanocarriers distributed in a plethora of inorganic and organic nanosystems. Among these aims, it is worth highlighting controlled and sustained target release, protection from degradation and reduction of side-effects [3–7].

Important advancements in preclinical and clinical studies have been achieved, since single/combined drugs or gene delivery were successfully used where functionalized nanocarriers were applied to. Thus, the substantial increase in the number of published studies in the last few years can explain significant improvements in the effectiveness and safety of well-established drugs due to the use of nanocarrier systems. This approach avoids the development of new molecules, which is overall an expensive process that can take several years to be properly elaborated. Simultaneously, substantial advancements in the biomedical application of nanostructured systems were achieved due to the understanding of how the properties such as the size, shape, and surface chemistry are capable of significantly changing the behavior of these materials, both *in vitro* and *in vivo*. Nowadays, the management of these properties has enabled rational drug-delivery systems capable of reaching different tissues in the human body, focusing singular aims [8–14].

Other advancements refer to the development of hybrid nanosystems capable of combining different organic-organic and organic-inorganic materials; superior features can be achieved through the combination of materials with different chemical compositions. Polymer-hybrid nanoparticles can be prepared based on the combination of inorganic constituents such as metal oxide nanoparticles, graphene, carbon nanotubes, silica and polymers. On the other hand, blending organic compounds (phospholipids, proteins and lipids) to natural or synthetic polymers can result in novel hybrid nanosystems capable of combining the advantages of these biomacromolecules to those of tailor-made synthetic polymers. The combination of different properties in hybrid systems can enable several sets of advantages over non-hybrid platforms, such as improvements in bloodstream circulation time, premature leakage, low encapsulation rate and unspecific release kinetics [15–17]. Furthermore, synthetic tunability enables preparing nanoparticles to co-encapsulate different therapeutic/treatment agents presenting different release profiles in order to simultaneously cover dissimilar therapeutics or imaging modalities [18,19].

More specifically, hybrid nanosystems have been used in many recent projects focused on cancer treatment that have been achieving

* Corresponding author.
E-mail address: soares@unifei.edu.br (D.C. Ferreira Soares).

https://doi.org/10.1016/j.biopha.2020.110695
Received 19 June 2020; Received in revised form 5 August 2020; Accepted 26 August 2020
Available online 10 September 2020

Table 1
Some examples and applications of hybrid nanoparticles formulated to enable the delivery of important therapeutic agents.

Hybrid	Encapsulated drug	Main Features	Authors (Ref.)
LPHNPs	Docetaxel	Clearance behavior of NPs in mice up to 72 h after the injection.	Dehaini, D. et al. [20]
	Gemcitabine hydrochloride (GEM)	Longer circulation time; GEM-loaded LPHNs can be used to enhanceantitumor drug effectiveness in breast cancer treatments.	Yalcin, T.E.et al. [21]
	Methotrexate (MTX)	Results of characterization *in vitro* have shown promising therapeutic effectiveness after drug dose reduction.	Tahir, N. et al. [22]
	Cisplatin	Promising platform to enable controlled cisplatin delivery in cancer therapy.	Khan, M.M. et al. [23]
	Paclitaxel	Enhances the EPR effect; Promising for oral delivery of PTX against resistant breast cancer.	Danhier, F. et al. and Zhang, T. et al. [24,25]
Micelles	Cisplatin	No significant toxicity effects on MCF-7 cell line; Very promising approach used for cisplatin delivery.	Rezaei, S.J. T. et al. [26]
	Cisplatin	The coupling of platinum (IV) complexes to dendrimers is a strategy that leads to compounds with promising biological activity;	Sommerfeld, N.S.et al. [27]
Dendrimers	Docetaxel	The dendrimer-based theranostic nanoplatform is promising for targeted chemotherapy and CT imaging of FAR-expressing tumors *in vivo*.	Zhu, J.et al. [28]
	Plitidepsin	Plitidepsin-containing carriers was evaluated in four cancer cell-lines and showed similar anticancer activity in the current standard drug formulation.	Fedeli, E. et al. [29]
	Simvastatin	Activity against human prostate cancer	Sedki, M. et al. [30]
Magnetic nanoparticles	Curcumin	The anticancer properties of nanocarriers were evidently shown by cytotoxic studies conducted with MCF-7 breast cancer cell lines.	Kamaraj, S. et al. [31]
	Doxorubicin	DOX release percentage in hybrid nanogels was more than that of hollow ones, whereas hollow nanogels presented higher loading capacity	Hajebi, S. *et.al.* [32]
Nanogels	Dexibuprofen	Highly porous and amorphous nanogels have shown significant dexibuprofen release in aqueous medium; Formulations are nontoxic and biocompatible.	Khalid, Q. et al. [33]

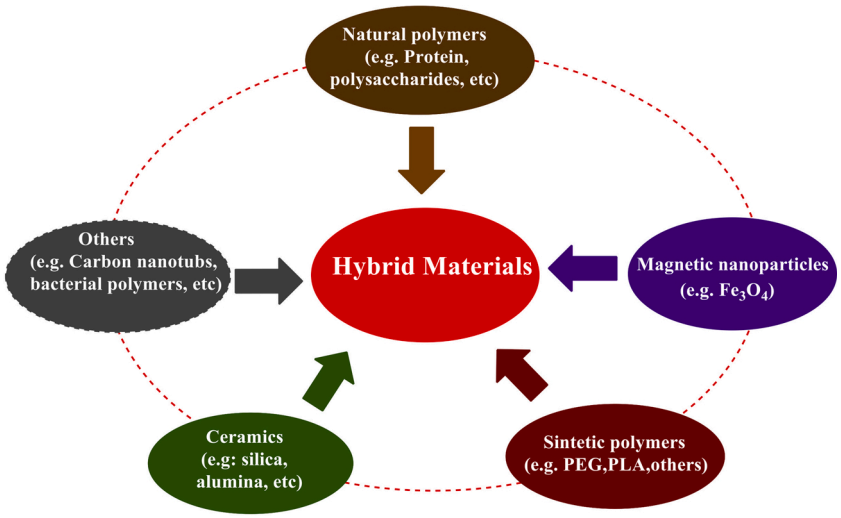

Fig. 1. Hybrid conjugates organic-organic or inorganic-inorganic combining the proprieties of two or more materials. They include MNPs, ceramics, carbon nanotubs, natural polymers and others.

relevant results. Table 1 summarizes examples and applications of hybrid nanoparticles recently formulated to enable the delivery of important anticancer therapeutic agents.

2. Why to synthesize hybrid conjugates?

The main goal of using polymers in conjugates to produce hybrid materials for drug delivery applications lies on stabilizing and improving the therapeutic activity of standalone drugs, because there is urgent demand for the development of effective carrier systems. The combination of two or more materials can change their individual properties and create hybrid materials with new and unique features. Synergistic and hybrid properties derive from the extremely high superficial surface area among the phases, in which the physical and chemical properties of polymers can be transmitted to inorganic materials (or biological polymers); consequently, they can change biodistribution, solubility and improve the system stability. Furthermore, the conjugation among the materials can increase bloodstream circulation time, as well as maintain biological actions. Fig. 1 shows the possibilities of finding hybrid materials.

Attaching synthetic polymers at atomic level, rather than blending them, is a significant breakthrough in polymer science since it enables combining the advantageous properties of both polymers, without inconveniences such as the separation phase, which is seen when natural polymers or inorganic particles get blended. This process has a mutlfold set of advantages, but its main focus lies on increasing conjugates solubility and/or stabilit and, consequently, on decreasing toxicity of the system [34–36]. More specifically, the delivery of cytotoxic drugs, such as antitumor agents, requires advanced therapeutic strategies because, nowadays, these drugs are based on conventional systemic biodistribution and present low specificity and selectivity [37]. For example, although metals have favorable magnetic properties, their high toxicity profile makes them unsuitable for biomedical use without proper and stable surface treatment [36]. On the other hand, although proteins present high activity and specificity, they have some limitations such as inherent protein biorecognition and, consequently, short half-life, poor stability, low solubility and immunogenicity.

Surface conjugation of polymers in proteins has rectified these

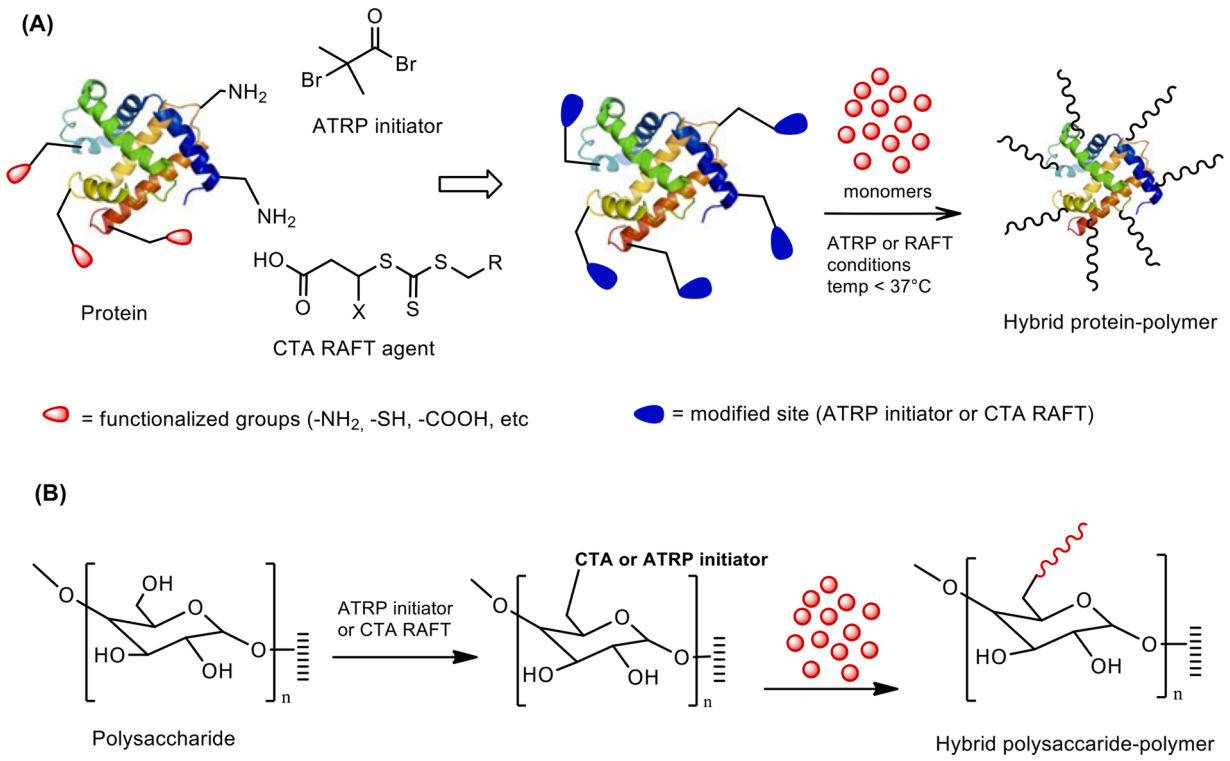

Fig. 2. (A) Grafting-from or *in situ* polymerization approach for synthesizing conjugates hybrid protein-polymer and (B) hybrid polysaccharide-polymer.

shortcomings, since protein-polymer conjugates have improved their physical stability, increased their half-life and made them non-immunogenic. Furthermore, these conjugates show a unique combination of properties deriving from both biologic and synthetic materials that can be individually used to elicit the desired effect [38]. Different synthetic pathways can be used to generate hybrid materials; however, the current study focused on the synthesis of hybrid nanoparticles based on the living radical polymerization technique, the so-called "Reversible Deactivation Radical Polymerization" (RDRP), with emphasis on conjugates enabled through the "grafting-from" approach.

3. Chemical changes for hybrid obtaiment purposes

Abuchowski et al. have conjugated monomethoxy-PEG (mPEG) to bovine serum albumin (BSA) for the first time in 1977 [39]. The generated conjugates have shown lower immunogenic response in animal models than the BSA native protein. After this discovery, researchers have found a promising field to develop new formulations with fewer side effects in several diseases, mainly chemotherapy drugs. Subsequently, new scientific studies started investigating the use of PEG conjugates, mainly of PEG-proteins, in both organic and inorganic conjugates due to their hydrophilic and neutral nature. Furthermore, PEG presents low opsonization rates and long circulation time in the bloodstream, which is the reason why it was approved by the Food and Drug Administration (FDA) [40]. The first PEGylated protein was approved by the FDA in 1990. Since then, PEG bioconjugation has been extensively used for protein modification purposes, which enabled several PEGylated proteins to be approved for clinical use [41]. Although only PEG conjugates are currently available in the market, many formulations with alternative polymers are under development and/or at stage 3 of clinical trials [41,42]. It is worth mentioning that when the first conjugates were merged, the adopted synthesis strategies required multiple steps or complex purification procedures, which led to final products presenting low yield, as well as hindered the progress in the field and the approval of these conjugates [40].

The need of synthesizing macromolecules with controlled sequences and configurations has led to advancements in polymer synthesis, mainly to reversible deactivation radical polymerization (RDRP) techniques, such as Atom Transfer Radical Polymerization (ATRP) or

Reversible Addition-Fragmentation Chain Transfer (RAFT). These approaches enable controlling chain length, monomer content and, to some degree, the monomer sequence, in an accurate and reproducible way [43]. RDRP techniques are efficient in forming conjugates both on organic surfaces, such as proteins or other natural polymers, and on inorganic surfaces, such as silica, iron oxide, carbon nanotubes, among others. The current study has addressed the latest advancements in generating these conjugates based on RDRP.

3.1. Advancements in organic-organic hybrid nanoparticles

The development of RDRP techniques has expanded the versatility in the synthesis of new hybrid conjugates. Overall, conjugation processes based on RDRP approaches, whose basic principle lies on introducing an anchoring layer in a given substrate (organic or inorganic), enable polymers for grafting-to, grafting-from, or grafting-through the substrate. Both strategies were already well described in several reviews and articles [44–47].

The grafting-from approach is the most efficient and promising strategy based on RDRP [48]. According to this approach, a protein [Fig. 2A) or another precursor such as polysaccharides (cellulose, chitosan, starch, among others) [Fig. 2B] is firstly modified by using an initiator to enable polymerization or reversible addition-fragmentation chain transfer (RAFT). Subsequently, the polymerization process is enabled by the modified precursor, mainly through ATRP or RAFT polymerization [49]. The major advantage of the grafting-from approach lies on the purification of the generated conjugates. They can be purified through simple dialysis, which enables removing the unreacted monomer, the initiator, among others. On the other hand, the grafting-to approach often presents low reaction yield. In addition, the purification between two large molecules is often tedious and requires using preparative gel-filtration chromatography. The advantage of grafting-to lies on pre-synthesized polymer use, which allows

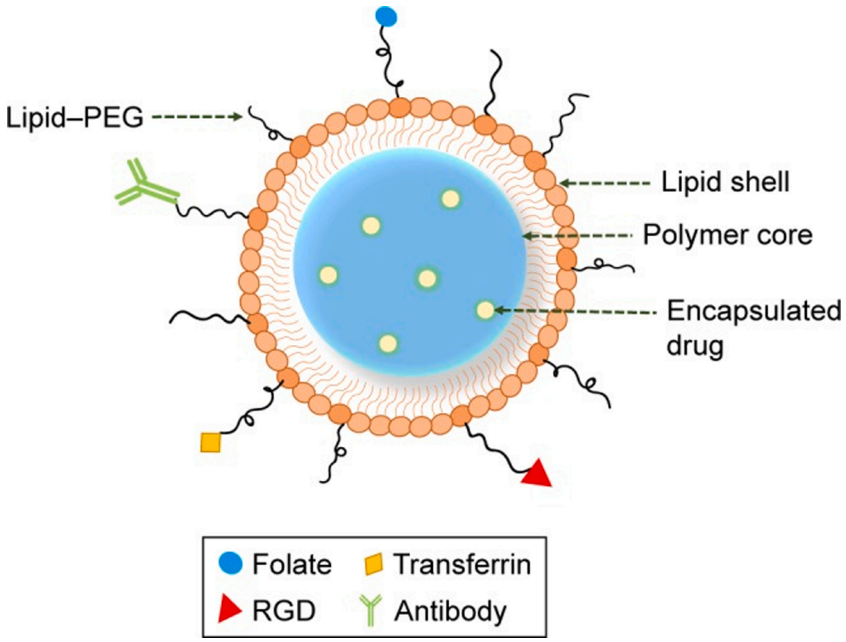

Fig. 3. The general structure of a lipid-polymer hybrid nanoparticle (LPHNP) that contains a core constituted by polymer chains and encapsulated drug. The lipid portion is located in the exterior layer (shell) in which is capable to be conjugated to different target agents (arginylglycylaspartic acid - RDG), antibodies, folate, transferrin, and other small lipid-PEG chains. reproduced with permission from Mukherjee et al., 2019 [47].

characterizing it. Furthermore, in the case of protein-polymer conjugates, this approach avoids protein exposure to potentially denaturing polymerization conditions [50]. Finally, the grafting-from approach enables preparing polymers with high grafting degree by using modified surfaces due to low steric hindrance during polymerization [44,48]. The advantages and disadvantages of the three main RDRP approaches are well summarized in our previous study review [51].

Protein/polymer conjugation can improve the stability, increase the solubility and enhance the systemic circulation of different proteins, as well as acting reducing the immunogenicity and antigenicity, which can lead to several interesting applications in the biomedical field [52]. Several proteins were transformed into macroinitiators or macro Chain Transference Agents (CTAs) [53] and applied for conjugate synthesis purposes, based on the use of different monomers [51,54–56]. Polysaccharides present highly hydrophilic structures; thus, their conjugation with different types of organic and inorganic nanoparticles, can significantly enhance their solubility in aqueous medium - these conjugates can self-assemble in nanostructures. In addition, when it comes

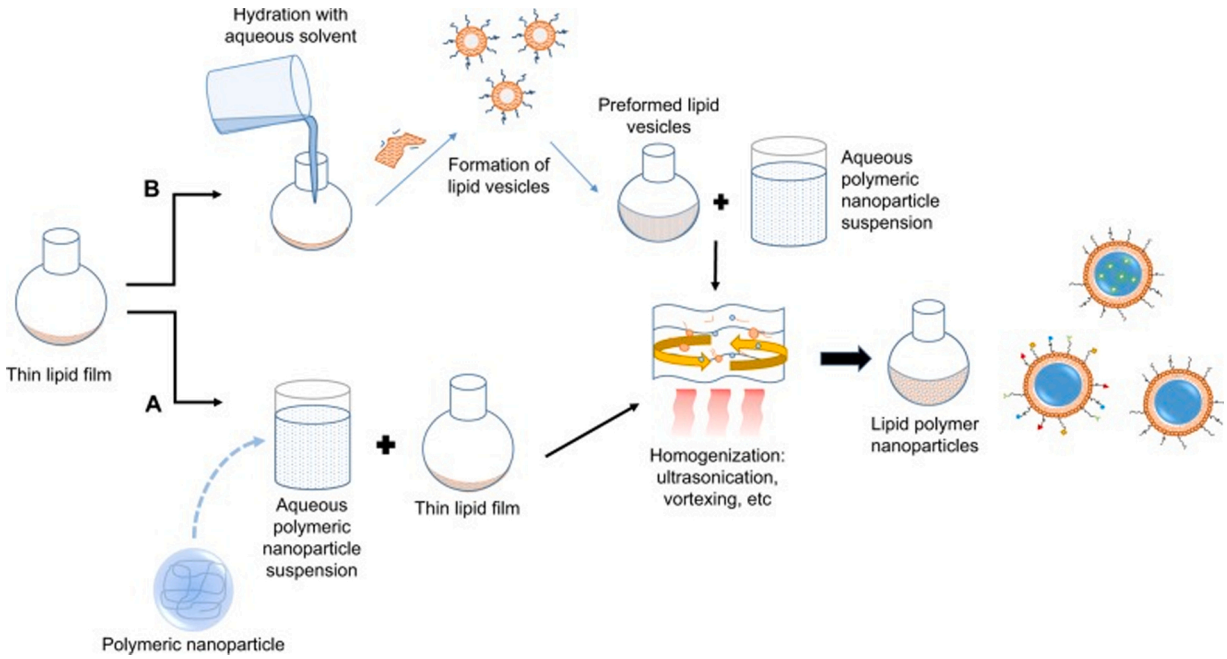

Fig. 4. Different approaches to prepare lipid-polymer hybrid nanoparticles (LPHNPs) through the two-step method. In the method (A) an aqueous suspension of polymeric nanoparticles is added to the pre-formed thin lipidic film. On the other hand, in the method (B), pre-formed lipid vesicles are added to the polymeric nanoparticles. In both methods, the next step is the homogenization phase were the hybrid nanoparticles are obtained. Reproduced with permission from Mukherjee et al., 2019 [47].

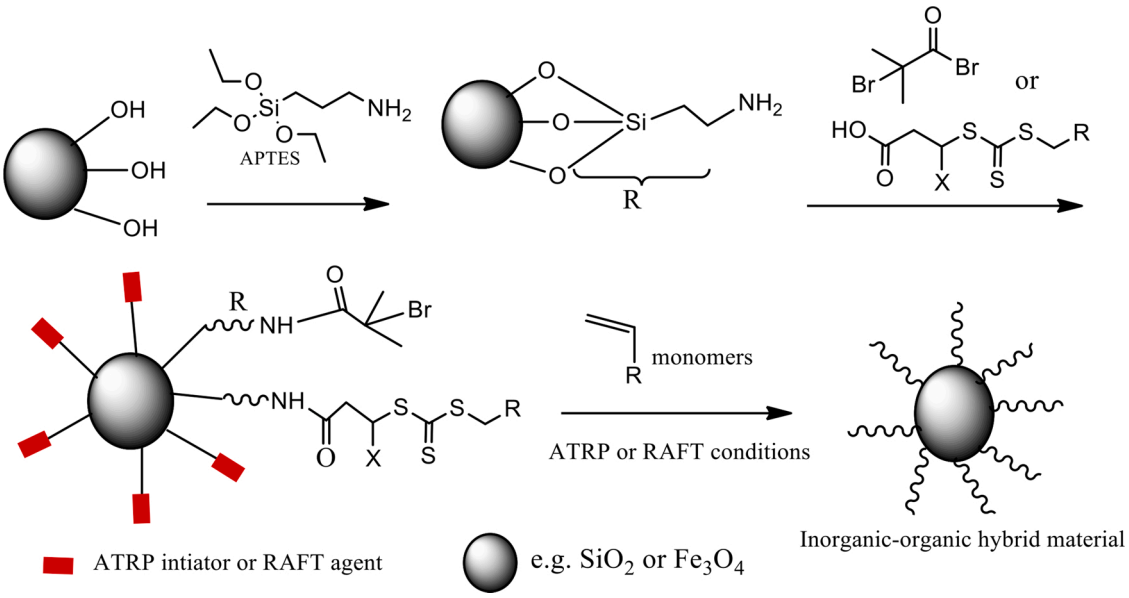

Fig. 5. Schematic illustration of the synthesis of hybrid nanoparticles (silica or iron oxide) coated with synthetic polymers *via* "grafting-from".

to drug delivery applications, they show longer circulation time in the bloodstream and significantly accumulate in tumor tissues [57].

Lipid–polymer hybrid nanoparticles (LPHNP) are another nanoparticle class that has emerged as the next-generation drug delivery platform. Polymeric nanoparticles (NPs) and lipid nano-carriers (*e.g.*, solid lipid nanoparticles and/or liposomes) are two different drug delivery systems; some formulations were approved by the US FDA for clinical use. However, each of these systems presented some drawbacks such as rapid drug diffusion and leakage, non-specific release, dose-related toxicity and uncontrolled drug release, when they were used as carriers, in separate [22]. These LPHNP classes have emerged to overcome the disadvantages of using polymeric nanoparticles and lipid systems, in separate. They consist in three different components, as shown in Fig. 3: (*i*) inner polymeric core enclosing the active therapeutic moiety; (*ii*) lipid monolayer surrounding the polymer core, and (*iii*) outer lipid–PEG layer, whose function lies on stabilizing and prolonging the systemic circulation to assure longer particle retention time in the body [47]. Given their distinctive structural design, LPHNs show high mechanical integrity and stability *in vivo*, as well as optimized drug entrapment and favorable pharmacokinetic profile. A recent study conducted by Yalcin et al. (2020) has investigated the application of antitumoral drug gemcitabine hydrochloride (GEM) loaded LPHNs to enhancepatients' chemotherapeutic response. Pharmacokinetic studies *in vivo* conducted with rats have investigated the advantage of GEM-loaded LPHNs over the commercial product Gemko®; GEM-loaded LPHNs presented longer circulation time [21].

Conventional methods used to prepare LPHNPs in the first studies comprised two stages, as shown in Fig. 4. A) Direct addition of previously formed polymeric NPs to dried lipid film, or B) preformed NPs addition to preformed lipid vesicles, based on the initial hydration of thin lipid films [47]. Nowadays, other nonconventional methods and optimized methodologies have been used to produce LPHNPs; among them, one finds the spray drying process [58] or single-step nanoprecipitation method [23] or emulsification–solvent evaporation [59].

3.2. Advancements in inorganic-organic hybrids

Despite the substantial advancements in the delivery system field in the last two decades, which enabled developing significant amounts of therapeutic agents, some challenges are yet to be overcome. In fact, the development of advanced technologies plays an essential role in assuring successful drug delivery in target sites. To the best of our knowledge, these inorganic-organic hybrids were not yet approved by the FDA for clinical use; however, many formulations are currently under evaluation in clinical trials; thus, their approval remains pending [5]. Therefore, further research efforts should aim at overcoming the existing technical challenges in oral drug delivery systems in order to prove their feasibility for clinical use [60].

The same techniques used for organic-organic hybrid preparation purposes can also be adopted for inorganic-organic hybrid synthesis, according to which, organic polymers are covalently linked to the surface of inorganic precursors such as magnetic nanoparticles [36,37,61], silica [62], metal-organic frameworks (MOFs) [63], among others. As previously mentioned, the grafting-from method uses polymerization initiators connected by covalent bond to the surface of the substrate to form polymer chains on inorganic (or organic) surfaces. This method can be applied to the surface of several geometric forms, such as nanoparticles and porous materials (*e.g.* silica), metals, metal oxides and natural compounds. Furthermore, it enables the production of hybrid materials with high grafting density [64].

Silica is one of the most versatile solid substrates; based on the synthesis method by Stöber, it is readily available in a wide variety of particle sizes, with high uniformity and narrow size distributions. Many researchers have produced hybrid materials using silica as RDRP precursor to enable greater control over synthesized nanoparticles [65,66]. Studies about controlled drug delivery systems have been widely expanded by the combination between mesoporous silica nanoparticles and several polymers. Silica polymer conjugates can control drug release, prevent premature drug leakage, provide sustained drug release and, consequently, improve therapeutic index and mitigate adverse effects [67,68].

Another important class of inorganic nanoparticles lies on magnetic nanoparticles (MNPs) based on metals and oxide metals. Unfortunately, metallic nanoparticles have high toxicity and oxidative sensitivity, and it makes them unsuitable for biomedical use without proper and stable surface treatment [36,69]. The overall scheme used for hybrid nanoparticle preparation is shown in Fig. 5. Firstly, nanoparticles (silica or iron oxide) were functionalized with APTES (3-aminopropyltriethoxy silane) and subjected to sequential reactions to 2-bromoisobutyrate (ATRP initiator) [65] or RAFT transfer agent [66]. Finally, the system was grafted with synthetic polymers.

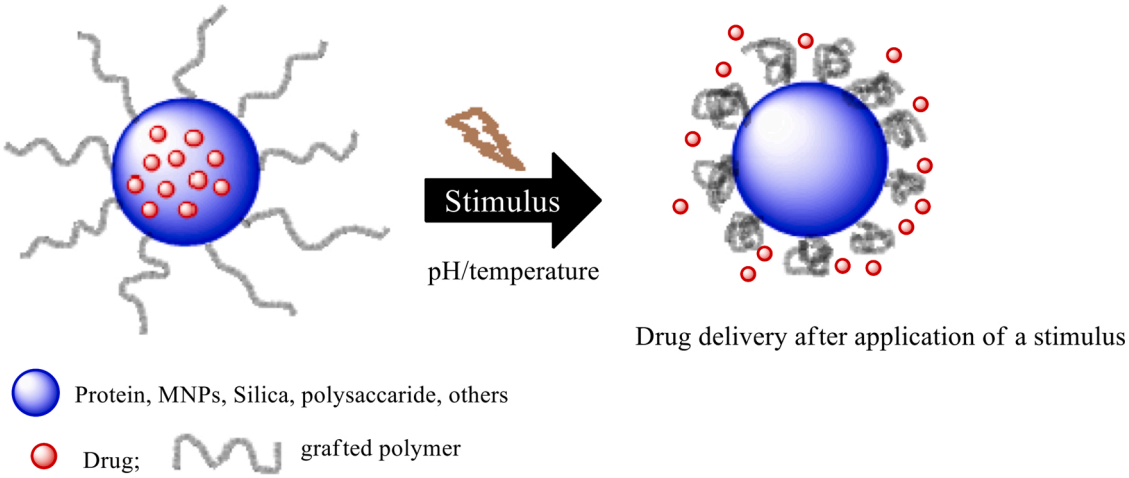

Fig. 6. Mechanism of a drug delivery system after stimulus application or tumor environments.

3.3. Synthesis of smart hybrid materials

Smart conjugated polymers are an important class of novel materials used for several advanced applications, with emphasis on drug delivery. These materials are amphiphilic macromolecules capable of possessing hydrophilic and hydrophobic portions. The hydrophilic portion can be uncharged or charged (anionic, cationic or zwitterionic) and interact with surrounding water molecules, whereas the hydrophobic portion is often composed of hydrocarbon chains that tend to minimize its exposure to water [70].

Nowadays, studies focus on investigating the stimulus-sensitive nanocarriers for drug delivery purposes, with emphasis on the likelihood of controlling drug delivery and release to a specific site at the desired time. Some polymers can introduce smart behaviors that respond to external stimuli such as conformation changes, solubility, changes in hydrophilic and hydrophobic balance, as well as in the release behavior of drug molecules. The most important smart delivery systems are the ones whose pH, temperature, ionic strength, light and redox potential stimuli can be changed.

Temperature- and pH-sensitive materials are the most widely explored stimuli for drug delivery applications in cancer treatment research, since the microenvironment around tumor cells is different from that surrounding healthy cells (lower pH and higher temperature); moreover, such a microenvironment can be use for passive targeting. For example, pH-sensitive nanoparticulate systems remain stable at physiologic pH 7.4, but they degrade to release the active drug target tissues presenting lower pH values [70]. On the other hand, temperature-sensitive nanosystems can destabilize their structure in tumor environments to enable controlled drug release [71]. Fig. 6 shows the mechanism of a drug delivery system after a stimulus application on tumor environments.

The review conducted by Lombard et al. (2019) [71] has described recent advancements in smart nanocarriers composed of organic and inorganic materials used for drug delivery applications. The ability to accurately control chain length and the architecture of hybrid materials based on RDRP techniques may result in smart surfaces with improved properties for application in molecular biology and in the science of materials. The ATRP and RAFT techniques can enable site-specific changes in a given precursor (organic or inorganic) and maintain conjugate's bioactivity. Combining the broad range of available monomers, initiators and catalysts for ATRP and RAFT polymerization - based on the grafting-from method (*in situ* polymerization) to graft polymers on proteins, silica, iron oxide, among others, - enables developing smart hybrid materials with stimuli-responsive polymers capable of responding to external triggers such as temperature and pH and of maintaining the biological activity. This type of radical polymerization aims at reducing termination reactions and at enabling control over molecular weight; its distribution has enabled access to complex architectures and site-specific functions that were previously unachievable through conventional radical polymerizations. The uniformity in resulting properties is extremely important for therapeutic applications, as well as for the FDA approval [40,72].

4. Cellular uptake and cytotoxicity studies

Khan and collaborators (2019) have prepared hybrid nanoparticles based on lipid-chitosan (LPHNPs) use as potential carrier for cisplatin delivery [23]. The aforementioned authors have reported the superior biocompatibility of the system due to the combination of natural polymer chitosan and phospholipid S75 (soybean with 74 % of phosphatidylcholine). Different chitosan/lipid ratios were tested to get to the optimum features, which were achieved at lipid-polymer ratio of 20:1. The improved formulation has shown mean size of 200 nm and 89.2 % drug loading efficiency.Cell viability tests were applied to A2780 cells (ovarian carcinoma cells) treated with different concentrations of blank and cisplatin-loaded nanoparticles. Collected data have shown that blank nanoparticles were not capable of inducing significant cytotoxicity in the tested cells. On the other hand, cells treated with cisplatin solution or cisplatin-loaded LPHNPs presented a significantly cytotoxic profile. According to these authors, such findings can be explained by the relevant cell uptake of hybrid nanoparticles. Flow cytometry and fluorescence microscopy techniques have shown that LPHNPs loaded with Rhodamine (Rh-PE- red fluorescence) and Hoechst (blue fluorescence) dyes were successfully internalized by cells through the interaction between cell membrane and the lipid layer of nanoparticles [73].

Cisplatin-loaded chitosan hybrid nanoparticles proposed and produced by the authors have shown relevant lack of initial cisplatin burst release due to its entrapment in the inner polymer region, which is protected by outer lipid cover. Furthermore, cisplatin presented prolonged and controlled release profile in the experiments, and this outcome was attributed to the lipid layer of the system and, to a lesser extent, to the polymer matrix whose release depends exclusively on the diffusion process.

Yalcin et al. (2020) have produced LPHNs based on the use of DSPE-mPEG$_{2000}$ [phosphatidylcholine (SPC), and 1,2-distearoyl-sn-glycero-3-phosphoethanolamine-N-[methoxy (polyethylene glycol)-2000] (ammonium salt)], PLGA 50:50 and PLGA 65:35 (60:40 mass ratio) added with the antitumor drug 'Gemcitabine' (GEN) [74]. The aforementioned authors have evaluated the ability of the system to enhance GEN's chemotherapeutic response. Fluorescence imaging experiments conducted with MDA-MB-231 and MCF-7 cells (human breast cancer), based on labeled LPHNs (coumarin-6) use and on DAPI staining, were

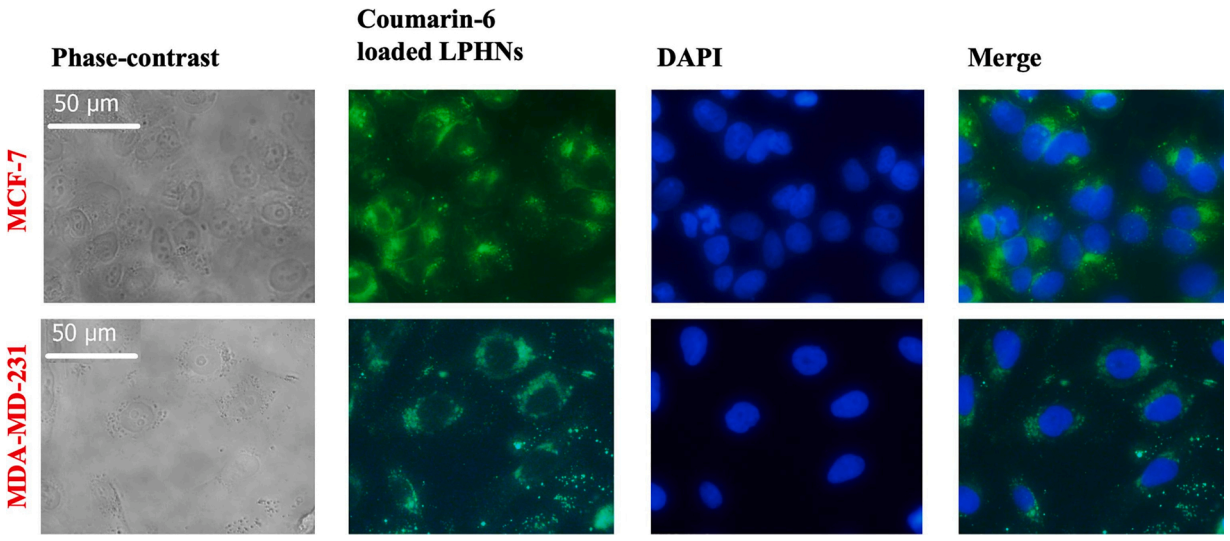

Fig. 7. *In vitro* uptake study of COUMARIN-6-LPHNPs IN MCF-7 and MDA-MB-231 cells. Reproduced with permission from Yalcin et al., (2020) [74].

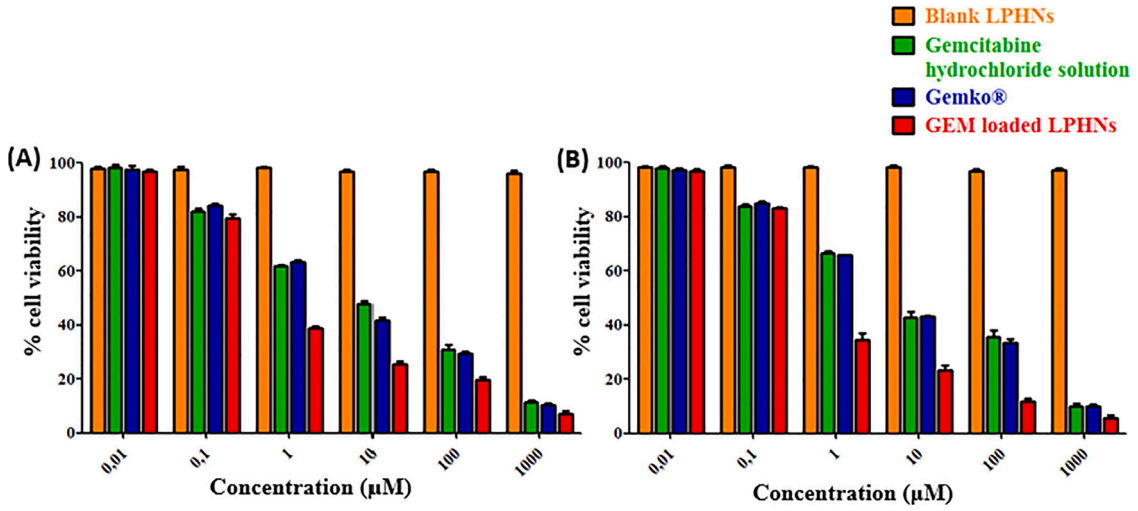

Fig. 8. Biocompatibility and viability of MFC-7 and MDA-MB-231 cells treated with free Gemcitabine (hydrochloride solution or Gemko®) and encapsulated in LPHNs. Values expressed as mean ± SD, n = 3. Reproduced with permission from Yalcin et al., (2020) [74].

carried out in order to evaluate the uptake behavior of nanoparticles - results are shown in Fig. 7. Images have evidenced that LPHNs were distributed in the cytoplasm surrounding the nuclei of cells in both models (green image). Based on the merged image, green dots stand out in the nuclei area, a fact that indicates satisfactory nanoparticle internalization process.

Based on the MTT assay, theses authors have investigated the biocompatibility and viability of MFC-7 and MDA-MB-231 cells treated with free Gemcitabine (hydrochloride solution and Gemko®) or encapsulated in LPHNs at concentrations of 0.01, 0.1, 1, 10, 100, and 1000 µM, (Fig. 8 - (A) MCF-7 and (B) MDA-MB-231 cells). The blank formulation presented excellent biocompatible profile in both tumor cell models at all tested concentrations. LPHNs were significantly capable of inducing death in a significant number of cells - except for cells treated at concentrations of 0.01 and 0.1 µM - in comparison to free drug solution and Gemko. IC_{50} of 0.38 ± 0.01 and 0.40 ± 0.04 µM were determined for LPHNs in MCF-7 and MDA-M-231 cells, respectively. These values were approximately 80 times higher than the ones recorded for cells treated with the free drug (gemcitabine hydrochloride).

Hybrid nanoparticles produced in the current study enabled significant improvement in the pharmacokinetic profile and effectiveness of GEM, as wel as reached biological half-life 4.2 times longer than that of commercial formulation Gemko®. Furthermore, the hybrid system presented longer circulation time, which was crucial to significantly reduce tumor volume in the treated mice in comparison to control groups comprising animals treated with Gemko® or untreated animals.

5. Preclinical applications

Dehaini et al. (2016) have developed a system comprising lipid-polymer hybrid nanoparticles (LPHNPs) to improve docetaxel tumor-penetration properties by using folate as targeting agent [20]. The developed formulation was based on the use of phospholipid DSPE-m-PEG_{2000}) and PLGA-COOH [carboxylic acid-terminated poly(lactic-co--glycolic acid). The aforementioned authors have investigated the circulation time of nanoparticles labeled with DID (1,13-dioctadecyl-3, 3,33,33- tetramethylindodicarbocyanine, 4-chlorobenzenesulfonate) dye and administered in xenograft mice (KB cells) - results are shown in Fig. 9 (a). Data have shown that nanoparticles were cleared from the bloodstream following a two-compartment model, with half-life elimination of 11.5 h. Furthermore, approximately 10 % of the administered dose remained in mice's blood after 24 h. Finally, the authors observed

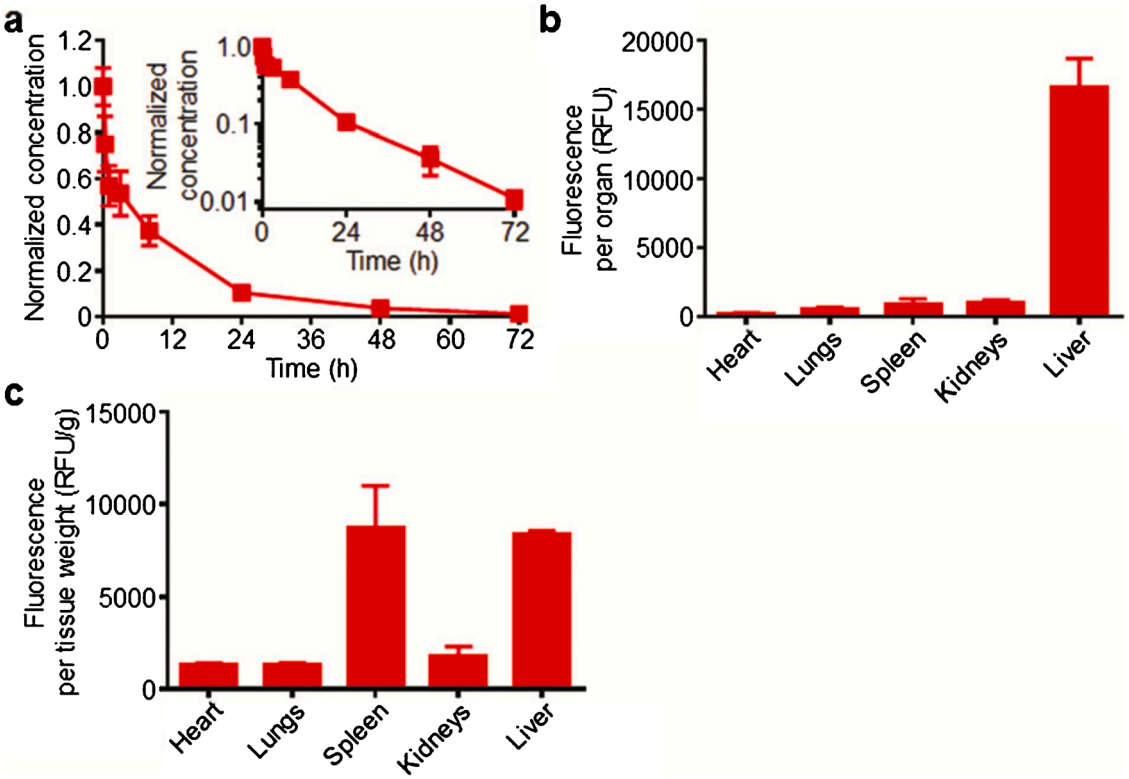

Fig. 9. Preclinical evaluation of LPHNPs. (a) Clearance behavior of nanoparticles in mice until 72 h after the injection. (b) and (c) biodistribution profile of nanoparticles in different tissues. Reproduced with permission from Dehaini et al., (2016) [53].

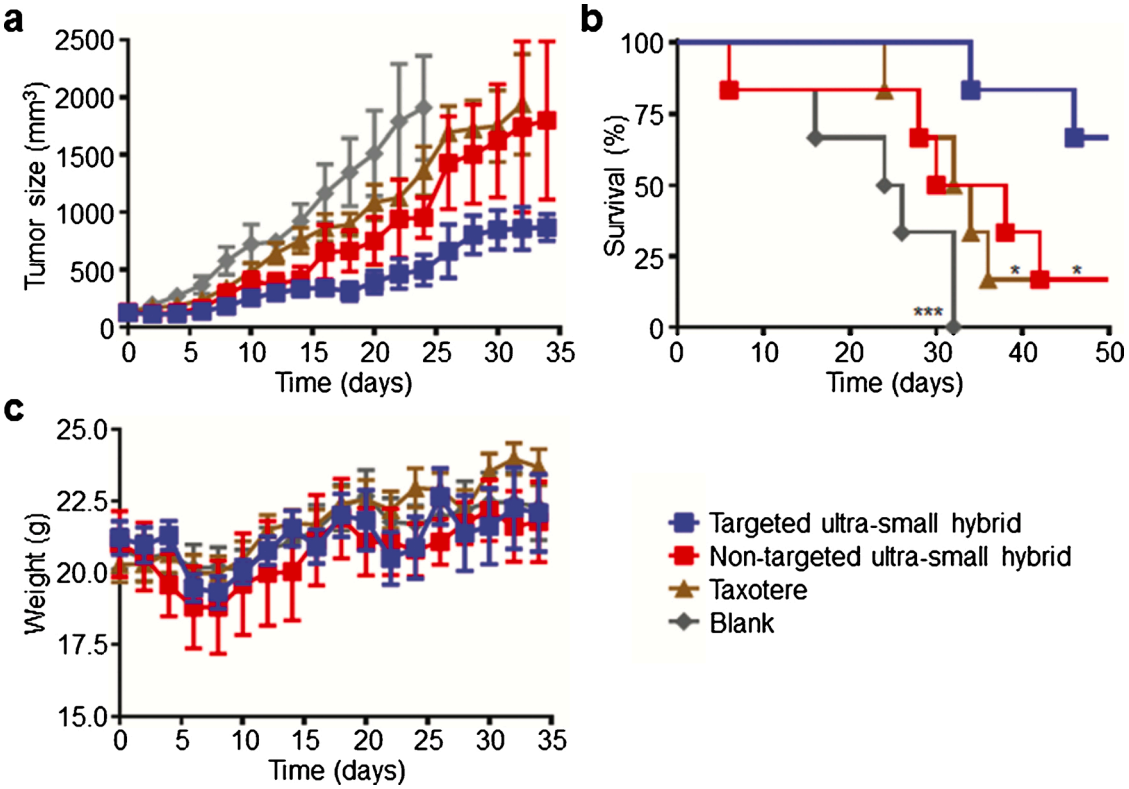

Fig. 10. Preclinical investigations of xenograft tumor-bearing (Kb - CCL-17 cells)mice treated with LPHNPs loaded with docetaxel and controls constituted by non-folate nanoparticles (non-target LPHNPs), free docetaxel (Taxotere) and blank formulation. (a) evaluation of tumor growth rhythm until 35 days. Mice treated with blank formulation died after 25 days of injection. (b) survival curves. (c) mice weight gain profile studied for 35 days. Reproduced with permission from Dehaini et al., (2016) [20].

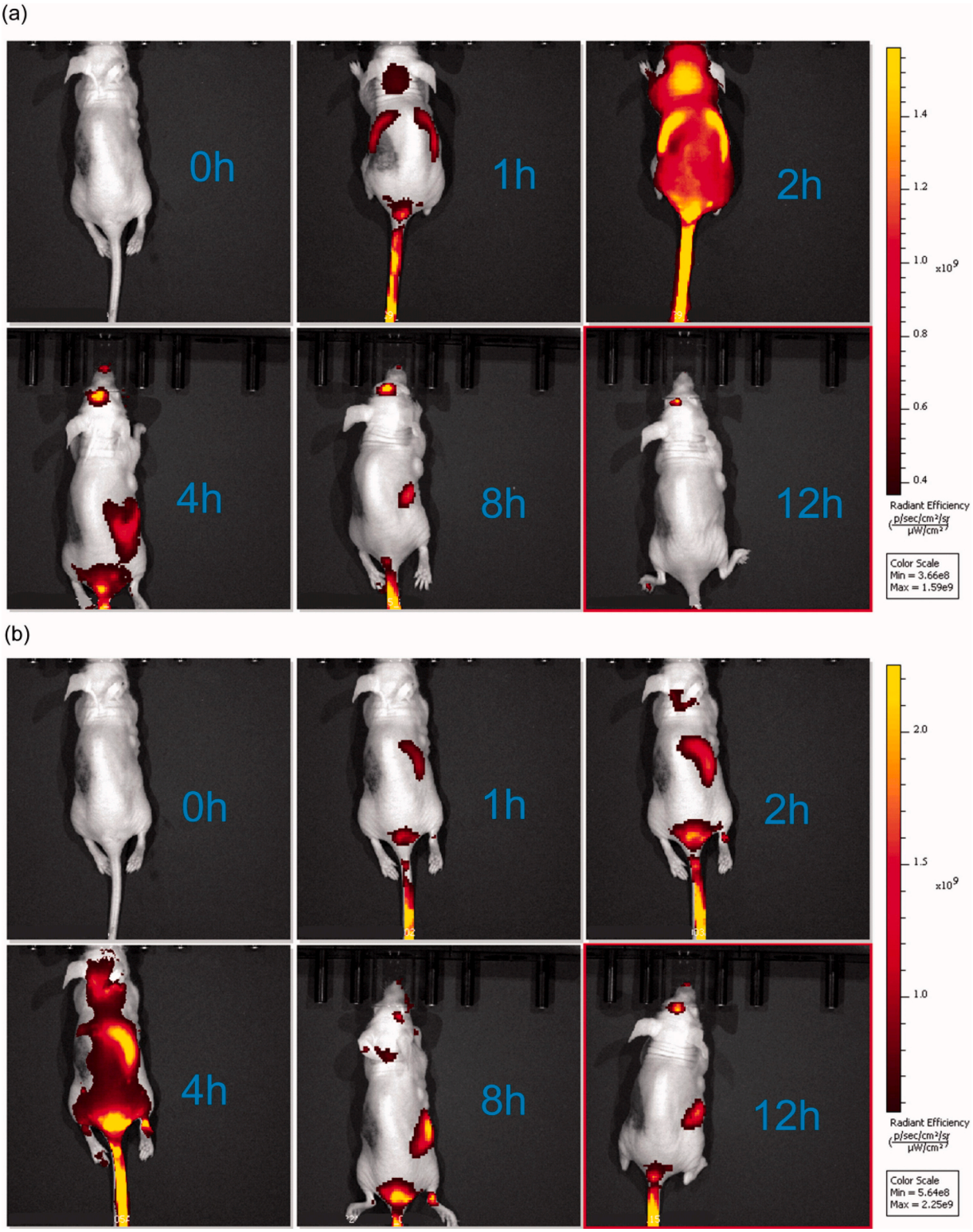

Fig. 11. Fluorescence imaging of xenograft bearing mice treated with (a) DOX + PSO-SLN (solid lipid nanoparticles) and (b) DOX + PSO-PLN (hybrid nanoparticles). Images were obtained at 0, 1, 2, 4, 8 and 12 h after the injection. Extracted with permission from Huang, et al., 2018 [75].

that significant amounts of delivered nanoparticles were uptaken by animals liver and spleen, after 24 h, likely due to phagocytic actions associated with animals' immunological system, as shown in Figs. 9 (b) and 11 (c).

Fig. 10 of the aforementioned study presents data about tumor uptake (a), animals' survival rate (b), and weight gain (c). Xenograft tumor-bearing mice (Kb - CCL-17 cells) were treated with LPHNPs loaded with docetaxel; controls were subjected to non-folate nanoparticles (non-target LPHNPs), free docetaxel (Taxotere), and blank formulation.

The target-hybrid system has shown effective positioning in deep regions within tumors, whereas the system loaded with antitumor agent

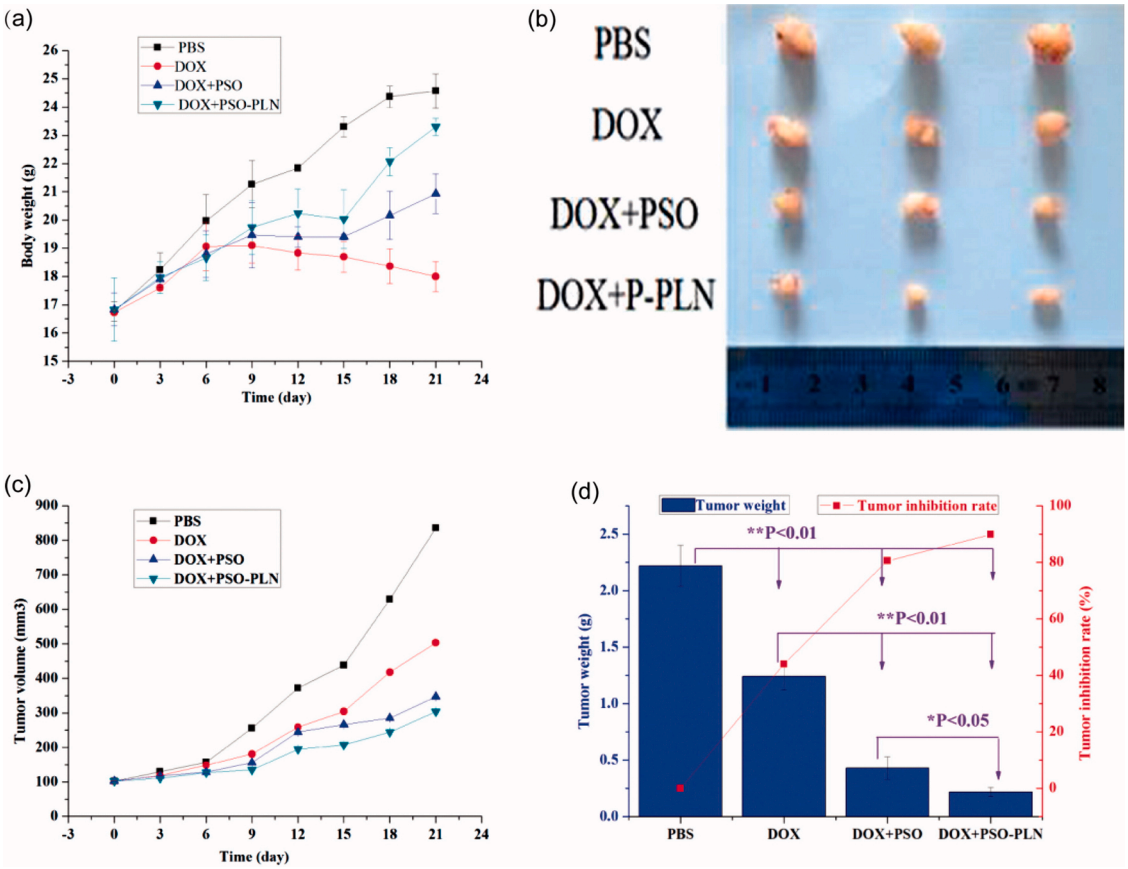

Fig. 12. Preclinical evaluation of xenografts bearing mice treated with free DOX, DOX + PSO, and DOX + PSO-PLN. The weight gain rhythm of animals is available in (a). The efficacy of the different formulations in the tumor growth inhibition, through 21 days, are available in (b), (c) and (d). The data represents the mean value ± S.D. Extracted with permission from Huang, et al., 2018 [75].

was capable of significantly slowing tumor growth, even in comparison to mice treated with non-target formulation, who presented similar behavior to those subjected to free drug. Furthermore, the authors observed that the system was capable of increasing animals' survival rate, although without significant body weight gain.

Huang and collaborators (2018) have performed a study focused on developing a nanosystem to be used against multidrug resistance (MDR), which is considered the main cause of failure in chemotherapy treatments [75]. The system comprised LPHNPs based on soybean phospholipids, as well as PLGA loaded with psoralen (psoralen-polymer-lipid-nanoparticles - PSO-PLN), which is a natural compound with relevant biological properties such as antitumor, antipsoriasis and anti-vitiligo activity. The aforementioned authors have evaluated drug accumulation in different groups of xenograft-bearing mice (MCF-7/ADR cells). Treatment groups comprised animals treated with PSO-PLN and the control, which comprised animals treated with solid lipid nanoparticles (PSO-SLN). PSO-SLN and PSO-PLN samples were labeled with indocyanine green (ICG). Fig. 11 (a) depicts fluorescence images of mice treated with PSO-SLN and free doxorubicin (DOX). Images of mice treated with DOX + PSO-PLN are shown in Fig. 11 (b). Based on the analysis applied to the data set, the authors attributed the best performance to the PSO-PLN system, which showed significantly longer drug persistence time in animals' liver and kidneys. These findings can be associated with the likely sustained-release effect of the hybrid system in comparison to that of the non-hybrid system.

In addition, the aforementioned authors have evaluated the antitumor activity of free DOX, DOX + PSO or DOX + PSO-PLN formulations by using the very same tumor model previously implanted in mice. Results presented in Fig. 12 (a) have shown that animals treated with free DOX had significant weight loss after 18 treatment days, a fact that indicates the relevant toxic nature of the free drug. However, Fig. 12 (b) and (c) allow comparing how different formulations used in the experiments were capable of slowing tumor growth. Animals treated with PBS solution (control) have shown tumors with significant volume; however, the best performance was recorded for animals treated with the DOX + PSO-PLN formulation, who presented 89.9 % tumor growth inhibition. On the other hand, free DOX and DOX + PSO were capable of inhibiting tumor growth by 44.0 % and 80.6 %, respectively [Fig. 12 (d)].

The hybrid formulation (PSO-PLN) has produced significant antitumor activity in comparison to the free drug; it may have happened due to sustained-release kinetic behavior. Furthermore, the developed formulation has increased DOX cytotoxicity *in vitro* and had significant action on the drug-resistant MCF-7/ADR xenograft model. If one takes into consideration all findings together, the produced hybrid nanosystem has shown potential advantages to treat drug-resistant breast cancer.

Xiong et al. (2017) have developed a novel hybrid nanoparticle system based on β-cyclodextrin-conjugated poly-L-lysine and on hyaluronic acid for co-delivery of oligoRNA and doxorubicin to enable nucleic acid delivery [76]. The hybrid system was capable of effectively delivering the drug and oligoRNA to tumor cells *via* CD44 receptor-mediated endocytosis, which was capable of significantly inhibiting cell proliferation. Preclinical investigations about the produced system have confirmed that nanoparticles were capable of specifically binding to CD44 receptors, which are often overexpressed on the surface of hepatocarcinoma cells (HCC). Results in biodistribution studies conducted with tumor-bearing nude mice have shown remarkable HCC-targeting property and relevant escape from the recognition of immune components after 24 h (Fig. 13a). Xu et al. (2017) have developed nanoparticles composed of sharp pH-responsive copolymers

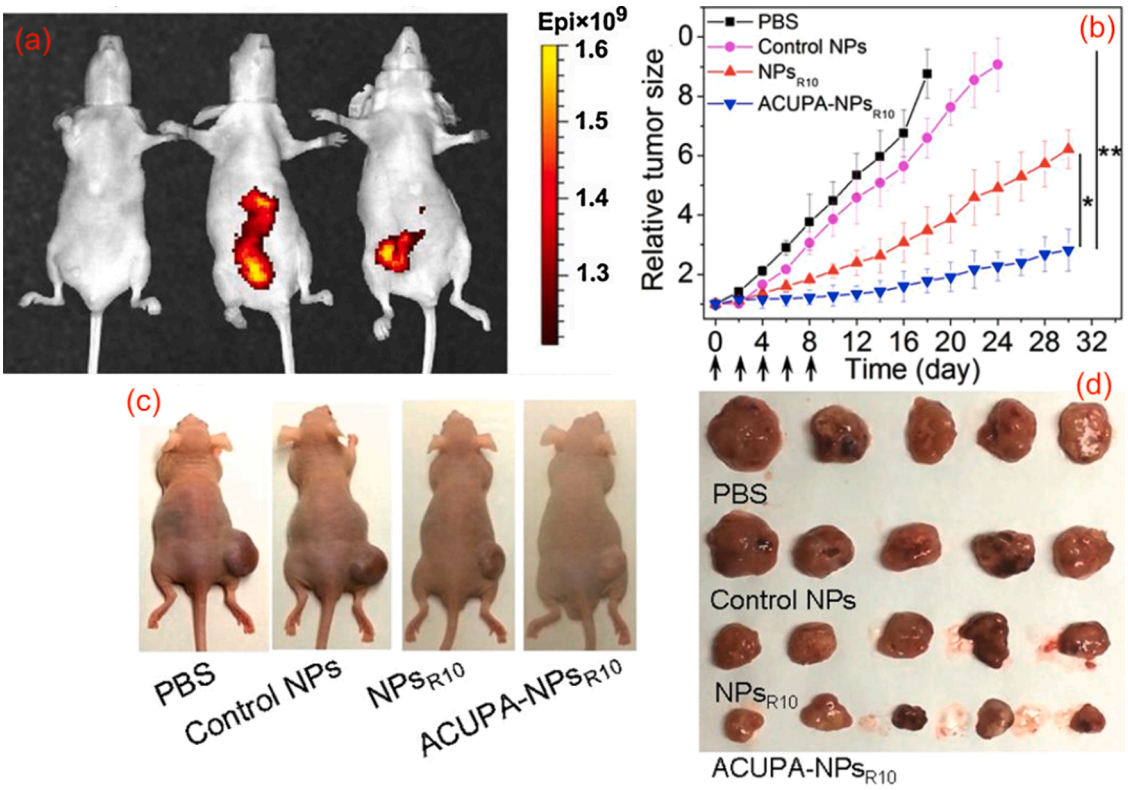

Fig. 13. Preclinical evaluation of two different hybrid nanosystems for nucleic acid delivery. In (a) are available biodistribution study conducted by Xiong et al., 2017, where an important tumor accumulation of the hybrid nanoparticles constituted by β-cyclodextrin-conjugated poly-l-lysine and hyaluronic acid co-delivering oligoRNA and doxorubicin was observed in tumor-bearing nude mice, after 24 h of the injection. In (b), (c) and (d) are a set of results obtained by Xu et al., 2017 which are available a study of relative tumor growth rhythm of the xenograft tumor-bearing mice treated with NPs composed of: (i) sharp pH-responsive copolymers containing the membrane-penetrating oligoarginine grafts, and an S, S-2-[3-[5-amino-1-carboxypentyl]ureido]pentanedioic acid (ACUPA) ligand that can specifically bind to prostate-specific membrane antigen (ACUPA-NPsr10); (ii) NPs without ACUPA ligand (NPsR10), (iii) NPs without grafting agent (Control NPs) and (iv) Phosphate-Buffered Saline solution (PBS). Modified with permission from Xiong et al., 2017 and Xu et al., 2017, respectively [76,77].

containing membrane-penetrating oligoarginine grafts and S, S-2-[3-[5-amino-1-carboxypentyl]ureido]pentanedioic acid (ACUPA$_{R10}$) ligand capable of specifically binding to prostate-specific membrane antigen for siRNA delivery, in order to evaluate the ability of hybrid nanoparticles to effectively deliver nucleic acids for therapeutic purposes [77]. The produced nanoparticles have shown the ability to escape from endosomes and to efficiently deliver siRNA to the cytoplasm of prostate tumor cells. This process has led to significant tumor growth inhibition due to specific recognition through ACUPA ligand, whereas animals subjected to control treatments presented significant tumor growth (Fig. 13b–d).

Gene therapy has enabled therapeutic strategies to be used against cancer since pDNA, siRNA or microRNA recorded relevant results in the control, development and growth of different tumor cell types [78,79]. The authors of the two herein cited studies have used the gene therapy approach to make tumor cells more susceptible to the action of anticancer drugs. Other studies have focused on investigating direct actions of the suicidal gene, such as apoptosis induction in tumor cells [80,81]. Unfortunately, high costs with research and with the advanced laboratory infrastructure required to do so, are a significant disadvantage of these applications.

6. Future trends

The development of new strategies focused on finding biocompatible hybrid materials has led to remarkable advancements in the biomedical field, in the last decade, with emphasis on the production of new drug carriers capable of reaching specific places such as tumor sites. The strategy of covalently attaching small initiator molecules to surfaces of natural polymers or inorganic biocompatible materials and of grafting polymers *in situ* from these surfaces - the so-called "*grafting-from*" - based on the ATRP or RAFT polymerization technique, has enabled preparing hybrid systems with a wide variety of properties. It is worth emphasizingthe responsive hybrid systems capable of responding to external triggers such as temperature and pH, as well as to maintain the biological activity. Materials produced based on these strategies have emerged as outstanding candidates for the next-generation platform of systems used for applications in this field.

On the other hand, the development of lipid polymer hybrid nanostructures appears to be a potential drug delivery platform. Such systems have versatile types of arrangements and are tunable in terms of release features and long-term behavior *in vivo*. These nanostructures can be used as therapeutics to deliver the optimum amount of drugs at the appropriate site, as well as to enable disease diagnosis. Furthermore, these LPHNPs can encapsulate more than one drug (codelivery), which is an important feature, since multiple-drug therapy is the treatment of choice for cancer cases; targeted drug delivery is a basic requirement in these treatments.

Nowadays, knowledge about the mechanism involved in the action of these hybrid systems remains incipient; thus, it is necessary conducting further studies on this topic. However, the advantages provided by the effective conjugation of polymers over organic surfaces such as mesoporous silica nanoparticles, magnetic nanoparticles and other biocompatible compounds, will allow researchers to develop better carrier systems. Such hybrids will be certainly capable of providing a more effective targeted delivery of anticancer drugs, opening room for innovative treatments and of contributing to the current therapeutic scenario.

Declaration of Competing Interest

The authors report no declarations of interest.

Acknowledgements

The authors would like to thank the Coordenação de Aperfeiçoamento de Pessoal de Nível Superior (CAPES), Fundação de Amparo à Pesquisa do Estado de Minas Gerais (FAPEMIG), and Conselho Nacional de Desenvolvimento Científico e Tecnológico (CNPq) for their financial support.

References

[1] N. Škalko-Basnet, Vanić, Lipid-based nanopharmaceuticals in antimicrobial therapy. Funct. Nanomater. Manag. Microb. Infect. A Strateg. to Address Microb. Drug Resist., Elsevier Inc., 2017, pp. 111–152, https://doi.org/10.1016/B978-0-323-41625-2.00005-3.

[2] B.S. Murty, P. Shankar, B. Raj, B.B. Rath, J. Murday, B.S. Murty, P. Shankar, B. Raj, B.B. Rath, J. Murday, Unique properties of nanomaterials. Textb. Nanosci. Nanotechnol., Springer, Berlin Heidelberg, 2013, pp. 29–65, https://doi.org/10.1007/978-3-642-28030-6_2.

[3] G. Tiwari, R. Tiwari, S. Bannerjee, L. Bhati, S. Pandey, P. Pandey, B. Sriwastawa, Drug delivery systems: an updated review, Int. J. Pharm. Investig. 2 (2012) 2, https://doi.org/10.4103/2230-973x.96920.

[4] L. Liu, Q. Ye, M. Lu, Y.C. Lo, Y.H. Hsu, M.C. Wei, Y.H. Chen, S.C. Lo, S.J. Wang, D. J. Bain, C. Ho, A new approach to reduce toxicities and to improve bioavailabilities of platinum-containing anti-cancer nanodrugs, Sci. Rep. 5 (2015) 1–11, https://doi.org/10.1038/srep10881.

[5] J.K. Patra, G. Das, L.F. Fraceto, E.V.R. Campos, M.D.P. Rodriguez-Torres, L. S. Acosta-Torres, L.A. Diaz-Torres, R. Grillo, M.K. Swamy, S. Sharma, S. Habtemariam, H.S. Shin, Nano based drug delivery systems: recent developments and future prospects 10 Technology 1007 Nanotechnology 03 Chemical Sciences 0306 Physical Chemistry (incl. Structural) 03 Chemical Sciences 0303 Macromolecular and Materials Chemistry 11 Medical and Health Sciences 1115 Pharmacology and Pharmaceutical Sciences 09 Engineering 0903 Biomedical Engineering Prof Ueli Aebi, Prof Peter Gehr, J. Nanobiotechnol. 16 (2018), https://doi.org/10.1186/s12951-018-0392-8.

[6] P.-C. Lee, B.-S. Zan, L.-T. Chen, T.-W. Chung, Multifunctional PLGA-based nanoparticles as a controlled release drug delivery system for antioxidant and anticoagulant therapy, Int. J. Nanomed. Vol.14 (2019) 1533–1549, https://doi.org/10.2147/IJN.S174962.

[7] K.M. Vargas, Y.-S. Shon, Hybrid lipid–nanoparticle complexes for biomedical applications, J. Mater. Chem. B 7 (2019) 695–708, https://doi.org/10.1039/C8TB03084G.

[8] A. Sen Gupta, Role of particle size, shape, and stiffness in design of intravascular drug delivery systems: insights from computations, experiments, and nature, Wiley Interdiscip. Rev. Nanomed. Nanobiotechnol. 8 (2016) 255–270, https://doi.org/10.1002/wnan.1362.

[9] M. Caldorera-Moore, N. Guimard, L. Shi, K. Roy, Designer nanoparticles: Incorporating size, shape and triggered release into nanoscale drug carriers, Expert Opin. Drug Deliv. 7 (2010) 479–495, https://doi.org/10.1517/17425240903579971.

[10] J.K. Patra, G. Das, L.F. Fraceto, E.V.R. Campos, M.D.P. Rodriguez-Torres, L. S. Acosta-Torres, L.A. Diaz-Torres, R. Grillo, M.K. Swamy, S. Sharma, S. Habtemariam, H.S. Shin, Nano based drug delivery systems: recent developments and future prospects, J. Nanobiotechnology 16 (2018) 1–33, https://doi.org/10.1186/s12951-018-0392-8.

[11] F. Bakar-Ates, E. Ozkan, C.T. Sengel-Turk, Encapsulation of cucurbitacin B into lipid polymer hybrid nanocarriers induced apoptosis of MDAMB231 cells through PARP cleavage, Int. J. Pharm. 586 (2020) 119565, https://doi.org/10.1016/j.ijpharm.2020.119565.

[12] C.T. Sengel-Turk, N. Ozmen, F. Bakar-Ates, Design, characterization and evaluation of cucurbitacin B-loaded core–shell-type hybrid nano-sized particles using DoE approach, Polym. Bull. (2020), https://doi.org/10.1007/s00289-020-03256-7.

[13] S. Bou, X. Wang, N. Anton, R. Bouchaala, A.S. Klymchenko, M. Collot, Lipid-core/polymer-shell hybrid nanoparticles: synthesis and characterization by fluorescence labeling and electrophoresis, Soft Matter 16 (2020) 4173–4181, https://doi.org/10.1039/D0SM00077A.

[14] M. Hamdi, H.M. Abdel-Bar, E. Elmowafy, K.T. Al-Jamal, G.A.S. Awad, An integrated vitamin E-coated polymer hybrid nanoplatform: a lucrative option for an enhanced in vitro macrophage retention for an anti-hepatitis B therapeutic prospect, PLoS One 15 (2020) e0227231, https://doi.org/10.1371/journal.pone.0227231.

[15] S. Krishnamurthy, R. Vaiyapuri, L. Zhang, J.M. Chan, Lipid-coated polymeric nanoparticles for cancer drug delivery, Biomater. Sci. 3 (2015) 923–936, https://doi.org/10.1039/c4bm00427b.

[16] N.S. Koseva, J. Rydz, E.V. Stoyanova, V.A. Mitova, Hybrid protein-synthetic polymer nanoparticles for drug delivery. Adv. Protein Chem. Struct. Biol., Academic Press, 2015, pp. 93–119, https://doi.org/10.1016/bs.apcsb.2014.12.003.

[17] J. Park, S.H. Wrzesinski, E. Stern, M. Look, J. Criscione, R. Ragheb, S.M. Jay, S. L. Demento, A. Agawu, P. Licona Limon, A.F. Ferrandino, D. Gonzalez, A. Habermann, R.A. Flavell, T.M. Fahmy, Combination delivery of TGF-β inhibitor and IL-2 by nanoscale liposomal polymeric gels enhances tumour immunotherapy, Nat. Mater. 11 (2012) 895–905, https://doi.org/10.1038/nmat3355.

[18] O. Eckardt, C. Pietsch, O. Zumann, M. Von Der Lühe, D.S. Brauer, F.H. Schacher, Well-defined SiO2@P(EtOx-stat-EI) core-shell hybrid nanoparticles via sol-gel processes, Macromol. Rapid Commun. 37 (2016) 337–342, https://doi.org/10.1002/marc.201500467.

[19] C. He, J. Lu, W. Lin, Hybrid nanoparticles for combination therapy of cancer, J. Control. Release 219 (2015) 224–236, https://doi.org/10.1016/j.jconrel.2015.09.029.

[20] D. Dehaini, R.H. Fang, B.T. Luk, Z. Pang, C.M.J. Hu, A.V. Kroll, C.L. Yu, W. Gao, L. Zhang, Ultra-small lipid-polymer hybrid nanoparticles for tumor-penetrating drug delivery, Nanoscale 8 (2016) 14411–14419, https://doi.org/10.1039/c6nr04091h.

[21] S. Ilbasmis-Tamer, S. Takka, Antitumor activity of gemcitabine hydrochloride loaded lipid polymer hybrid nanoparticles (LPHNs): in vitro and in vivo, Int. J. Pharm. 580 (2020) 119246, https://doi.org/10.1016/j.ijpharm.2020.119246.

[22] N. Tahir, A. Madni, V. Balasubramanian, M. Rehman, A. Correia, P.M. Kashif, E. Mäkilä, J. Salonen, H.A. Santos, Development and optimization of methotrexate-loaded lipid-polymer hybrid nanoparticles for controlled drug delivery applications, Int. J. Pharm. 533 (2017) 156–168, https://doi.org/10.1016/j.ijpharm.2017.09.061.

[23] M.M. Khan, A. Madni, V. Torchilin, N. Filipczak, J. Pan, N. Tahir, H. Shah, Lipid-chitosan hybrid nanoparticles for controlled delivery of cisplatin, Drug Deliv. 26 (2019) 765–772, https://doi.org/10.1080/10717544.2019.1642420.

[24] F. Danhier, P. Danhier, C.J. De Saedeleer, A.-C. Fruytier, N. Schleich, A. des Rieux, P. Sonveaux, B. Gallez, V. Préat, Paclitaxel-loaded micelles enhance transvascular permeability and retention of nanomedicines in tumors, Int. J. Pharm. 479 (2015) 399–407, https://doi.org/10.1016/j.ijpharm.2015.01.009.

[25] T. Zhang, J. Luo, Y. Fu, H. Li, R. Ding, T. Gong, Z. Zhang, Novel oral administrated paclitaxel micelles with enhanced bioavailability and antitumor efficacy for resistant breast cancer, Colloids Surf. B Biointerfaces 150 (2017) 89–97, https://doi.org/10.1016/j.colsurfb.2016.11.024.

[26] S.J.T. Rezaei, E. Sarijloo, H. Rashidzadeh, S. Zamani, A. Ramazani, A. Hesami, E. Mohammadi, pH-triggered prodrug micelles for cisplatin delivery: preparation and In Vitro/Vivo evaluation, React. Funct. Polym. 146 (2020) 104399, https://doi.org/10.1016/j.reactfunctpolym.2019.104399.

[27] N.S. Sommerfeld, M. Hejl, M.H.M. Klose, E. Schreiber-Brynzak, A. Bileck, S. M. Meier, C. Gerner, M.A. Jakupec, M. Galanski, B.K. Keppler, Low-generation polyamidoamine dendrimers as drug carriers for platinum(IV) complexes, Eur. J. Inorg. Chem. 2017 (2017) 1713–1720, https://doi.org/10.1002/ejic.201601205.

[28] J. Zhu, G. Wang, C.S. Alves, H. Tomás, Z. Xiong, M. Shen, J. Rodrigues, X. Shi, Multifunctional dendrimer-entrapped gold nanoparticles conjugated with doxorubicin for pH-Responsive drug delivery and targeted computed tomography imaging, Langmuir 34 (2018) 12428–12435, https://doi.org/10.1021/acs.langmuir.8b02901.

[29] E. Fedeli, A. Lancelot, J. Dominguez, J. Serrano, P. Calvo, T. Sierra, Self-assembling hybrid linear-dendritic block copolymers: the design of nano-carriers for lipophilic antitumoral drugs, Nanomaterials 9 (2019) 161, https://doi.org/10.3390/nano9020161.

[30] M. Sedki, I.A. Khalil, I.M. El-Sherbiny, Hybrid nanocarrier system for guiding and augmenting simvastatin cytotoxic activity against prostate cancer, Artif. Cells Nanomed. Biotechnol. 46 (2018) S641–S650, https://doi.org/10.1080/21691401.2018.1505743.

[31] S. Kamaraj, U.M. Palanisamy, M.S.B. Kadhar Mohamed, A. Gangasalam, G. A. Maria, R. Kandasamy, Curcumin drug delivery by vanillin-chitosan coated with calcium ferrite hybrid nanoparticles as carrier, Eur. J. Pharm. Sci. 116 (2018) 48–60, https://doi.org/10.1016/j.ejps.2018.01.023.

[32] S. Hajebi, A. Abdollahi, H. Roghani-Mamaqani, M. Salami-Kalajahi, Hybrid and hollow Poly(N,N-dimethylaminoethyl methacrylate) nanogels as stimuli-responsive carriers for controlled release of doxorubicin, Polymer (Guildf) 180 (2019) 121716, https://doi.org/10.1016/j.polymer.2019.121716.

[33] Q. Khalid, M. Ahmad, M. Usman Minhas, Hydroxypropyl-β-cyclodextrin hybrid nanogels as nano-drug delivery carriers to enhance the solubility of dexibuprofen: characterization, in vitro release, and acute oral toxicity studies, Adv. Polym. Technol. 37 (2018) 2171–2185, https://doi.org/10.1002/adv.21876.

[34] W. Jiang, B. Shang, L. Li, S. Zhang, Y. Zhen, Construction of a genetically engineered chimeric apoprotein consisting of sequences derived from lidamycin and neocarzinostatin, Anticancer Drugs 27 (2016) 24–28, https://doi.org/10.1097/CAD.0000000000000300.

[35] J. Li, F. Cao, H. liang Yin, Z. jian Huang, Z. tao Lin, N. Mao, B. Sun, G. Wang, Ferroptosis: past, present and future, Cell Death Dis. 11 (2020) 1–13, https://doi.org/10.1038/s41419-020-2298-2.

[36] L. Hajba, A. Guttman, The use of magnetic nanoparticles in cancer theranostics: toward handheld diagnostic devices, Biotechnol. Adv. 34 (2016) 354–361, https://doi.org/10.1016/j.biotechadv.2016.02.001.

[37] L. Mohammed, D. Ragab, H. Gomaa, Bioactivity of hybrid polymeric magnetic nanoparticles and their applications in drug delivery, Curr. Pharm. Des. 22 (2016) 3332–3352, https://doi.org/10.2174/1381612822666160208143237.

[38] E.M. Pelegri-O'Day, E.-W. Lin, H.D. Maynard, Therapeutic Protein–Polymer, Conjugates: advancing beyond PEGylation, J. Am. Chem. Soc. 136 (2014) 14323–14332, https://doi.org/10.1021/ja504390x.

[39] A. Abuchowski, J.R. McCoy, N.C. Palczuk, T. van Es, F.F. Davis, Effect of covalent attachment of polyethylene glycol on immunogenicity and circulating life of bovine liver catalase, J. Biol. Chem. 252 (1977) 3582–3586.

[40] E.M. Pelegri-O'Day, E.-W. Lin, H.D. Maynard, Therapeutic Protein–Polymer, Conjugates: advancing beyond PEGylation, J. Am. Chem. Soc. 136 (2014) 14323–14332, https://doi.org/10.1021/ja504390x.

[41] F. Moncalvo, M.I. Martinez Espinoza, F. Cellesi, Nanosized delivery systems for therapeutic proteins: clinically validated technologies and advanced development strategies, Front. Bioeng. Biotechnol. 8 (2020), https://doi.org/10.3389/fbioe.2020.00089.

[42] F.S. Mozar, E.H. Chowdhury, Impact of PEGylated nanoparticles on tumor targeted drug delivery, Curr. Pharm. Des. 24 (2018) 3283–3296, https://doi.org/10.2174/1381612824666180730161721.

[43] A.J. Russell, S.L. Baker, C.M. Colina, C.A. Figg, J.L. Kaar, K. Matyjaszewski, A. Simakova, B.S. Sumerlin, Next generation protein-polymer conjugates, AIChE J. 64 (2018) 3230–3245, https://doi.org/10.1002/aic.16338.

[44] N. Vanparijs, S. Maji, B. Louage, L. Voorhaar, D. Laplace, Q. Zhang, Y. Shi, W. E. Hennink, R. Hoogenboom, B.G. De Geest, Polymer-protein conjugation via a 'grafting to' approach – a comparative study of the performance of protein-reactive RAFT chain transfer agents, Polym. Chem. 6 (2015) 5602–5614, https://doi.org/10.1039/C4PY01224K.

[45] M.S. Messina, K.M.M. Messina, A. Bhattacharya, H.R. Montgomery, H.D. Maynard, Preparation of biomolecule-polymer conjugates by grafting-from using ATRP, RAFT, or ROMP, Prog. Polym. Sci. 100 (2020) 101186, https://doi.org/10.1016/j.progpolymsci.2019.101186.

[46] M. Macchione, C. Biglione, M. Strumia, Design, synthesis and architectures of hybrid nanomaterials for therapy and diagnosis applications, Polymers (Basel) 10 (2018) 527, https://doi.org/10.3390/polym10050527.

[47] A. Mukherjee, A.K. Waters, P. Kalyan, A.S. Achrol, S. Kesari, V.M. Yenugonda, Lipid-polymer hybrid nanoparticles as a nextgeneration drug delivery platform: state of the art, emerging technologies, and perspectives, Int. J. Nanomed. 14 (2019) 1937–1952, https://doi.org/10.2147/IJN.S198353.

[48] M.L. Tebaldi, H. Charan, L. Mavliutova, A. Böker, U. Glebe, Dual-stimuli sensitive hybrid materials: ferritin-PDMAEMA by grafting-from polymerization, Macromol. Chem. Phys. 218 (2017) 1600529, https://doi.org/10.1002/macp.201600529.

[49] M.L. Tebaldi, H. Charan, L. Mavliutova, A. Böker, U. Glebe, Dual-stimuli sensitive hybrid materials: ferritin-PDMAEMA by grafting-from polymerization, Macromol. Chem. Phys. 218 (2017) 1600529, https://doi.org/10.1002/macp.201600529.

[50] N. Vanparijs, S. Maji, B. Louage, L. Voorhaar, D. Laplace, Q. Zhang, Y. Shi, W. E. Hennink, R. Hoogenboom, B.G. De Geest, Polymer-protein conjugation via a 'grafting to' approach – a comparative study of the performance of protein-reactive RAFT chain transfer agents, Polym. Chem. 6 (2015) 5602–5614, https://doi.org/10.1039/C4PY01224K.

[51] M.L. Tebaldi, A.L.C. Maia, F. Poletto, F.V. de Andrade, D.C.F. Soares, Poly(-3-hydroxybutyrate-co-3-hydroxyvalerate) (PHBV): current advances in synthesis methodologies, antitumor applications and biocompatibility, J. Drug Deliv. Sci. Technol. 51 (2019) 115–126, https://doi.org/10.1016/j.jddst.2019.02.007.

[52] W. Zhao, F. Liu, Y. Chen, J. Bai, W. Gao, Synthesis of well-defined protein–polymer conjugates for biomedicine, Polymer (Guildf.) 66 (2015) A1–A10, https://doi.org/10.1016/j.polymer.2015.03.054.

[53] P. De, M. Li, S.R. Gondi, B.S. Sumerlin, Temperature-regulated activity of responsive polymer−protein conjugates prepared by grafting-from via RAFT polymerization, J. Am. Chem. Soc. 130 (2008) 11288–11289, https://doi.org/10.1021/ja804495v.

[54] H. Murata, C.S. Cummings, R.R. Koepsel, A.J. Russell, Polymer-based protein engineering can rationally tune enzyme activity, pH-dependence, and stability, Biomacromolecules 14 (2013) 1919–1926, https://doi.org/10.1021/bm4002816.

[55] W. Zhao, F. Liu, Y. Chen, J. Bai, W. Gao, Synthesis of well-defined protein-polymer conjugates for biomedicine, Polym. (United Kingdom) 66 (2015) A1–A10, https://doi.org/10.1016/j.polymer.2015.03.054.

[56] B. Trzebicka, R. Szweda, D. Kosowski, D. Szweda, Ł. Otulakowski, E. Haladjova, A. Dworak, Thermoresponsive polymer-peptide/protein conjugates, Prog. Polym. Sci. 68 (2017) 35–76, https://doi.org/10.1016/j.progpolymsci.2016.12.004.

[57] F. Seidi, R. Jenjob, T. Phakkeeree, D. Crespy, Saccharides, oligosaccharides, and polysaccharides nanoparticles for biomedical applications, J. Control. Release 284 (2018) 188–212, https://doi.org/10.1016/j.jconrel.2018.06.026.

[58] S. Maghrebi, C.A. Prestidge, P. Joyce, An update on polymer-lipid hybrid systems for improving oral drug delivery, Expert Opin. Drug Deliv. 16 (2019) 507–524, https://doi.org/10.1080/17425247.2019.1605353.

[59] V. Dave, R.B. Yadav, K. Kushwaha, S. Yadav, S. Sharma, U. Agrawal, Lipid-polymer hybrid nanoparticles: development & statistical optimization of norfloxacin for topical drug delivery system, Bioact. Mater. 2 (2017) 269–280, https://doi.org/10.1016/j.bioactmat.2017.07.002.

[60] B. Homayun, X. Lin, H.-J. Choi, Challenges and recent progress in oral drug delivery systems for biopharmaceuticals, Pharmaceutics 11 (2019) 129, https://doi.org/10.3390/pharmaceutics11030129.

[61] X. Tian, L. Zhang, M. Yang, L. Bai, Y. Dai, Z. Yu, Y. Pan, Functional magnetic hybrid nanomaterials for biomedical diagnosis and treatment, Wiley Interdiscip. Rev. Nanomed. Nanobiotechnol. 10 (2018) e1476, https://doi.org/10.1002/wnan.1476.

[62] Z. Xu, X. Ma, Y.-E. Gao, M. Hou, P. Xue, C.M. Li, Y. Kang, Multifunctional silica nanoparticles as a promising theranostic platform for biomedical applications, Mater. Chem. Front. 1 (2017) 1257–1272, https://doi.org/10.1039/C7QM00153C.

[63] X. Wang, L. Liu, Y. Luo, H. Zhao, Bioconjugation of biotin to the interfaces of polymeric micelles via in situ click chemistry, Langmuir 25 (2009) 744–750, https://doi.org/10.1021/la802810w.

[64] M. Flejszar, P. Chmielarz, Surface-initiated atom transfer radical polymerization for the preparation of well-defined organic–inorganic hybrid nanomaterials, Materials (Basel) 12 (2019) 3030, https://doi.org/10.3390/ma12183030.

[65] Z. Du, X. Sun, X. Tai, G. Wang, X. Liu, Synthesis of hybrid silica nanoparticles grafted with thermoresponsive poly(ethylene glycol) methyl ether methacrylate via AGET-ATRP, RSC Adv. 5 (2015) 17194–17201, https://doi.org/10.1039/C4RA17013J.

[66] J. Moraes, K. Ohno, T. Maschmeyer, S. Perrier, Synthesis of silica–polymer core–shell nanoparticles by reversible addition–fragmentation chain transfer polymerization, Chem. Commun. 49 (2013) 9077, https://doi.org/10.1039/c3cc45319g.

[67] E. Bagheri, L. Ansari, K. Abnous, S.M. Taghdisi, F. Charbgoo, M. Ramezani, M. Alibolandi, Silica based hybrid materials for drug delivery and bioimaging, J. Control. Release 277 (2018) 57–76, https://doi.org/10.1016/j.jconrel.2018.03.014.

[68] G. Pan, T. ting Jia, Q. xia Huang, Y. yan Qiu, J. Xu, P. hao Yin, T. Liu, Mesoporous silica nanoparticles (MSNs)-based organic/inorganic hybrid nanocarriers loading 5-Fluorouracil for the treatment of colon cancer with improved anticancer efficacy, Colloids Surf. B Biointerfaces 159 (2017) 375–385, https://doi.org/10.1016/j.colsurfb.2017.08.013.

[69] S. Palanisamy, Y.-M. Wang, Superparamagnetic iron oxide nanoparticulate system: synthesis, targeting, drug delivery and therapy in cancer, Dalton Trans. 48 (2019) 9490–9515, https://doi.org/10.1039/C9DT00459A.

[70] M. Nabila, N. Jahan, D.E. Penheiro, Polymeric nanoparticles for targeted delivery in cancer treatment: an overview, Int. J Pharm Sci Rev Res 52 (2018) 101–111.

[71] D. Lombardo, M.A. Kiselev, M.T. Caccamo, Smart nanoparticles for drug delivery application: development of versatile nanocarrier platforms in biotechnology and nanomedicine, J. Nanomater. 2019 (2019) 1–26, https://doi.org/10.1155/2019/3702518.

[72] I. Cobo, M. Li, B.S. Sumerlin, S. Perrier, Smart hybrid materials by conjugation of responsive polymers to biomacromolecules, Nat. Mater. 14 (2015) 143–159, https://doi.org/10.1038/nmat4106.

[73] Y. Guo, L. Wang, P. Lv, P. Zhang, Transferrin-conjugated doxorubicin-loaded lipid-coated nanoparticles for the targeting and therapy of lung cancer, Oncol. Lett. 9 (2015) 1065–1072, https://doi.org/10.3892/ol.2014.2840.

[74] T.E. Yalcin, S. Ilbasmis-Tamer, S. Takka, Antitumor activity of gemcitabine hydrochloride loaded lipid polymer hybrid nanoparticles (LPHNs): in vitro and in vivo, Int. J. Pharm. 580 (2020) 119246, https://doi.org/10.1016/j.ijpharm.2020.119246.

[75] Q. Huang, T. Cai, Q. Li, Y. Huang, Q. Liu, B. Wang, X. Xia, Q. Wang, J.C.C. Whitney, S.P.C. Cole, Y. Cai, Preparation of psoralen polymer–lipid hybrid nanoparticles and their reversal of multidrug resistance in MCF-7/ADR cells, Drug Deliv. 25 (2018) 1044–1054, https://doi.org/10.1080/10717544.2018.1464084.

[76] Q. Xiong, M. Cui, Y. Bai, Y. Liu, D. Liu, T. Song, A supramolecular nanoparticle system based on β-cyclodextrin-conjugated poly-l-lysine and hyaluronic acid for co-delivery of gene and chemotherapy agent targeting hepatocellular carcinoma, Colloids Surf. B Biointerfaces 155 (2017) 93–103, https://doi.org/10.1016/j.colsurfb.2017.04.008.

[77] X. Xu, J. Wu, Y. Liu, P.E. Saw, W. Tao, M. Yu, H. Zope, M. Si, A. Victorious, J. Rasmussen, D. Ayyash, O.C. Farokhzad, J. Shi, Multifunctional envelope-type siRNA delivery nanoparticle platform for prostate cancer therapy, ACS Nano 11 (2017) 2618–2627, https://doi.org/10.1021/acsnano.6b07195.

[78] B. Arjmand, B. Larijani, M. Sheikh Hosseini, M. Payab, K. Gilany, P. Goodarzi, P. Parhizkar Roudsari, M. Amanollahi Baharvand, N. sadat Hoseini Mohammadi, The Horizon of Gene Therapy in Modern Medicine: Advances and Challenges, 2019, pp. 33–64, https://doi.org/10.1007/5584_2019_463.

[79] A. del Pozo-Rodríguez, A. Rodríguez-Gascón, J. Rodríguez-Castejón, M. Vicente-Pascual, I. Gómez-Aguado, L.S. Battaglia, M.Á. Solinís, Gene Therapy, 2019, pp. 321–368, https://doi.org/10.1007/10_2019_109.

[80] S.-N. Jeong, S.Y. Yoo, Novel oncolytic virus armed with Cancer suicide gene and normal vasculogenic gene for improved anti-tumor activity, Cancers (Basel) 12 (2020) 1070, https://doi.org/10.3390/cancers12051070.

[81] U. Altanerova, J. Jakubechova, K. Benejova, P. Priscakova, V. Repiska, A. Babelova, B. Smolkova, C. Altaner, Intracellular prodrug gene therapy for cancer mediated by tumor cell suicide gene exosomes, Int. J. Cancer (2020), https://doi.org/10.1002/ijc.33188 ijc.33188.